Title
Functional characterization of transcription elongation machinery in HIV transcription and latency

Author
Li, Zichong

Publication Date
2018

Peer reviewed|Thesis/dissertation

Functional characterization of transcription elongation machinery in HIV transcription and latency

By

Zichong Li

A dissertation submitted in partial satisfaction of the

requirements for the degree of

Doctor of Philosophy

in

Molecular and Cell Biology

in the

Graduate Division

of the

University of California, Berkeley

Committee in charge:

Professor Qiang Zhou, Chair

Professor Britt Glaunsinger

Professor James Hurley

Professor Fenyong Liu

Fall 2018

Abstract

Functional characterization of transcription elongation machinery

in HIV transcription and latency

by

Zichong Li

Doctor of Philosophy in Molecular and Cell Biology

University of California, Berkeley

Professor Qiang Zhou, Chair

This dissertation is mainly focused on developing therapeutic strategies to eradicate the human immunodeficiency virus-1 (HIV-1) from infected individuals. Although HIV-1 could be suppressed in infected individuals through combined anti-retroviral therapy (cART), a latent reservoir remains in every infected individual. The reservoir is mainly composed of latently infected resting $CD4^+$ T cells. Since the exceedingly long half-life of the resting $CD4^+$ T cells and the unpredictability of when the latent HIV-1 inside them would become active, life-long medication is needed to prevent the resurgence of HIV/AIDS. The following researches are for seeking and characterizing novel drug targets, testing/repurposing drugs to reactivate latent HIVs, exposing them for recognition and clearance by host immune system, thus purging HIV from infected individuals.

The first part of this dissertation proves that RNA polymerase II (Pol II) transcription elongation is a key step during the reversal of HIV latency. Using the CRISPR/Cas9 technique and complementation assays, I find the human transcription elongation factors ELL2 and AFF1 play predominate roles in HIV-1 transcription in $CD4^+$ T cells. I further discover that, compared with their orthologs, ELL2 and AFF1 constitute only a minor subset of the Super Elongation Complexes (SECs), but are the preferred functional partners for the HIV Tat protein. Through artificially elevating the levels of ELL2 and AFF1 in the cells, latent HIV could be efficiently reactivated. In summary, these results shed light on the mechanisms of the elongation step in HIV transcription and lay the ground work for future researches to develop novel avenues to stimulate the HIV transcription elongation and reactivate the latent viruses.

The second part of this dissertation is a follow up of one of my earlier studies that identified that the bromodomain protein Brd4 promotes HIV latency by binding to the viral LTR to inhibit Tat-induced transcription. Here, I discover that the LTR of latent HIV has low acetylated histone H3 (AcH3) but high AcH4 content, which recruits Brd4 to inhibit Tat-transactivation. Furthermore, I find the lysine acetyltransferase KAT5 but not the paralogs KAT7 and KAT8 promotes HIV latency through acetylating H4 on the provirus. Antagonizing KAT5 removes AcH4 and Brd4 from HIV LTR, enhances

loading of the Super Elongation Complex, and interferes with the establishment of latency. Thus, the KAT5-AcH4-Brd4 axis is a key regulator of HIV latency and a potential therapeutic target for eradicating latent HIV reservoirs.

The third part of this dissertation uses the CRISPR-inhibition (CRISPRi) technology to extensively screen the functions of all the 20,000 human genes in maintaining HIV latency. The result not only includes several known genes, but also discovers several so far unreported genes playing vital roles in HIV latency. Through verification in cell line models, I found inhibition of these genes could significantly reactivate latent HIV. Excitingly, several hits in the screen are subunits of proteasomes, and there are FDA-approved drugs targeting proteasomes. To test the effect of these drugs on reactivating latent HIV, I isolated primary $CD4^+$ T cells from 13 ART-suppressed HIV-1 infected individual and used the drugs at different concentrations and in combination with other drugs to treat the cells. The results demonstrate that the FDA-approved proteasome inhibitors could indeed significantly enhance the reversal of HIV latency, without inducing global T cell activation or proliferation.

In summary, this dissertation proves that enhancing the activity of the human transcription elongation machinery is an effective avenue to reverse HIV-1 latency. The insights gained in this dissertation could potentially benefit future therapeutic intervention to eradicate HIV/AIDS.

To Charles Robert Darwin

Table of Contents

List of Figures and Tables

Chapter 2

Chapter 3

Chapter 4

List of Symbols and Abbreviations

AcH3	Acetylated Histone H3
AcH4	Acetylated Histone H4
bp	base pair
cART	combined anti-retroviral therapy
CRISPR	Clustered Regularly Interspaced Short Palindromic Repeats
CRISPRi	CRISPR interference
HIV	human immunodeficiency virus
UNAIDS	Joint United Nations Program on HIV/AIDS
KAT	lysine acetyltransferase
LTR	long terminal repeat
nt	nucleotide
PAF1c	Polymerase Associated Factor complex
Pol II	RNA polymerase II
PrEP	pre-exposure prophylaxis
P-TEFb	Positive transcription elongation factor b
REACT	Reiterative Enrichment and Authentication of CRISPRi Targets
SEC	Super Elongation Complex
SIV	simian immunodeficiency virus
snRNP	small nuclear ribonucleoproteins
TAR	Trans-acting Response Element
Tat	Trans-Activator of Transcription
WHO	World Health Organization

Acknowledgements

I would like to thank my advisor, Dr. Qiang Zhou, for giving me the opportunity to receive the best education in the world. His tremendous passion and enthusiasm for research have been motivating and inspiring me all the time, and his persistent supports and guidance have made everything in my dissertation possible.

I would like to acknowledge all the members, both past and present, of the Zhou lab for making the lab an enjoyable place to work. I have learned an incredible amount from each person.

I am very grateful to my committee members Drs. Britt Glaunsinger, James Hurley, and Fenyong Liu for their time and guidance.

I am also very grateful to the MCB department, particularly the professors who taught MCB 200 (2013), MCB 210 (2014), and MCB 230 (2014). These courses laid out the foundation for my critical thinking and independent researching abilities.

I also want to thank my students while I was teaching as a graduate student instructor in Fall 2014 (MCB 32L), Spring 2016 (MCB 102), and Fall 2018 (MCB 132). Their incredibly good attitude and tremendous amount of curiosity greatly energized me both personally and academically. And I also want to thank the professors who taught these courses, especially Dr. Michael Botchan, whose encouragement and approval of my teaching performance greatly enhanced my confidence of choosing teaching as part of my future career.

I also want to thank the Tang Opportunity Fund, Berkeley International Office, and the Irving H. Wiesenfeld fellowship for financial support, and my family for financial and spiritual support.

Chapter 1

General Introduction

A brief evolutionary and epidemiological history of HIV

Although the acquired immune deficiency syndrome (AIDS) was first formally identified as a clinical syndrome in 1981 (1-3), the origin of HIV/AIDS is much more ancient. Using a molecular clock based on the constant average rate of evolution of viral sequences, the common ancestor of the main group of HIV-1 has been dated to around the 1920s (4). That is when the Simian Immunodeficiency Virus (SIV) was transmitted from chimpanzee to humans through cross-species blood contact, most likely during hunting activities in west central Africa (5). Further sequence analyses revealed that SIV in chimpanzee was the result of recombination between two distinct forms of SIVs from two different species of monkeys (6).

Given the close relatedness of chimpanzees and humans and the long existence of chimpanzee-hunting activities in west central Africa, the chimpanzee-to-human cross-species transmission likely had happened numerous times in history. However, only in the early twentieth century did HIV spread across the world, likely due to the vastly increased human populations, interactions, migrations, and the widespread use of unsterile injections associated with colonialism in Africa (7-9). According to World Health Organization (WHO), more than 70 million people worldwide have been infected and about 35 million people have died of HIV since the beginning of the epidemic. At the end of 2017, about 37 million people in the world were living with HIV. It is estimated that HIV-1 was introduced from central Africa to Haiti around 1967, taken from Haiti to the United States around 1969, and eventually entered male gay communities in New York City in 1971 and from there spread to San Francisco in 1976 (10,11). According to Centers for Disease Control and Prevention, in the United States, about 1.2 million people were living with HIV at the end of 2015, and 38,500 people became newly infected in that year.

Current status of anti-HIV therapy

The advent of combined antiretroviral therapy (cART) in 1996 transformed HIV infection from a speedy death sentence to a manageable chronic condition (12,13). There are six classes of antiretroviral drugs that target different phases of HIV lifecycle: fusion inhibitors, nucleoside reverse transcriptase inhibitors, nucleotide reverse transcriptase inhibitors, non-nucleoside reverse transcriptase inhibitors, integrase inhibitors, and protease inhibitors. To maximally suppress HIV replication and avoid resistance, the standard of care is to use combinations of three antiretroviral drugs from at least two different classes (14). Due to the high mutation rate of replicating HIV, treatment discontinuations cause rapid resistance development (15). In recently years, pharmaceutical companies combined multiple antiretroviral drugs into a single pill taken once daily. These fixed-dose combinations greatly reduce pill burden, increase adherence and long-term effectiveness (16).

Besides cART, which suppresses viral replication in infected individuals, pre-exposure prophylaxis (PrEP) is a major breakthrough in recent years as a way to reduce the risk of HIV-negative people acquiring HIV infection (17). PrEP administers Truvada, a nucleotide reverse transcriptase inhibitor to uninfected people that are regularly involved in high-risk behaviors (18). When used properly, PrEP could significantly

reduce the risk of contracting HIV (19). However, due to the high cost, PrEP is still out of reach for most of the high-risk populations (20).

Another and arguably the ultimate approach to end HIV epidemic is HIV vaccine. However, due to the rapid generation of escape mutations, multiple trials showed no efficacy (21-25), except RV 144. Also known as the Thai trial, RV 144 administered the combination of two vaccines, ALVAC and AIDSVAX, which previously failed on their own, to volunteers primarily at heterosexual risk for HIV infection. The results, with a p-value of 0.04, demonstrated that the rate of HIV infection among volunteers who received the experimental vaccine was 31.2% lower than the rate of HIV infection in volunteers who received the placebo (26). This encouraging result indicates that combinations of different vaccines are more effective than single vaccines, possibly due to the increased difficulty for the virus to generate escape mutations that could resist both componential vaccines. The RV 144 trial also demonstrated that the combination of ALVAC and AIDSVAX is safe and well tolerated, thus suitable for further trials with larger-scale in more diverse populations (27).

One major problem with the current fight against HIV/AIDS is the limited coverage of cART to people with HIV infection. According to WHO, in 2017, the global coverage of cART was only 47%. This is due to the limited diagnosis rate, the limited resources to distribute cART medications, and the limited effectiveness of cART. On average, in 2017, only 75% people with HIV were diagnosed of their infection, among those diagnosed, 79% were on cART, and among those on cART, 81% achieved viral suppression (i.e. with undetectable viral load in blood). The encouraging scenario is that these ratios are steadily increasing annually. To end global HIV epidemic by 2030, the 90-90-90 goal has been proposed by the Joint United Nations Program on HIV/AIDS (UNAIDS) and WHO: that by 2020, 90% of people living with HIV will be diagnosed, 90% of the diagnosed people will be on sustained cART, and 90% of the people on cART will achieve viral suppression (28). Encouragingly, in 2016, Sweden became the first country to achieve the 90-90-90 goal (29). However, globally, the progress is uneven, since most of the undiagnosed and untreated populations are in low- and middle-income counties especially in Africa (30). For example, in 2014 and 2015, in one of the provinces in South Africa most heavily affected by HIV, only 52% of HIV-infected men and 65% of HIV-infected women were diagnosed (31). Therefore, considerable resources should be focused on the developing countries in order to achieve the 90-90-90 goal and end global HIV epidemic (32).

Another major drawback of the current anti-HIV therapy, with cART at the core, is its side effects when being taken for decades as the infected population age (33-35). These side effects, including but not limited to hypersensitivity or allergic reactions, heart disease, diabetes, lactic acidosis, kidney-, liver-, or pancreas-damage, and peripheral neuropathy, are the main reasons of therapy dropout, which leads to quick viral resurgence and development of viral resistance to cART (36-40). Another drawback of cART is its high cost, estimated to be over $400,000 per lifetime treatment (41,42), constitutes a grave financial burden, especially for developing countries with the largest HIV-infected populations (43,44). The reason that the virus persists for decades and requires lifelong adherence to cART is the latent stage in HIV's life cycle.

Transcriptional silencing leads to HIV latency, a primary obstacle for a cure

Like other members of *Retroviridae*, HIV's life cycle requires integration of the reverse-transcribed viral genome into the host genome as a provirus. After integration, the fate of the provirus depends on both cellular determinants and the features of HIV itself (45,46). While most of the integrated viruses get into active life cycles at the expense of killing the host cells, a minor population of them gets into latency while retaining their ability to enter active replication in a future time. The latent lifestyle grants HIV an evolutionary advantage by enhancing its transmission across target-cell-poor mucosa (47). Clinically, the latently infected cells, primarily resting $CD4^+$ T cells, serve as a viral reservoir that that necessitates lifelong antiretroviral therapy (ART) (48,49). Of the estimated 78 million people infected to date, the only one documented case of cure, Timothy Ray Brown (the "Berlin patient"), achieved an apparent clearance of the latent reservoir after receiving myeloablative haemopoietic stem cell transplantations from a homozygous CCR5-Δ32 donor (50,51).

Although the radical approaches in the case of the Berlin patient are not applicable to the broader population, this case does indicate that chronic HIV infection is curable if the latent reservoir could be sufficiently reduced (52). Toward this goal, a leading strategy relies on using latency reversing agents (LRAs) to reactivate the latent proviruses in ART-suppressed HIV-infected individuals, thus exposing the infected cells to be killed by the host immune system and/or therapeutic reagents (45,53,54). This strategy (nicknamed "shock and kill" or "kick and kill") requires exhaustive knowledge about the mechanisms involved in the establishment, maintenance, and reversal of HIV latency.

HIV latency is the result of multiple obstacles that block the proviral transcription (55): (1) In chronically infected cells, the histones on the chromosomal locations integrated by HIV proviruses could be depleted of the acetylation modifications, which are generally required for a relaxed chromosomal structure amenable to the loading of the transcription machinery, thus preventing the transcription initiation (56-58). (2) The sequestration of the transcription factors NF-κB and NFAT, which bind to HIV's 5' long terminal repeat (LTR) and recruit RNA polymerase II (Pol II) at the beginning of the proviral transcription, thus reducing the initiation of HIV transcription (59-62). (3) The promoter-proximal pausing of Pol II on HIV LTR abolishes productive transcription elongation. After initiation, Pol II pauses at around 62 bp downstream of the transcription start site, due to the intrinsic features of HIV promoter and the effect of negative host factors (63,64). Before the pausing of Pol II, a stretch of 59 nt RNA leader sequence is transcribed and folds into a specific stem-loop structure, named TAR (stands for Trans-Activation Response) element. To release the paused Pol II into active transcription involves the most unique feature of HIV transcription: Tat-dependent transcription elongation (65), as described below.

Tat is a key regulatory protein in HIV transcription and latency reversal

Unlike other simpler retroviruses, HIV, as a lentivirus, encodes additional regulatory proteins to control its life cycle. One such protein, Tat (stands for "Trans-Activator of Transcription"), a small protein consisting of between 86 and 101 amino acids depending on the subtype, plays a critical role in the transcription of HIV provirus.

Tat stimulates HIV transcription elongation by releasing the paused Pol II into productive transcription (46). Early studies demonstrate that Tat binds to a bulge structure in the stem of the TAR RNA element, and in doing so potently stimulates the elongation but not initiation step of HIV transcription (66-70).

The fact that Tat protein is encoded by HIV genome that it helps transcribe constitutes a powerful positive feedback mechanism. This mechanism underlies the stochastic nature of the establishment and reversal of HIV latency (71-73). During latency establishment, small reductions in initiation rates could be enough to restrict Tat production and lead to entry into latency. On the other hand, even extremely rare cases of productive transcription elongation in latently infected cells could be enough to generate the initial amount of Tat to trigger full-scale latency reversal through the positive feedback loop (46). Because of the Tat-dependent stochastic nature of HIV transcription, significant portions of the replication-competent proviruses in the latent reservoir remain uninduced even after maximal T cell activation, thus increasing the barrier to HIV-1 cure (74,75).

Besides binding to TAR, Tat functions through interacting with several host factors related to transcription elongation. Early studies identified P-TEFb (stands for positive transcription elongation factor b) as a direct Tat-interaction partner that is required for Tat transactivation (76-79). After being recruited by Tat onto TAR that is adjacent to the paused Pol II, the CDK9 subunit of P-TEFb phosphorylates the carboxyl-terminal domain (CTD) of the large subunit of paused Pol II, thus releasing it into productive transcription elongation (80-82). As an important transcription elongation factor related to stimulating the transcription of numerous human genes (83), the majority of P-TEFb in the cells is sequestered in 7SK snRNP (84,85), a large multi-subunit RNA-protein complex that regulate the levels of a pool of active P-TEFb available in the cells (86-88). Adding another layer of Tat's function, it can increase the active pool of P-TEFb by competing with HEXIM1, one of the subunits of 7SK snRNP (89). Besides these earlier discoveries, in the past decade, a major advance in our understanding of Tat's function is the recognition that Tat stimulates HIV transcription elongation through more than one mechanism, thanks to the purification and characterization of Super Elongation Complex (SEC) as a novel Ta-interaction partner.

Discovery of SEC as a major co-factor of Tat

Aiming to identify additional factors that may interact with P-TEFb in the presence of Tat, in 2010, two groups reported the results of affinity purifications in HeLa and HEK293-based cell lines (90,91). Their mass spectrometry results indicate that the Tat co-factors are much more than previously expected: In addition to P-TEFb, Tat also interacts with 7SK snRNP (91), and most importantly, as identified by both of the two groups, Tat's interaction with P-TEFb is part of a larger protein-protein complex that contains, besides P-TEFb, additional transcription elongation factors. Among them are AFF1, AFF4, ELL1, ELL2, EAF1, ENL, and AF9 (90,91). Because this complex contains multiple transcription elongation factors that work through distinctive mechanisms to enhance transcription elongation, it is named "super elongation complex (SEC)" (92).

Besides P-TEFb, the other active components of SEC are ELL2 and ELL1. They are paralogous proteins that were first identified in 1996-1997 (93,94). Functionally, ELL2 and ELL1 increase the catalytic rate of Pol II transcription elongation (95). Importantly, in human cells, the protein level of ELL2, but not the paralogous ELL1, is tightly regulated by polyubiquitination and proteasomal degradation pathways (96).

The other two paralogous proteins in SEC are ENL, and AF9. They interact with Polymerase-Associated Factor complex (PAFc) to connect SEC to Pol II on chromatin (97). Of note, besides PAF1c, additional recruiters/docking sites of SEC have also been reported, including the human mediator subunit Med26. In the case of Med26, it N terminal domain interacts with EAF1, which stands for "ELL-associated factor 1", thus recruits SEC to mediator that is part of the Pol II elongation complex (98).

AFF4 and AFF1 serve as scaffold proteins in SEC. They are long, flexible, and internally disordered proteins with small hydrophobic patches that interact with P-TEFb, ELL1/2 and ENL/AF9 (99-101). Interestingly, they not only serve to assemble SEC, but also stimulates TAR recognition by Tat and enables Tat to extract P-TEFb from 7SK snRNP (102,103).

Of note, SEC is present not only in HIV-infected cells, but also in uninfected cells, and is required for the transcription of MLL chimera targets in leukemic cells (92), as well as global regulation of gene expression in embryonic stem cells (104).

The Tat-SEC axis is a drug target for HIV transcription latency reversal

Since its discovery, SEC had been implicated in Tat-induced HIV transcription. In the next few years, efforts had been made to elucidate, in $CD4^+$ T cells, how much SEC contributes to the HIV transcription and latency reversal. Before the discovery of SEC, an interesting observation had been made that another P-TEFb interaction partner, Brd4, could inhibit Tat-induced HIV transcription (105,106). Detailed mutagenic studies and reporter assays indicate that a short domain at the extreme C-terminal of Brd4 interacts with P-TEFb and is responsible for inhibiting Tat-induced HIV transcription (106). Since Brd4 could not assemble P-TEFb into SEC as Tat does, these early observations imply that a possible competitive relationship may be present between Tat and Brd4 in terms of determining whether P-TEFb goes into SEC or not.

The invention of a Brd4-specific small molecular inhibitor, JQ1 (107), greatly facilitated the testing of this hypothesis. Brd4 interacts with acetylated chromatins (thus locate on HIV provirus) through the two acetyl-lysine recognition motifs, or bromodomains located at its N-terminus. By competitively binding to the bromodomains, JQ1 removes Brd4 from chromatin. In one of my earlier publications, I found that JQ1 reverses HIV latency in $CD4^+$ T cells through antagonizing Brd4's inhibition of Tat-transactivation (108). JQ1 dissociates Brd4 from the HIV promoter, allowing Tat to recruit SEC to LTR to stimulate HIV transcription elongation (108). More important, I found that JQ1 synergizes with prostratin, another LRA that activates NF-κB through protein kinase C (PKC) pathway. Similar results were also reported by others (109,110). In the following years, multiple studies had confirmed the efficacy of JQ1 in reversing HIV latency, and its synergy with PKC agonists (111,112). These results demonstrate the

feasibility of targeting the Tat-SEC axis to reverse HIV latency and herald more studies on the detailed mechanisms that underlie this axis.

To purge latent HIV reservoir requires combined therapeutic approaches

Since the discovery of the latent reservoir, efforts have been made to purge the reservoir by reversing HIV latency. Based on the earlier observations that the viral reactivation is concomitant with T cell activation (113,114), the first clinical trials sought to activate T cells *in vivo* by co-administration of antibodies against CD3 and interleukin-2 (115,116). However, the results demonstrate that these T cell activation reagents are highly toxic to participants without significant perturbation of the latent reservoir. In the following years, multiple LRAs that do not activate T cells have been tested in human trials. These LRAs were well tolerated *in vivo*, but their effect on the enhancement of HIV transcription is low, and they could not induce any obvious reduction of the latent reservoir (117,118). The modest results of the current LRAs inspire me to search for novel cellular mechanisms that maintain HIV latency, and, by targeting these mechanisms in combination with the current LRAs, to better enhance the transcription of latent HIV and expose the viral reservoir.

Chapter 2

A minor subset of Super Elongation Complexes plays a predominant role in reversing HIV-1 latency

(This work was originally published in *Molecular and cellular biology* as: Li, Z., Lu, Z., & Zhou, Q. (2016). A minor subset of super elongation complexes plays a predominant role in reversing HIV-1 latency. *Molecular and cellular biology*, MCB-00994.)

Summary

Promoter-proximal pausing by RNA polymerase (Pol) II is a key rate-limiting step in HIV-1 transcription and latency reversal. The viral Tat protein recruits human Super Elongation Complexes (SECs) to paused Pol II to overcome this restriction. Despite the recent progress in understanding the functions of different subsets of SECs in controlling cellular and Tat-activated HIV transcription, little is known about the SEC subtypes that help reverse viral latency in CD4+ T cells. Here, we used the CRISPR-Cas9 genome-editing tool to knock out the gene encoding the SEC subunit ELL2, AFF1, or AFF4 in Jurkat/2D10 cells, a well-characterized HIV-1 latency model (119). Depletion of these proteins drastically reduced spontaneous and drug-induced latency reversal by suppressing HIV-1 transcriptional elongation. Surprisingly, a low-abundance subset of SECs containing ELL2 and AFF1 was found to play a predominant role in cooperating with Tat to reverse latency. By increasing the cellular level/activity of these Tat-friendly SECs, we could potently activate latent HIV-1 without using any drugs. These results implicate the ELL2/AFF1-SECs as an important target in the future design of a combinatorial therapeutic approach to purge latent HIV-1.

Introduction

HIV-1 latency, which is characterized by transcriptional silence of the integrated proviruses, is the principal impediment to eradication of viral infection. Although anti-retroviral therapy (ART) has been used successfully to drive HIV-1 into this silent state thereby decreasing the plasma viremia to undetectable levels, the proviruses can quickly resume transcription and active replication once ART is interrupted (54). To obtain a real cure for HIV/AIDS, one strategy nicknamed 'shock and kill' has been proposed to eliminate the latent viral reservoirs by first activating the proviruses in infected cells. This is followed by the next phase where spread of the activated viruses can be suppressed by ART and the virus-producing cells are eliminated simultaneously (46).

A number of cytokines and small molecule drugs that include histone deacetylase inhibitors (HDACi), protein kinase C agonists, BET bromodomain inhibitors and others have been tested for their latency-reversing potentials (45,120). However, virtually all of them have been found to display low efficacy and/or unacceptable side effects, which have limited their clinical use (120). Thus, better and more specific means to activate the latent proviruses are urgently needed, which can only be achieved through in-depth characterization of the molecular mechanism and factors that control viral latency.

Without stimulation, RNA Polymerase II (Pol II) that transcribes the integrated proviral DNA has a strong tendency to pause and then terminate near the transcription start site, resulting in the production of only short transcripts (65). This abortive transcription presents a major hurdle to efficient escape of HIV-1 from latency (46). To overcome this hurdle, a multi-component complex containing the viral-encoded Tat protein and its specific host co-factors must form on the nascent 5' end of the HIV-1 transcript, which folds into a stem-loop structure called the TAR (Trans-Activation Response) RNA. This Tat/TAR-containing complex converts the paused Pol II into a highly processive form capable of generating the full-length HIV-1 transcripts (65). In 2010, a set of human transcription factor complexes, called the Super Elongation Complexes (SECs), was identified as the specific Tat co-factor (91,97). A typical SEC contains CDK9 and cyclin T (CycT; either CycT1 or T2), collectively referred to as P-TEFb, as well as one of each of the three pairs of homologous proteins: ELL1/ELL2, AFF1/AFF4, and ENL/AF9 (90-92). Owing to the ability of these proteins to create multiple different combinations among them, a fairly large family of related SEC complexes exists in vivo (121,122).

The P-TEFb component of a SEC stimulates transcriptional elongation through phosphorylating the Pol II carboxyl-terminal domain (CTD) and negative elongation factors (65). The ELL1/2 subunit, on the other hand, can directly increase the catalytic rate of Pol II by suppressing transient pausing (123). As these two elongation stimulatory factors act simultaneously on a single polymerase complex at the HIV-1 promoter, they synergistically boost viral transcription (90,122). In addition to P-TEFb and ELL1/2, AFF1/AFF4 is another essential SEC component due to its ability to serve as a flexible scaffold to recruit all the other subunits into a complete complex (97,99).

Our recent structural and biochemical analyses indicate that AFF1/4 and Tat bind right next to each other to the surface of CycT1, and that this arrangement significantly enhances the interaction between Tat and P-TEFb (100). Compared to AFF1, AFF4

displays greatly diminished ability to promote the Tat-P-TEFb binding because of a critical amino acid variation between the two AFF proteins (122). While this functional difference was observed mostly in HeLa and HEK293 cells, it remains to be determined whether it also exists in HIV-1's natural host, CD4+ T cells. Unlike AFF1 that stimulates the Tat-P-TEFb interaction, the human BET bromodomain protein BRD4 competes with Tat for binding to P-TEFb, leading to the inhibition of Tat-transactivation (105,106). Importantly, a small molecule inhibitor termed JQ1 has been shown to antagonize BRD4's inhibitory effect through occupying its bromodomains. This in turn promotes the Tat-P-TEFb/SEC binding, Tat-transactivation, and the exit of HIV-1 from latency (108-110).

Despite the recognition of the key role that the SECs play in HIV-1 transcription, little is known about how they may control viral latency. Specifically, it remains to be seen to what extent the reversal of latency depends on the SECs and whether any particular members of the SEC family may exert a predominant role in this process. Furthermore, it is unclear whether the cellular level/activity of a SEC can be manipulated in CD4+ T cells to efficiently reverse latency in the absence of any chemical inducers that have serious side effects.

Previously, it has been difficult to answer these questions due to the frequently encountered partial effectiveness of RNA interference (RNAi) in silencing gene expression. In the present study, we used the state-of-the-art CRISPR-Cas9 genome-editing tool to knock out (KO) the gene encoding the SEC subunit ELL2, AFF1, or AFF4 in 2D10 cells, a well-characterized Jurkat T cell-based HIV-1 latency model (119). Depletion of these SEC subunits significantly reduced both spontaneous and drug-induced latency reversal by suppressing viral transcription at the stage of elongation. Surprisingly, despite its very low abundance, a minor subset of SECs was found to play a predominant role in facilitating the Tat-dependent latency exit. Furthermore, by simply elevating the cellular level/activity of these Tat-friendly SECs, we were able to efficiently reverse latency without using any drugs.

Experimental Procedures

Generation of knockout (KO) and rescue cell lines

The procedures for disrupting the genes encoding the SEC subunits ELL2, AFF1, and AFF4 using the CRISPR-Cas9 system in the Jurkat-based 2D10 cell line (119) have been described previously (124). The plasmid vector pSpCas9(BB)-2A-Puro (PX459) that expresses Cas9 and sgRNA was from Addgene (plasmid # 48139). The sgRNA and genotyping primer sequences used in the procedures are listed in Table 2-1. The positive KO clones were identified by Sanger sequencing of the genomic amplicons obtained with the TA Cloning Kit (Life Technologies), and the loss of expression of the disrupted genes was verified by immunoblotting of the target proteins.

A pcDNA3-based vector expressing FLAG-tagged ELL2 (ELL2-F) was stably introduced into the ELL2 KO cell line ΔELL2 by nucleofection. Rescue clones

expressing varying levels of ELL2-F were obtained by sorting of single cells, selection in G418 at 400 μg/ml for 16 days, and finally anti-Flag immunoblotting.

Generation of stable AFF1- or AFF4-knockdown (KD) HeLa cells

The shRNA sequences that target AFF1 (shAFF1; 5'-CCGGGCCTCAAGTGAAGTTTGACAACTCGAGTTGTCAAACTTCACTTGAGGCTTTTTG-3') and AFF4 (shAFF4: 5'-CCGGGCACCAGTCTAAATCTATGTTCTCGAGAACATAGATTTAGACTGGTGCTTTTTG-3'), respectively, were cloned into the lentiviral vector pLKO.1. shRNA targeting GFP was used as a non-target control. Lentivirus production and infection of HeLa cells were conducted as previously described (102).

Detection of HIV-1 latency reversal

To test the effects of SEC subunit KO and the rescues on spontaneous and drug-induced latency reversal, 1 x 10^6 WT or the various KO cells were treated with 1 nM PMA, 2 μM prostratin, 1 μM JQ1, or 0.1% DMSO as a negative control. After the treatment for 16 hours, the cells were subjected to FACS analysis to detect the GFP fluorescence. Data were analyzed using the Flowjo (Tree Star) software by first selecting living cells using the FS/SS gates, and then reading the GFP-positive percentage for each sample under the same threshold throughout the experiment. The percentage of GFP(+) cells and the standard deviation for each sample were calculated based on the triplicate treatments.

Reverse transcription followed by quantitative real-time PCR (RT-qPCR) analysis

Total RNA was extracted by TRIzol reagent (Life Technology) from drug-treated or untreated WT Jurkat/2D10 cells or the various KO cell lines and reversed transcribed using random hexamer primers (Life Technology). The cDNA was amplified with the DyNAmo HS SYBR Green qPCR kit (Fisher F-410L) on a CFX96 system (Bio-Rad) using the HIV-1 LTR forward primer 5'-GGGTCTCTCTGGTTAGACCAG-3' in combination with either HIV-1 LTR reverse primer-1: 5'-GGGTTCCCTAGTTAGCCAGAG-3', or reverse primer-2: 5'-CTGCTAGAGATTTTCCACACTGAC3' to examine the levels of the short, just initiated and longer, elongated HIV-1 transcript, respectively (125). All reactions were performed in triplicates with melting curves to ensure specificity. The PCR signals were normalized to that of GAPDH and displayed.

Co-immunoprecipitation

Approximately 5 × 10^8 WT or KO cells were swollen in hypotonic buffer A (10 mM HEPES-KOH [pH 7.9], 1.5 mM $MgCl_2$, and 10 mM KCl) for 10 minutes and then centrifuged at 362g for 10 min. The nuclei were extracted with Dounce tissue homogenizer in buffer C (20 mM HEPES-KOH [pH 7.9], 0.4 M NaCl, 25 % glycerol, 0.2 mM EDTA, 1.5 mM $MgCl_2$, 0.2 % NP-40, and 1 × protease inhibitor cocktail). Nuclear extracts were mixed with 4 μg specific antibodies or control normal IgG and incubated at 4℃ for 3 hours. Subsequently, 15 μl protein-A beads (Life Technology) were added into each reaction and the mixtures were rotated at 4℃ overnight. The beads were then washed extensively with buffer D (20 mM HEPES-KOH [pH 7.9], 0.3 M KCl, 15 %

glycerol, 0.2 mM EDTA, 0.2 % NP-40, 1 × protease inhibitor cocktail) and eluted with 30 ul 0.1 M glycine (pH 2.0). For Western blot, 2% of the total input for immunoprecipitation (IP) and 25% of the IP eluate were loaded into each NE and IP lane, respectively.

Results

Generation of Jurkat/2D10-based AFF1, AFF4 or ELL2 KO cell lines using the CRISPR-Cas9 system

Using the CRISPR-Cas9 system (124), we introduced double-strand breaks into the first exon of the ELL2 and AFF4 genes as well as the second exon of the AFF1 gene in the Jurkat-based 2D10 cells, a post-integrative latency model developed by the Karn laboratory (119). The HIV-1 sequence contained in this cell line encodes a partially attenuated Tat variant H13L as well as the short-lived d2EGFP reporter protein in place of the *nef* gene. The positive knockout (KO) clones were identified by Sanger sequencing, which detected frame-shift mutations resulting from non-homologous end-joining repair in both alleles of the target genes (Fig. 2-1 and Table 2-1). The complete loss of protein expression by the target genes was also verified by Western analysis of the KO cell lysates (Fig. 2-1).

Two different clones each of the AFF1- and AFF4-KO were obtained by using two separate single guide (sg)RNA sequences that target distinct regions of the AFF1 or 4 gene (Fig. 2-1 and Table 2-1). These twin AFF1/4-KO clones will be analyzed in key experiments below to ensure that the results obtained can indeed be attributed to the loss of AFF1 or 4 but not some unintended off-target effects of the sgRNAs and the CRISPR-Cas9 system. For the single ELL2 KO clone, we will perform rescue experiments by reintroduction of wild-type (WT) or mutant ELL2-expressing constructs as a way to rule out any off-target effects (see below).

It is important to point out that our efforts to obtain homozygous ELL1 KO were unsuccessful despite the use of two distinct sgRNA sequences and sequencing at least 34 different clones (Table 2-1). Only heterozygous KO cells in which one allele was found to contain a frame-shift mutation, while the other had an in-frame deletion or insertion that restored the ELL1 open reading frame, were obtained. These observations suggest that ELL1 is an essential gene, a notion that is supported by a recent genome-wide study showing that the sgRNA sequences for ELL1 were significantly more depleted than those for ELL2, AFF1, and AFF4 in a negative selection screen (126).

AFF1, AFF4 and ELL2 are differentially required by various agents to reverse HIV-1 latency

We next performed FACS analysis to examine the effect of the ELL2, AFF1 or AFF4 KO on abilities of several well-known latency-reversing small molecules to promote the HIV-1 LTR (Long Terminal Repeat)-dependent GFP expression. Representative FACS plots are shown in Fig. 2-2A, and based on theses and others the processed data are summarized in bar graphs in Fig. 2-2B-E. First of all, when treated with the vehicle control DMSO, only a small percentage (~1.2%) of WT cells became

GFP-positive, and the loss of any of the three SEC components was found to further reduce this spontaneous, basal level exit from latency (Fig. 2-2B). Notably, between the two AFF proteins, AFF4 KO produced a more pronounced effect (<0.1% GFP+ cells) than did AFF1 KO (~0.5%) in suppressing this process.

As for the drug-induced latency reversal, all three SEC subunits were shown to be important in this process, although the responses to their KO varied from compound to compound. The BET bromodomain inhibitor JQ1 is known to activate HIV-1 transcription by antagonizing BRD4's inhibition of the Tat-P-TEFb/SEC interaction, thereby stimulating the Tat/SEC-dependent viral transcription (108,110). We have recently demonstrated that the AFF1-containing SECs are preferentially employed by Tat to trans-activate the HIV-1 LTR (122). Consistent with these observations, the JQ1-induced latency reversal was strongly dependent on AFF1 (from 47% in WT cells to ~2-3% GFP+ cells remaining in the KO population; Fig. 2-2C) but much less so on AFF4 (47% to 18%). PMA and prostratin, on the other hand, function primarily by activating Protein Kinase C (PKC) and hence NF-κB, which then binds to and stimulates transcription from the viral LTR. Compared to JQ1's strong reliance on AFF1, latency reversal by these two compounds was not so much decreased by the AFF4 or AFF1 KO (at least 14% GFP-positive cells still remaining) and moreover, it was affected somewhat similarly by the loss of AFF1 or AFF4 (Fig. 2-2D & 2-2E).

Among the three latency-reversing compounds tested, JQ1 displayed the highest sensitivity to the KO of ELL2 (Fig. 2-2C), whereas prostratin was the least sensitive (Fig. 2-2E) and PMA in the middle (Fig. 2-2D). The strong dependence on ELL2 by JQ1 is consistent with the earlier demonstrations that the Tat-SEC complex plays an especially important role in allowing JQ1 to reverse HIV-1 latency (108). Later, we will investigate whether the homologous ELL1 protein can rescue the ELL2 KO to enable JQ1 to regain this ability.

KO of SEC subunits suppresses latency reversal by decreasing HIV-1 transcriptional elongation

In the above latency reversal assay, the two independent AFF1 or AFF4 KO clones, which were generated with sgRNAs targeting two different regions of AFF1 or AFF4, produced nearly identical responses under all treatment conditions (Fig. 2-2B-E). The twin AFF1/4 KO clones also behaved the same in many other experiments below, thus ruling out their displayed phenotypes as potential off-target effects of CRISPR-Cas9. Thus, for simplicity of presentation, results obtained with just one clone each of the AFF1/4 KO (ΔAFF1-sg1 and ΔAFF4-sg1) will be discussed henceforth.

In light of the above GFP data showing the KO-induced decrease in HIV-1 LTR activity, we wanted to further investigate whether the decrease occurred at the transcription initiation or elongation level. To this end, RT-qPCR reactions containing two distinct pairs of LTR primers (125) that can distinguish between a just initiated short (59-nt) HIV-1 transcript and an elongated longer form (190-nt) were performed (Fig. 2-3A). Consistent with the notion that the SEC is exclusively involved in the elongation control, production of the short HIV-1 RNA, i.e. transcription initiation, was mostly unaffected by loss of any of the three SEC subunits (Fig. 2-3B). This was true not only

for JQ1, the BRD4 antagonist and Tat/SEC activator, which elevated production of the 59-nt transcript, i.e. initiation, by only ~2-fold compared to DMSO, but also for PMA and prostratin, the two PKC/NF-κB activators, which stimulated this process by nearly 80-fold.

In contrast to HIV-1 initiation, the production of the longer 190-nt transcript, i.e. transcription elongation, was sensitive to KO of SEC subunits, although the degree of sensitivity varied under different treatment conditions (Fig. 2-3C). Just like the situations encountered above in the GFP reporter assay, between AFF1 and AFF4, the low, basal level elongation in DMSO-treated cells was extremely sensitive to the loss of AFF4 but not AFF1. In contrast, the activated elongation in JQ1-treated cells was completely gone only after the KO of AFF1 but not AFF4 (Fig. 2-3C), reinforcing the notion that JQ1 acts primarily by stimulating the Tat/SEC-dependent HIV-1 elongation and that the AFF1-SEC is preferentially utilized in this process (108,110,122). As for HIV-1 elongation in cells treated with either PMA or prostratin, it was similarly sensitive to the loss of AFF1 or AFF4, although the dependence of the two compounds on AFF1/4 was a few orders of magnitude lower than that of JQ1 on AFF1 (Fig. 2-3C).

Finally, just like the KO of AFF1/4, the KO of ELL2 did not much affect the HIV-1 initiation, but uniformly decreased basal as well as activated HIV-1 elongation under all treatment conditions (Fig. 2-3B & 2-3C), confirming this protein as a key contributor to the SEC-mediated elongation stimulation. Together, the above data indicate that even though the three latency-reversing agents can preferentially target different stages of HIV-1 transcription (PMA and prostratin primarily activate the NF-κB-mediated initiation, whereas JQ1 mostly the Tat-stimulated elongation), the SEC-dependent HIV-1 elongation is an indispensible step that all three compounds must activate, either directly or indirectly, in order to efficiently promote the viral exit from latency.

Latency reversal in KO cell lines is restored by re-introduction of the missing proteins or in some cases their functional homologues

To investigate whether the homologous ELL (ELL1 and ELL2) and AFF (AFF1 and AFF4) proteins may possess redundant functions in promoting the exit from HIV-1 latency, we expressed them individually from nucleofected cDNAs in WT Jurkat/2D10 and the three SEC subunit-KO cell lines. With the exception of AFF4-F (Flag-tagged AFF4), this resulted in an increase in basal level GFP production in WT cells (Fig. 2-4A). However, compared to ELL2-F, ELL1-F was significantly less effective in this process. Upon close examination, we suspected that even this relatively weak stimulatory effect was likely caused by ELL1-F's much higher accumulation than ELL2-F in nucleofected cells (Fig. 2-4A, bottom panel). Indeed, when the expression of the two ELL proteins was adjusted to about the same level, ELL1-F completely lost the ability to activate GFP expression (Fig. 2-4B). Thus, between the two homologous pairs of SEC subunits, only the introduction of extra ELL2, or to a smaller extent, AFF1 into WT cells was able to promote the non-drug induced latency reversal, suggesting that these two SEC subunits are normally present at levels or in states that are suboptimal for the reversal.

In the various KO lines, the spontaneous latency reversal was restored or even elevated to levels higher than that seen in WT cells upon re-introduction of the cDNAs

encoding the missing proteins. For example, significantly elevated GFP production was observed when ELL2-F but not ELL1-F was reintroduced into the ELL2 KO cells (Fig. 2-4B). A smaller increase was seen only after ELL1-F was expressed at a much higher level than ELL2-F or when extra AFF1-F was introduced (Fig. 2-4A). The specificity of the rescue has effectively ruled out the phenotypes displayed by the ELL2 KO cells as off-target effects.

Similar to the situation found in the ELL2 KO cells, ectopic expression of AFF1-F but not AFF4-F in the AFF1 KO cells was able to reverse latency beyond the level detected in WT cells (Fig. 2-4A). In contrast, introduction of not only AFF4-F but also AFF1-F into the AFF4 KO cells was able to elevate the level of GFP production to that of WT cells, although the introduction of ELL1-F or ELL2-F completely failed to produce such an effect (Fig. 2-4A). The observations that AFF1 effectively complemented the loss of AFF4 but AFF4 was unable to replace AFF1 suggest that during spontaneous latency reversal, AFF1 possesses all the essential functions that AFF4 does but not *vice versa*.

Next, we repeated the above rescue experiment under the JQ1-treatment conditions. The data in Fig. 2-4C indicate that although the overall percentages of GFP(+) cells upon exposure to JQ1 were much higher than those obtained under basal, non-drug induced conditions, the JQ1-induced latency reversal responded very similarly to the introduction of ELL1/2 and AFF1/4 into WT and the KO cell lines (compare Fig. 2-4C with Fig. 2-4A). Despite this overall similarity, there was a noticeable difference between the two with regard to the responses displayed by the AFF4 KO cells. While the introduction of extra ELL2 into this line failed to enhance basal GFP production (Fig. 2-4A), it was almost as effective as the introduction of either AFF1 or AFF4 in rescuing the JQ1-induced latency reversal (Fig. 2-4C). Previously, it has been shown that JQ1 activates HIV-1 transcription and reverses viral latency through mostly the Tat/SEC-dependent pathway (108,110) and that the SEC subunits ELL2 and AFF1 play an especially important role in this process (90,122). Given these revelations, it is likely that the extra ELL2 or AFF1 introduced into the AFF4 KO cells was used to assemble the Tat-friendly, ELL2/AFF1-containing SECs that efficiently promoted latency reversal in the absence of AFF4.

Given the demonstration that ELL1 and ELL2 possess similar activities in stimulating transcriptional elongation *in vitro* (93), it is intriguing that the two proteins displayed non-redundant functions during HIV-1 latency reversal. To determine the underlying mechanism, we replaced the N-terminal transactivation domain of ELL1 (aa 1-291) with the corresponding region in ELL2 (aa 1-290) and determined the abilities of the overexpressed WT and engineered ELL1 protein (E2N-E1C-F) to promote the exit of HIV provirus from latency in the ELL2 KO-2D10 cells (Fig. 2-4D). While WT ELL1 was largely inactive in this assay, the presence of the N-terminal domain of ELL2 dramatically enhanced the ability of the engineered ELL1 to reverse viral latency to a level similar to that caused by WT ELL2 (compare Fig. 2-4A and 2-4D). This result suggests that the different abilities of the two ELL proteins to reverse latency can be attributed to their distinct N-terminal Pol II-binding domains.

ELL2 synergizes with AFF1 overexpression or BRD4 knockdown to reverse HIV-1 latency in the absence of any chemical inducers

Having observed that ELL2 played an exceptionally important role in promoting the exit of HIV from latency, we further explored the potential of using either ELL2 overexpression alone or in combination with other manipulations to reverse latency in the absence of any chemical inducers. Toward this goal, the ELL2 KO cell line was used as the basis to generate a series of stable lines expressing varying levels of ELL2-F as indicated by anti-ELL2 immunoblotting (Fig. 2-5A, bottom panel). While no ELL2 was detected in ΔE2-R1, the ELL2 levels in ΔE2-R2 and ΔE2-R3 cells were 1.3-, and 3.1-times higher than that of endogenous ELL2 in WT cells, respectively.

When these clones were analyzed by FACS, the expression of ELL2-F was found to increase the percentage of GFP(+) cells in each population in a dose-dependent manner (Fig. 2-5A). More importantly, the overexpressed ELL2-F alone in ΔE2-R3 cells was able to single-handedly produce 18% GFP(+) cells, again supporting the idea that ELL2 in WT Jurkat/2D10 cells is normally present in an amount or state that is inadequate for efficient HIV-1 transcription and latency reversal.

Previously, we and others have shown that the BET bromodomain protein BRD4 acts as a direct competitor of HIV-1 Tat for binding to P-TEFb/SEC and that the inactivation of BRD4 alleviates this inhibition to promote Tat-stimulation of HIV transcription and exit from latency (105,106,108,110). Consistent with these observations, the siRNA-mediated knockdown (KD) of BRD4 expression was found to strongly synergize with ELL2 overexpression to reverse HIV-1 latency in ΔE2-R3 cells [11% and 17% GFP(+) cells were caused by siBRD4 and ELL2 overexpression alone, respectively, versus 85% caused by the combination of the two; Fig. 2-5B].

Not only did the KD of BRD4, which resulted in more SECs that could be bound by Tat and thus amounted to an elevation of the effective SEC level in ΔE2-R3 cells, strongly promote the drug-free exit from latency, a similar effect was also produced by the direct overexpression of the SEC subunit AFF1-F but not AFF4-F in these cells (Fig. 2-5C and 2-5D). This latter result once again highlights the functional difference between the two AFF proteins in promoting the Tat/SEC-dependent latency reversal. Further analyses have shown that this functional difference can be traced to a single amino acid variation between AFF1 and AFF4. Compared to WT AFF1, AFF1 V67M, in which Val67 was replaced with the bulkier Met found at a homologous position (amino acid 62) in AFF4, lost the ability to reverse latency in ΔE2-R3 cells (Fig. 2-5E). In contrast, AFF4 M62V, which contains Val at position 62 instead of the normal Met, gained the ability and became much more effective than WT AFF4 in the assay.

We have recently shown that in HeLa cells, the above-mentioned reciprocal exchange of amino acids between AFF1 and AFF4 alters the abilities to these two proteins to promote Tat binding to P-TEFb/SEC and activation of HIV-1 transcription (122). The current study has further extended these observations into the Jurkat/2D10-based latency model by showing that the single amino acid difference between the two AFF proteins allows AFF1 but not AFF4 to strongly synergize with ELL2 to reverse latency in a Tat/SEC-dependent manner.

AFF1 is present in only a minor subset of SECs

We have recently reported that as structural scaffold, AFF1 and AFF4 nucleate the formation of separate SECs with largely non-overlapping functions in HeLa cells (122). However, the relative abundance of the AFF1- and AFF4-SECs inside a cell has not been determined and it is unclear whether the two AFF proteins assemble their SECs with a similar or different efficiency. To address this issue, we took advantage of the AFF1 and AFF4 KO cell lines ΔAFF1-sg1 and ΔAFF4-sg1 and performed anti-CDK9 immunoprecipitations (IP) in nuclear extracts and examined the association of a panel of signature SEC subunits with CDK9 by immunoblotting.

Surprisingly, other than causing an about 50% increase in the level of AFF4 bound to CDK9, the AFF1 KO produced little noticeable effect on CDK9's interactions with ELL1, ELL2, ENL, and AF9 (Fig. 2-6A). In contrast, the AFF4 KO greatly reduced the amounts of these SEC components associated with CDK9 but had no significant effect on the AFF1-CDK9 interaction (Fig. 2-6B). Although the amount of CDK9 sequestered in the total SEC population in ΔAFF4-sg1 cells was significantly decreased, the AFF4 KO had little impact on the ability of AFF1 to nucleate the assembly of the AFF1-SECs and thus selectively retain CDK9 in this sub-population (Fig. 2-6C). Together, these results suggest that in Jurkat/2D10 cells, AFF4 is the main scaffolding protein responsible for formation of the vast majority of the SECs, whereas AFF1 is assembled into only a minor subset of the total SEC population. Importantly, it is the latter subset of SECs that has been shown above to play a predominant role in supporting HIV-1 transactivation and escape from latency. Unlike AFF1/4, ELL2 does not play a structural role during SEC assembly (90,99). As expected, the ELL2 KO had no obvious effect on interactions of CDK9 with the remaining SEC subunits (Fig. 2-6D).

To investigate the contributions of AFF1 and AFF4 to SEC assembly in a different cell type, we repeated the above experiment in engineered HeLa cells, in which the expression of AFF1 or AFF4 had been stably knocked down (KD) by target-specific shRNAs (shAFF1 & shAFF4). The shRNA that targets GFP (shGFP) was used as a negative control. Very similar to the situations encountered in the Jurkat/2D10-based KO cells (Fig. 2-6A & 2-6B), the KD of AFF1 in HeLa cells had little effect on the interactions of ELL2, ENL, and AF9 with CDK9 when compared to the shGFP control, whereas the AFF4 KD drastically reduced these interactions (Fig. 2-6E). Thus, in HeLa cells, AFF4 was also used as the predominant scaffolding protein to assemble most of the SECs.

Despite the similarity between the two cell types, there were also obvious differences. First, unlike the AFF4 KO in Jurkat/2D10 cells that has led to a dramatic decrease in the level of the CDK9-bound ELL1 (Fig. 2-6B), the KD in HeLa cells actually elevated the ELL1 level in both the anti-CDK9 immunoprecipitates as well as the nuclear extract (NE) through an unknown mechanism (Fig. 2-6E). Secondly, the ELL2 level in HeLa NE was decreased markedly upon AFF4 KD (Fig. 2-6E), but only very slightly in Jurkat/2D10 cells after the AFF4 KO (Fig. 2-6B). This decrease could be due to the loss of AFF4's protection of ELL2 from the E3 ubiquitin ligase Siah1 (96). Apparently the degree of protection varied between the two cell types. Finally, the KD of AFF1 or AFF4 in HeLa cells significantly increased binding of CDK9 to the remaining non-targeted AFF paralog (Fig. 2-6E), suggesting the existence of a robust compensatory relationship between the two AFF proteins in this cell line. In comparison, a somewhat

weaker compensation was detected in the Jurkat/2D10-based AFF1/4 KO cells (Fig. 2-6A & 6B). Since AFF4 is the predominant scaffolding protein for SEC assembly, its ability to compensate for the lost AFF1 through increased binding to CDK9 may also partially explain why the interactions of CDK9 with several signature SEC components remained largely unaffected by either AFF1 KD or KO.

Discussion

P-TEFb is a component of the multi-subunit SECs, and recent studies indicate that it is not the isolated P-TEFb but rather a complete SEC that is recruited by Tat to the HIV-1 promoter for efficient transcriptional activation (90,91,122). Although P-TEFb has been extensively studied and recognized as a key host factor required for HIV-1 to escape latency (127,128), the contribution by the non-P-TEFb part of a SEC to this process has not been determined. Furthermore, since the SECs belong to a fairly large family of related complexes (121), it remains to be tested whether the SEC subtype that has been shown to be key for Tat-activation of HIV-1 transcription in HeLa cells (122) is also important for the HIV provirus to escape latency in CD4+ T cells. To address these questions, the present study employs the CRISPR-Cas9 system to knock out the genes encoding three key SEC subunits AFF1, AFF4 and ELL2 in 2D10 cells, a well-characterized Jurkat T cell-based HIV-1 latency model (119). Through this loss-of-function approach that is much more rigorous than the RNAi-mediated knockdowns performed previously, we show that latency reversal, regardless of whether it was drug-induced or occurred spontaneously, was unable to proceed in the absence of these non-P-TEFb SEC subunits.

Among the three SEC subunits analyzed in the current study, AFF1 and AFF4 are characterized as scaffolding proteins required for assembly of the AFF1- and AFF4-containing SECs, respectively (90,102). Our data indicate that these two subsets of SECs are differentially required for HIV-1 latency reversal depending on how the process was induced. For example, spontaneous, basal level latency reversal depended more on the AFF4-SECs, whereas the JQ1-induced process was much more sensitive to the loss of the AFF1-SECs (Fig. 2-2B & 2-2C). Mirroring these different requirements, the JQ1-induced HIV-1 transcriptional elongation was strongly inhibited by the KO of AFF1 but much less so by KO of AFF4 (Fig. 2-3C). In contrast, basal HIV-1 elongation was extremely sensitive to the depletion of the AFF4- but not AFF1-SECs (Fig. 2-3C).

A likely explanation for the strong dependence on the AFF4-SECs for basal, spontaneous HIV-1 latency reversal and elongation is that a cellular recruitment factor such as the Polymerase-Associated Factor complex (PAFc) (97) or/and the mediator complex is likely responsible for attracting a SEC to the viral promoter under these Tat-free conditions. Between the AFF1- and AFF4-SECs, the latter have been shown in the current study to be strongly predominant in vivo (Fig. 2-6). Moreover, PAFc and mediator are not known to prefer one subtype over the other. Because of these reasons, the KO of AFF4 is expected to exert a bigger impact than the KO of AFF1 at this stage when only an extremely low level of viral transcription is triggered. In contrast, when cells are treated with JQ1, which antagonizes the BRD4 inhibition of the Tat-CycT1 interaction thereby boosting Tat's ability to recruit a SEC to the paused Pol II at the viral

promoter (108), the AFF1-SECs are preferentially selected because the Tat-CycT1 binding is stronger in the presence of AFF1 than AFF4 (108,122). Thus, even though the AFF1-SECs represent a minor subset of the total SEC population in vivo, they are preferentially used in JQ1-treated cells and play an especially critical role in Tat-dependent HIV-1 latency reversal and transcriptional elongation.

In addition to AFF1/4, the SEC subunit ELL2 has also been shown to occupy an important place in activating latent proviruses. Because of the failure to obtain an ELL1 KO line, it is difficult to directly assess the role of ELL1 in controlling this process. However, several pieces of evidence suggest that as a SEC subunit, it may not be as effective as ELL2 in supporting HIV-1 transcriptional elongation and escape from latency. First, except for the observations made in prostratin-treated cells, ELL2 KO caused more than 50% of reduction in both HIV-1 transcriptional elongation and latency reversal under basal as well as drug (JQ1 or PMA)-induced conditions (Fig. 2-2 and Fig. 2-3C). In other words, the remaining ELL1-containing SECs in the ELL2 KO cells have provided less than half of the total SEC activity under these conditions. In addition, ELL1 failed to rescue the loss of ELL2 when it was expressed at about the same level as that of ELL2, indicating that it was less active than ELL2 in supporting spontaneous and JQ1-induced latency reversal (Fig. 2-4B & 2-4C). A weak complementation was observed only after ELL1 was expressed to a much higher level (Fig. 2-4A). Mechanistically, our domain swapping experiment (Fig. 2-4D) reveals that differences between the N-terminal Pol II-binding domains of ELL1 and ELL2 underlie the different activities of the two ELL proteins in HIV-1 latency reversal. Future studies are needed to determine how the ELL2 N-terminal domain may establish a more productive interaction with Pol II at the HIV-1 promoter to activate viral transcription and reverse latency.

Another important finding of the present study is that by merely increasing the level/activity of the ELL2/AFF1-containing SECs in Jurkat/2D10 cells, we were able to efficiently reverse HIV-1 latency without using any drugs (Fig. 2-5), suggesting that this subset of SECs is normally a rate-limiting factor for Tat-transactivation in these cells. Since the simple introduction of extra Tat protein alone without the matching host cofactors produces only limited effects in reversing latency (129,130), an array of human proteins has been discovered to activate HIV-1 proviruses to various degrees in latently infected cells once their expression is enhanced or silenced (reviewed in (45)). However, in most cases this has not been a very effective strategy except for the p65 (RelA) subunit of NF-κB. The Greene laboratory reported in 2006 that overexpression of p65 was able to activate over 80% of the latent proviruses in Jurkat-based J-Lat cells (56).

This level of activation is similar to what we have accomplished in the current study through overexpressing ELL2 and AFF1 together (65% latency reversal) or combining ELL2 overexpression with BRD4 KD (85%). Both strategies can increase the effective concentrations of the ELL2/AFF1-contaning SECs that are targeted by Tat for HIV-1 transactivation. Given the pleiotropic functions NF-κB especially in the immune system and unacceptable side-effects of its activating drugs PMA and prostratin, the NF-κB pathway may not be an ideal therapeutic target for latency reversal (131). In contrast, the SECs appear to only selectively regulate a minor fraction of genes (104). In our ongoing efforts to identify additional, more druggable targets to achieve robust latency reversal, the ELL2/AFF1-contaning SECs merit serious considerations because efficient

and complete reversal cannot proceed without these low-abundance, Tat-specific SECs and their interactions with Tat.

It is important to point out that the present conclusion about the predominant effects of the ELL2/AFF1-contaning SECs in HIV latency reversal has been made in activated CD4+ T cells. A vital difference between quiescent memory CD4+ T cells and activated T cells is that the former have extremely low levels of active P-TEFb (127). Thus, the overexpression of ELL2 and AFF1, if it is to be used in a future therapeutic approach to reverse HIV latency, should most likely be combined with additional manipulations (e.g. treatment with a cocktail of cytokines (132) or prostratin (133)) that can increase the nuclear concentration of active P-TEFb without completely activating T cells.

Table 2-1. CRISPR-Cas9 genome targeting statistics

Gene	Targeted exon[1]	Genotyping primer sequence[2]	sgRNA sequence	On-target score[3]	No. of clones sequenced[4]	No. of KO clones[5]
ELL2	1	GAGCGCCCGGATCGCCGTCT CGTCGGAAAGTCCCGCAG	GAGCGCCCGGATCGCCGTCT	91	2	2
AFF4	1	AAGTGTTTTGTTGGGGTGGGTT GGTGAAGTACCCGCCGATG	AGAACGGGAAAGGCGGAATC	83	9	5
			TGCGTATGAAAGAACGGGAA	81	6	2
AFF1	2	CCTGCAGATGAAAAGCTTCCAC GTGCCATTTTAACTCAATTCCCCTG	CCTTCTCTCTAATTCGAAGC	89	5	2
			AGAGAAGGAAAGACGCAACC	73	2	1
ELL1	1	ATATGCAACAACTTGGGGCG CAGCTTCCCCCTATCACGGT	TCGTGCGGGCGGGTTAGCGA	98	10	0
			TCTGGCGCGGTAGCTCTCGA	93	24	0

[1] Position of sgRNA targeted exon within the gene.

[2] Sequences of primer pairs used to amplify targeted genomic regions for Surveyor Assay® and Sanger sequencing.

[3] Faithful on-target score predicted based on http://crispr.mit.edu/.

[4] Number of cell clones sequenced.

[5] Number of cell clones identified with homozygous fame-shift mutations by sequencing.

Figure 2-1. Verification of Jurkat/2D10-based knockout cell lines in which the genes encoding three SEC subunits are disrupted by CRISPR-Cas9. Nucleotide and predicted amino acid sequences surrounding the intended Cas9 cleavage sites (arrows) in wild-type ELL2 (A), AFF4 (B) and AFF1 (C) genes as well as their mutant alleles generated by CRISPR-Cas9 are shown. Insertions of extra nucleotides are indicated by underlined lowercase letters, deletions by capital letters containing strikethroughs, and the omitted nucleotides marked by four consecutive dots (….). In the names of the AFF1 and AFF4 KO (ΔAFF1/4) clones, sg1 and sg2 refer to two independent clones obtained by using two separate sgRNA sequences targeting different regions of each gene locus. Premature stop codons as a result of frame-shift mutations are indicated by a star (*). The loss of protein expression from the disrupted genes in the various KO clones was confirmed by immunoblotting with the indicated antibodies.

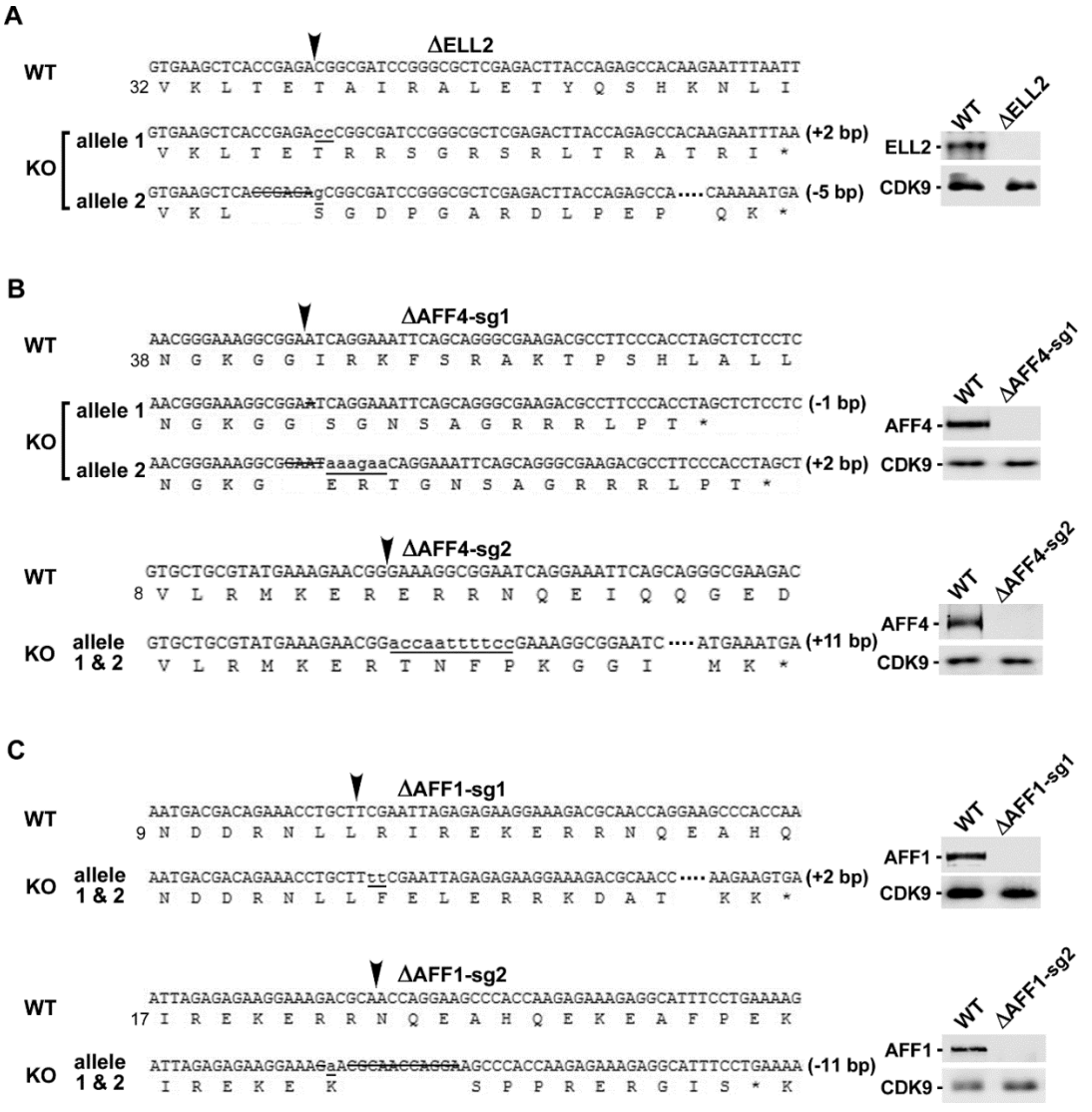

Figure 2-1

Figure 2-2. AFF1, AFF4 and ELL2 are differentially required by the various HIV-1 latency-reversing small molecules. A., B., C., D. & E. The indicated cell lines were exposed to the various agents labeled on top and then subjected to FACS analysis to determine the percentage of GFP(+) cells present in each cell population. WT: Wild-type Jurkat/2D10 cells. Representative FACS plots (A) and bar graphs (B-E) based on these and other plots were shown. Each column represents the average of three independent experiments, with the error bars indicating mean +/- standard deviation.

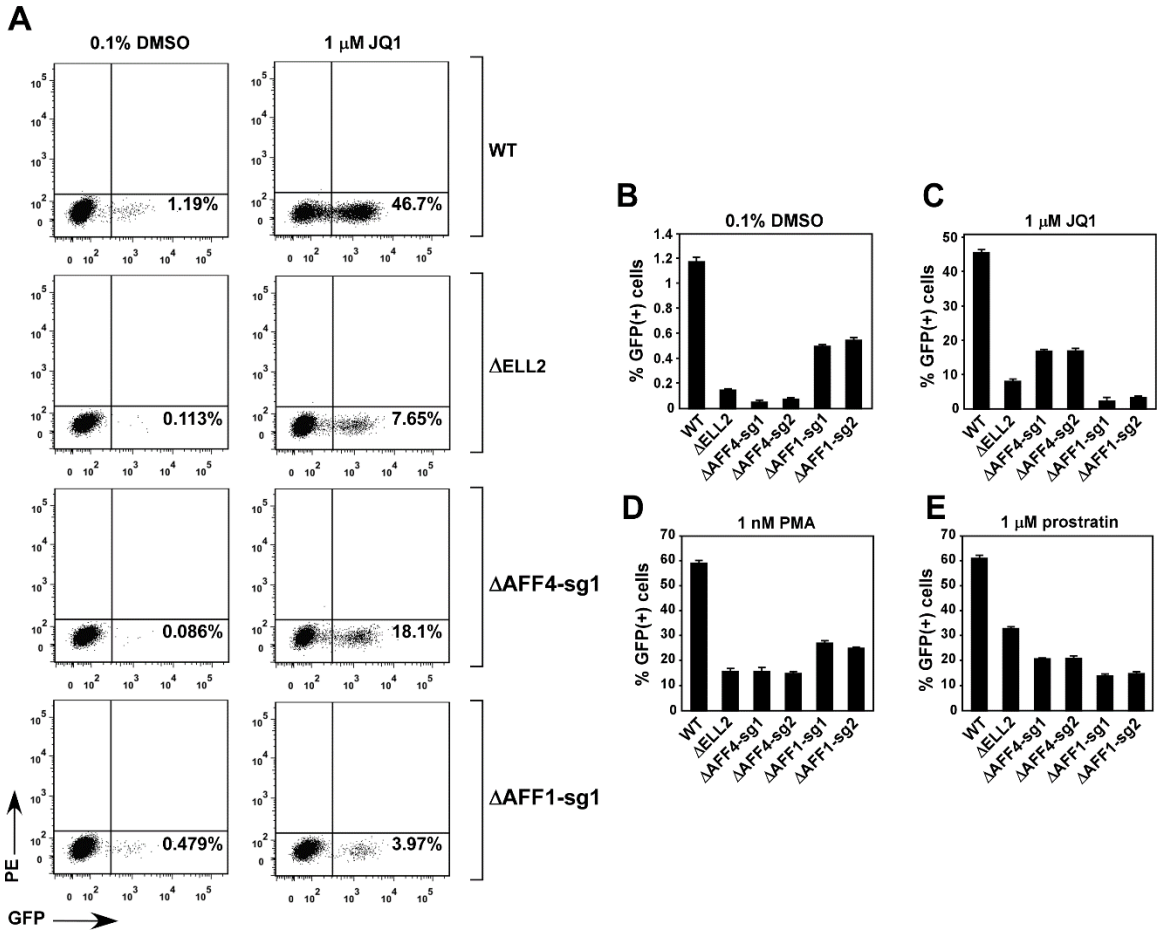

Figure 2-2

Figure 2-3. KO of SEC subunits suppresses latency reversal by inhibiting HIV-1 transcriptional elongation. A. A schematic diagram showing the various regions that make up the HIV-1 5' LTR and the positions of transcription start site (TSS) as well as the primer sets that were used in RT-qPCR reactions to quantify the short 59-nucloetide (nt) and long 190-nt HIV-1 transcripts. **B.** & **C.** RT-qPCR quantification of the short (B) and long (C) HIV-1 transcripts using the specific primers shown in A. The qPCR signals were normalized to that of GAPDH. Each column represents the average of three independent RT-qPCR measurements, with the error bars indicating mean +/- standard deviation.

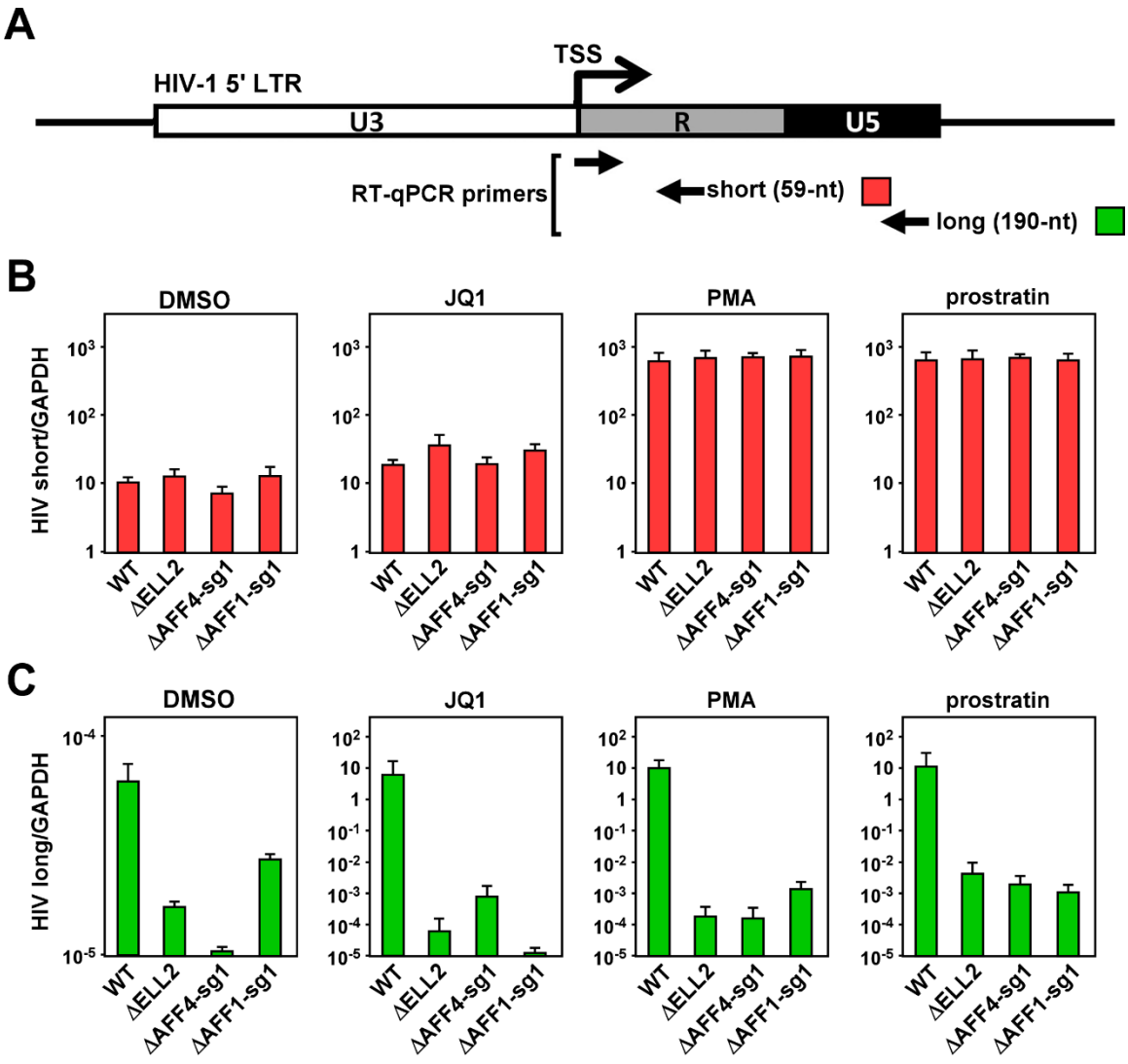

Figure 2-3

Figure 2-4. Restoration of HIV-1 latency reversal in SEC subunit-KO cell lines by reintroduction of the missing proteins or in some cases their functional homologues or an ELL2-ELL1 chimeric protein. A, B, C & D. Vectors expressing the indicated Flag-tagged SEC subunits (A-C) or the ELL2-ELL1 chimeric protein E2N-E1C-F (D) were nucleofected into WT Jurkat/2D10 cells or the various SEC subunit-KO cells derived from this cell line. Forty-eight hours later, the cells were either untreated (A, B & D) or treated with JQ1 for an additional 16 hours (C). The percentages of GFP(+) cells among the various cell populations were then determined by FACS and plotted in bar graphs, with the error bars representing mean +/- standard deviation from three independent measurements. The dashed lines mark the levels of latency activation achieved in WT cells containing an empty vector and are used as a reference. An aliquot of cells from each group was checked for levels of the indicated proteins by immunoblotting.

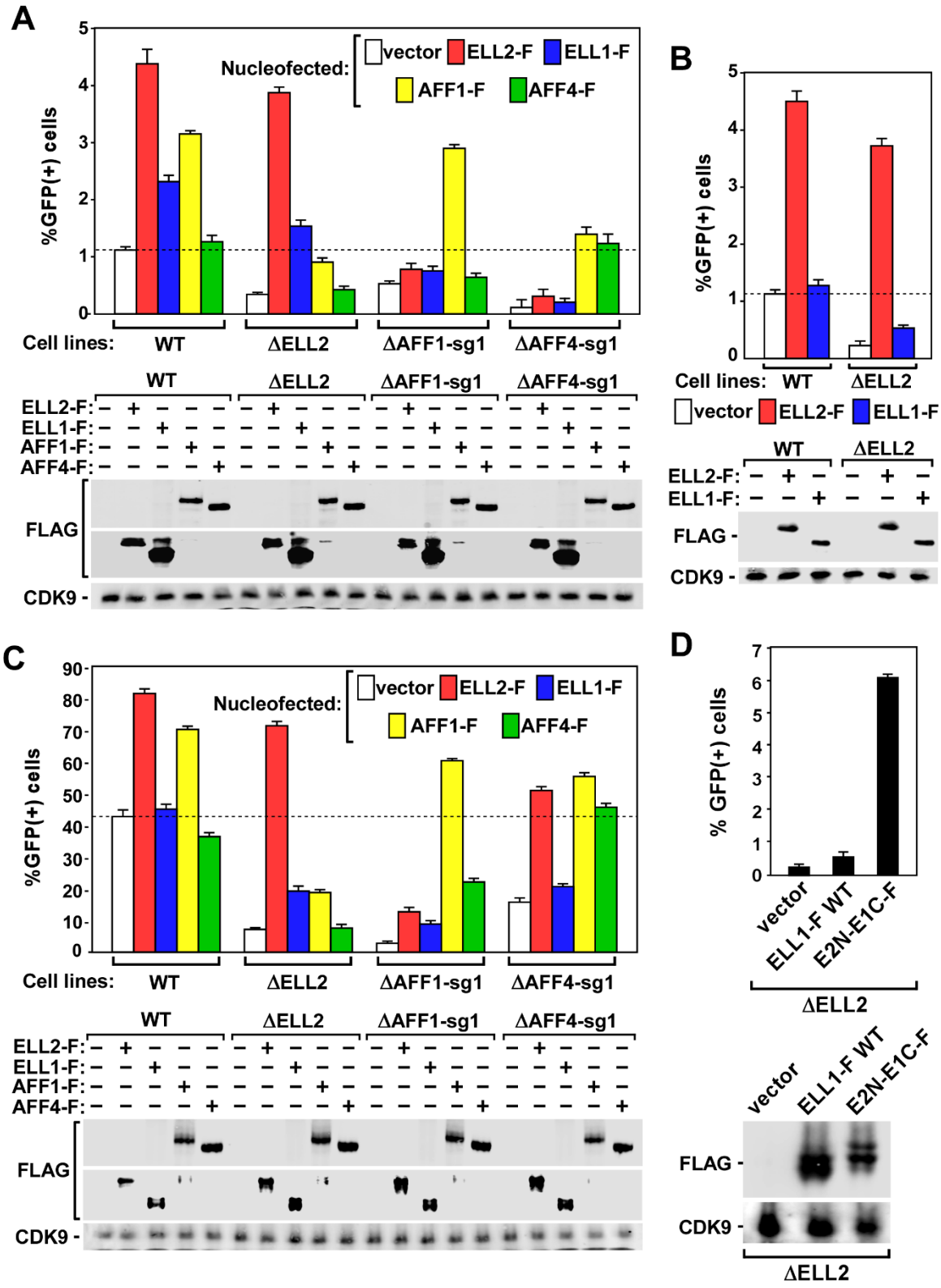
A
%GFP(+) cells
Nucleofected:
vector
ELL2-F
ELL1-F
AFF1-F
AFF4-F
Cell lines:
WT
ΔELL2
ΔAFF1-sg1
ΔAFF4-sg1
ELL2-F:
ELL1-F:
AFF1-F:
AFF4-F:
FLAG
CDK9
B
%GFP(+) cells
Cell lines:
WT
ΔELL2
vector
ELL2-F
ELL1-F
ELL2-F:
ELL1-F:
FLAG
CDK9
C
%GFP(+) cells
Nucleofected:
vector
ELL2-F
ELL1-F
AFF1-F
AFF4-F
Cell lines:
WT
ΔELL2
ΔAFF1-sg1
ΔAFF4-sg1
ELL2-F:
ELL1-F:
AFF1-F:
AFF4-F:
FLAG
CDK9
D
% GFP(+) cells
vector
ELL1-F WT
E2N-E1C-F
ΔELL2
vector
ELL1-F WT
E2N-E1C-F
FLAG
CDK9
ΔELL2

Figure 2-4

Figure 2-5. ELL2 synergizes with AFF1 overexpression or BRD4 knockdown to promote drug-free HIV-1 latency reversal. A. An ELL2-F expression vector was stably introduced into the ELL2 KO (ΔELL2) cells. Three independent clones (ΔE2-R1, 2 & 3) expressing different amounts of ELL2-F were selected based on anti-ELL2 immunoblotting (bottom) and examined for the percentages of GFP(+) cells by FACS analysis (top). **B.** ΔELL2 and ΔE2-R3 cells were nucleofected with either the BRD4-specific siRNA (siBRD4) or a control non-target siRNA (siNT) and examined by immunoblotting for the presence in cell lysates of the indicated proteins (bottom) and by FACS for the percentages of GFP(+) cells (top). **C.** & **D.** ΔELL2 and ΔE2-R3 were nucleofected with plasmids expressing nothing (-), AFF1-F (C), or AFF4-F (D) and then analyzed as in B. **E.** ΔE2-R3 cells were nucleofected with either an empty vector or plasmids expressing the indicated AFF1/4 proteins and then analyzed as in B.

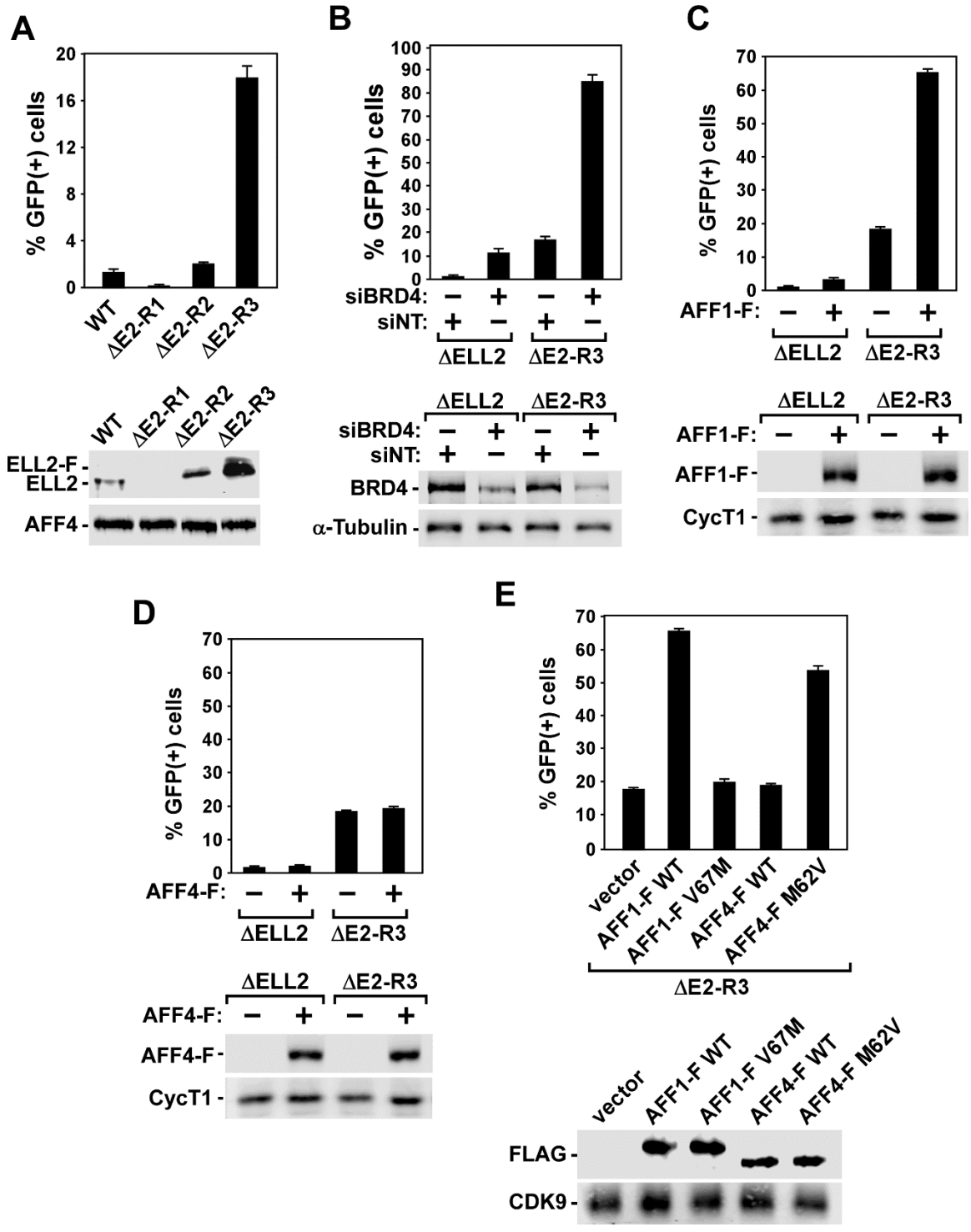
A
% GFP(+) cells
WT
ΔE2-R1
ΔE2-R2
ΔE2-R3
ELL2-F
ELL2
AFF4
B
% GFP(+) cells
siBRD4:
siNT:
ΔELL2
ΔE2-R3
BRD4
α-Tubulin
C
% GFP(+) cells
AFF1-F:
ΔELL2
ΔE2-R3
AFF1-F
CycT1
D
% GFP(+) cells
AFF4-F:
ΔELL2
ΔE2-R3
AFF4-F
CycT1
E
% GFP(+) cells
vector
AFF1-F WT
AFF1-F V67M
AFF4-F WT
AFF4-F M62V
ΔE2-R3
FLAG
CDK9

Figure 2-5

Figure 2-6. AFF1 is present in only a minor subset of SECs. A., B., C., & D. Nuclear extracts (NE) were prepared from wild-type (WT) Jurkat/2D10 cells or the Jurkat/2D10-based AFF1 KO (ΔAFF1-sg1, A), AFF4 KO (ΔAFF4-sg1, B & C), and ELL2 KO (ΔELL2, D) cells and subjected to immunoprecipitation (IP) with the specific anti-CDK9 (A, B, & D) or anti-AFF1 (C) antibody or non-specific, normal IgG as a control (ctl.). The immunoprecipitates were examined by immunoblotting for presence of the various proteins labeled on the left. **E.** NE from HeLa cells stably expressing the indicated shRNAs or nothing (-) were subjected to the same IP-immunoblotting analysis as in A.

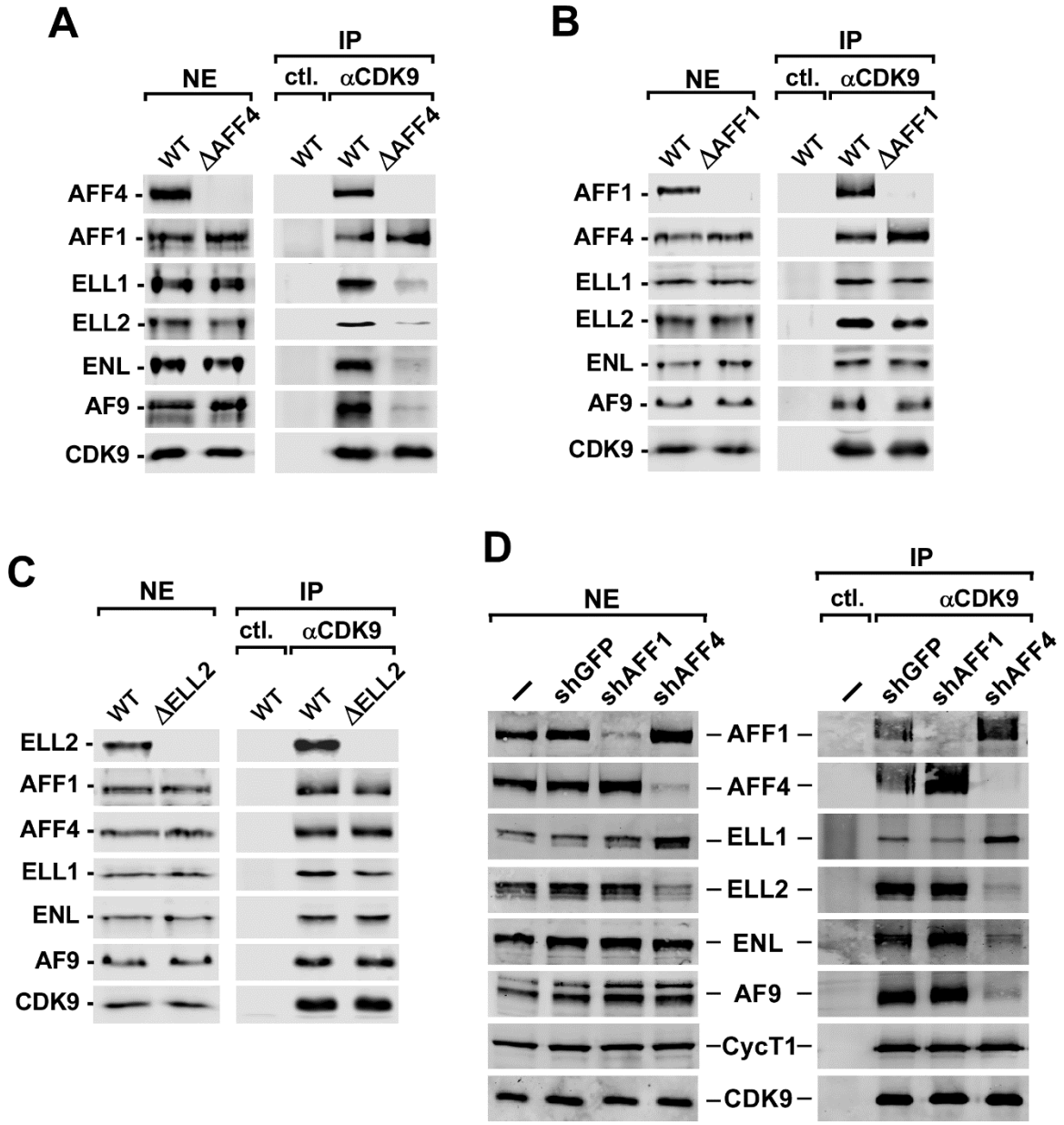

Figure 2-6

Chapter 3

The KAT5-Acetyl-Histone4-Brd4 axis silences HIV-1 transcription and promotes viral latency

(This work was originally published in *PLOS pathogens* as: Li, Z., Mbonye, U., Feng, Z., Wang, X., Gao, X., Karn, J., & Zhou, Q. (2018). The KAT5-Acetyl-Histone4-Brd4 axis silences HIV-1 transcription and promotes viral latency. *PLOS pathogens*, 14(4), e1007012.)

Summary

The bromodomain protein Brd4 promotes HIV-1 latency by competitively inhibiting P-TEFb-mediated transcription induced by the virus-encoded Tat protein. Brd4 is recruited to the HIV LTR by interactions with acetyl-histones3 (AcH3) and AcH4. However, the precise modification pattern that it reads and the writer for generating this pattern are unknown. By examining a pool of latently infected proviruses with diverse integration sites, we found that the LTR characteristically has low AcH3 but high AcH4 content. This unusual acetylation profile attracts Brd4 to suppress the interaction of Tat with the host super elongation complex (SEC) that is essential for productive HIV transcription and latency reversal. KAT5 (lysine acetyltransferase 5), but not its paralogs KAT7 and KAT8, is found to promote HIV latency through acetylating H4 on the provirus. Antagonizing KAT5 removes AcH4 and Brd4 from the LTR, enhances the SEC loading, and reverses as well as delays, the establishment of latency. The pro-latency effect of KAT5 is confirmed in a primary CD4+ T cell latency model as well as cells from ART-treated patients. Our data thus indicate the KAT5-AcH4-Brd4 axis as a key regulator of latency and a potential therapeutic target to reactivate latent HIV reservoirs for eradication.

Introduction

The recent development of novel immunotherapeutic agents such as the bispecific dual-affinity retargeting (DART) antibodies that can engage a bound cytotoxic T cell to destroy an HIV-infected cell through recognizing the viral envelope proteins on the latter's surface has fueled new optimism for finding a cure for HIV/AIDS(134). However, a major impediment to the cure effort is the latent viral reservoirs in long-lived CD4+ T cells that do not express any HIV protein/RNA, and thus cannot be recognized either by DART or by the host immune system(135).

HIV latency is the result of silenced proviral transcription due to multiple complementary mechanisms(53). To expose the latent reservoirs for accelerated clearance, numerous "latency-reversing agents" (LRAs) have been identified that target specific stages of the HIV transcription cycle(45). However, extensive *ex vivo* studies suggest that individual LRAs are not very potent and that combinations of LRAs will be required to effectively purge the latent reservoirs(120). Among the successful combinatorial *ex vivo* trials, inhibition of the BET bromodomain protein Brd4 with JQ1 strongly synergized with other LRAs to reverse viral latency(111,136). Although these *ex vivo* studies provide an important proof of concept, the available LRAs are either highly toxic or yet to be proven efficacious in clinical settings(53). Thus, better and safer LRAs are urgently needed.

Brd4 is known to use its two bromodomains to bind to acetylated histones H3 and H4 (AcH3 and AcH4) (137) and its C-terminal PID (P-TEFb-interacting domain) to recruit the human positive transcription elongation factor b (P-TEFb) to chromatin(105,138) to promote transcription of cellular primary response genes(139). Counterintuitively, during activation of HIV transcription by the viral-encoded Tat protein, Brd4 acts as a potent inhibitor(105,106). This is because Brd4, which is highly abundant *in vivo*, can directly compete with Tat for binding to the limited cellular supply of P-TEFb(105,106), the protein kinase that is an integral component of the multi-subunit Super Elongation Complex (SEC) used by Tat as a host cofactor for HIV transactivation(90,91). By removing Brd4 from the HIV long terminal repeat (LTR), JQ1 and other bromodomain inhibitors have been shown to reverse HIV latency by promoting the Tat-SEC formation, and consequently, Tat-transactivation(108,110). Antagonizing the Tat-SEC complex may not be the only way that Brd4 controls HIV latency. A recent study has shown that the short isoform of Brd4 (Brd4S) that lacks the PID can instead recruit the repressive SWI/SNF chromatin-remodeling complexes onto the latent HIV-1 promoter to repress transcription(140).

Given that targeting Brd4 can be a very effective strategy to purge latent HIV reservoirs(111,136), it is important to identify the prevailing histone acetylation pattern that allows Brd4 to be recruited and persistent on the HIV provirus. Knowing the exact Brd4 target on HIV chromatin and how it is created during latency establishment may help us devise more specific and efficient methods to displace Brd4 from the LTR for latency reversal. This will also help resolve the paradox that histone acetylation, which is typically associated with relaxed chromatin structure and HIV transactivation(141), can be used to attract Brd4 to silence proviral transcription. We therefore examined the status of AcH3 and AcH4 present on the LTR of a pool of latent HIV proviruses that had diverse integration sites. Our data indicate that upon entering latency, these proviruses displayed elevated levels of AcH4 and Brd4 but drastically reduced levels of AcH3 on

their LTR, raising the possibility that AcH4 is the primary histone modification responsible for attracting and retaining Brd4 on the silenced proviruses.

Three major histone acetyltransferases (HATs) are known to modify H4: KAT5 (Tip60) is known to acetylate lysines 5, 8, 12 and 16(142); KAT7 targets three out of the four positions; and KAT8 (MOF) modifies lysine16 exclusively(143). Our data indicate that downregulating the expression or activity of KAT5, but not KAT7 and KAT8, removed AcH4 and Brd4 from the HIV LTR, leading to the enhanced SEC loading, Tat-transactivation and escape from latency. Consistent with these results, our data further show that silencing KAT5 interfered with the establishment of latency. Together, these results have demonstrated a critical role for KAT5 and its acetylation of H4 in promoting Brd4's recruitment to the HIV LTR and establishment of latency. Furthermore, they reveal that inhibiting the KAT5-AcH4-Brd4 axis is potentially an effective strategy for activating the latent proviruses for subsequent eradication.

Experimental Procedures

CRISPRi-induced downregulation of KAT5, KAT7 and KAT8

To downregulate KAT5, KAT7 and KAT8 in Jurkat 2D10 cells (previously generated by Karn lab based on human CD4+ T cells Jurkat line (119)), vectors pHR-TRE3G-Krab-dCas9-P2A-mCherry(144) and pLVX-advanced-TetOn (gift from IGI, UC Berkeley) were packaged separately using a 3rd generation lentiviral packaging system and co-infected into Jurkat 2D10 cells. A clone (2D10-iI) expressing Krab-dCas9-HA-P2A-mCherry in response to doxycycline (Dox) treatment was picked by FACS, and verified by Western blot. DNA oligos containing sgKAT5#1 (sg1; 5'-GACTCAGTAGACCGCCAC-3'), sgKAT5#2 (sg2; 5'-GCCTCAGGCCGAGCCCTAGG-3'), sgKAT7#1 (sg1; 5'-GTGTATCAGTCCCAATCCTG-3'), sgKAT7#2 (sg2; 5'-GGGATCGTCCGCAGGATT-3'), and sgKAT8 (5'-GAGAGACGCGGCCCGGGGAT-3') were synthesized and cloned separately into the pSico-BFP-puro vector(144), which was then packaged and transduced into the 2D10-iI cells. After 1 μg/ml puromycin selection for 4 days, the stable CRISPRi-KAT5-sg1, CRISPRi-KAT5-sg2, CRISPRi-KAT7-sg1, CRISPRi-KAT7-sg2, and CRISPRi-KAT8 cell pools were treated with 1 μg/ml Dox for 72 hours and checked by RT-qPCR and Western blot with KAT5 (Invitrogen), KAT7 (Bethyl) and KAT8 antibodies (Invitrogen) for CRISPRi efficiency.

Reverse transcription and real-time PCR (RT-qPCR) assay

Total RNA from ~5×10^6 cells were extracted by RNeasy kit (Qiagen) and reverse transcribed using the M-MLV Reverse Transcriptase (VWR) with random hexamers (Invitrogen). The cDNAs were subjected to qPCR using a DyNAmo HS SYBR Green qPCR kit (Fisher) on a CFX96 machine (Bio-Rad) with the following primers: qKAT5-F (5'-AACCAGGACAACGAAGATGAG-3'), qKAT5-R (5'-GTCACCCATTCATCCAGACG-3'); qKAT7-F (5'-AGCCCTTCCTGTTCTATGTTATG-3'), qKAT7-R (5'-CATAGCCCTGTCTCATGTACTG-3'), qKAT8-F (5'-GGGAAAGAGATCTACCGCAAG-3'), qKAT8-R (5'-TCCACGTCAAAGTACAGTGTC-3'); qActB-F (5'-AGAGCTACGAGCTGCCTGAC-3'), qActB-R (5'-AGCACTGTGTTGGCGTACAG-3'); qLTR-F (5'-GGGTCTCTCTGGTTAGACCAG-3'), qLTR-59R (5'-

GGGTTCCCTAGTTAGCCAGAG-3'), qLTR-190R (5'-CTGCTAGAGATTTTCCACACTGAC-3'); qMYC-F (5'-TTCGGGTAGTGGAAAACCAG-3'), qMYC-R (5'-AGTAGAAATACGGCTGCACC-3'); qFOS-F (5'-TTGTGAAGACCATGACAGGAG-3'), qFOS-R (5'-CCATCTTATTCCTTTCCCTTCGG-3'); qJUNB-F (5'-AGCCCAAACTAACCTCACG-3'), qJUNB-R (5'-GGGCATCGTCATAGAAGGTC-3'). All reactions were carried out in triplicates. The PCR signals were normalized to those of ActB and displayed.

Cell line-based latency reversal assay

The CRISPRi-KAT5-sg1/sg2, CRISPRi-KAT8, or parental Jurkat 2D10 cells were first treated with the various LRAs or MG-149 (APExBIO) at the indicated concentrations for 20 hr, and then subjected to flow cytometry on a BD Bioscience LSR Fortessa X20 cytometer for GFP fluorescence. The data were analyzed using Flowjo™ software. Each drug treatment was done in 200 μl RMPI medium (Invitrogen) with 10% FBS (Gemini 900108 Lot A96C). To induce CRISPRi-mediated downregulation of KAT5 or KAT8, the CRISPRi-KAT5-sg1/sg2, CRISPRi-KAT8 cells were pre-treated for 48 hr with 1 μg/ml Dox before the LRA treatments. For control groups, 0.1% DMSO was used.

Generation of latently infected quiescent Th17 primary T cells

Naïve CD4+ T cells isolated from a previously frozen healthy donor leukapheresis pack (previously generated by Karn lab(145)) by negative selection using the EasySep™ Naïve CD4 T-cell isolation kit (19155RF; Stem Cell) were simultaneously treated with T-cell receptor activator magnetic beads and a Th17 polarization cytokine cocktail for 6 days as previously described(145). On Day 4, IL-2 was added to the cells at 60 IU/ml. Following Th17 polarization and during T-cell expansion, cells were either infected or not with a VSVG-pseudotyped pHR'-Nef+-CD8a/GFP viral construct by spinoculation. HIV-infected cells were later positively selected for by anti-CD8a magnetic separation. To generate quiescent T cells, infected cell populations were cultured in medium containing reduced concentrations of IL-2 (15 IU/ml) and IL-23 (12.5 μg/ml) for at least 2 weeks. Proviral latency was monitored by assessing for the expression of Nef and gp120 Env by immunofluorescence flow cytometry before and after T-cell receptor reactivation for 18 hr. Achievement of resting T cells was monitored by immunostaining for Ki67, cyclin D3, and pSer175 CDK9 under the same conditions.

Flow cytometry analysis of proviral reactivation in latently infected primary T cells

Primary resting Th17 cells, latently infected with HIV as described above, were pretreated or not for 30 min with MG-149 at varying concentrations (10 or 50 μM) prior to 24 or 48 hr challenge with either of the following stimuli: T-cell receptor activator anti-CD3/anti-CD28 antibody cocktail, JQ1 (at 1 μM or 5 μM), SAHA (500 nM), or ingenol (20 nM). Cells were washed once with 1X PBS and fixed in 4% formaldehyde for 15 min at room temperature prior to permeabilization with 1X BD Perm/Wash buffer (BD Biosciences). After blocking with a non-specific IgG for 15 min, cells were immunofluorescently stained for HIV Nef. Thereafter, these cells were washed three times with 1X permeabilization buffer and subjected to flow cytometry analysis using the LSR Fortessa instrument (BD Biosciences) equipped with the appropriate laser and filters.

Western blotting analysis of MG-149's effect on AcH4 levels in primary T cells

Approximately 2.4×10^7 memory CD4+ T cells were isolated by negative selection from a healthy donor leukapheresis pack containing 1.5×10^8 PBMCs.

Following the isolation, cells were allowed to recover overnight in 10 ml complete RPMI media supplemented with 60 IU/ml IL-2 and 1 mM SAHA and then divided equally into a 24-well plate and treated with varying concentrations of MG-149 for 24 hr. Whole cell extracts were mixed with 50 ml of a 2X SDS-PAGE sample buffer prior to microtip sonication to mechanically shear viscous DNA. Thereafter, the samples were boiled at 95 ℃ for 10 min and subjected to SDS-PAGE and immunoblotting analysis for N-terminally acetylated histone H4, total histone H4, and N-terminally acetylated histone H3. Densitometry analysis was performed using Quantity One software (Bio-Rad).

Measurement of HIV-1 mRNA in culture supernatants of primary cells from ART-treated patients

This part of the study has been approved by the Bioethics Review Committee of the Shenzhen Center for Disease Control and Prevention in China. All research participants gave written informed consent, and all subject data and specimens were coded to protect confidentiality. HIV-1–infected individuals enrolled in the study were based on the criteria of good response to suppressive ART and undetectable plasma HIV-1 RNA levels. The PBMCs from the $EDTA^+$ blood were isolated by Ficoll centrifugation. Approximately 10×10^6 PBMCs were cultured in 2 ml RPMI1640 medium containing 10% FBS. The cells were then treated with 0.2% DMSO, 50 ng PMA + 1 μM Ionomycin (PMA/I) as a positive control, 50 μM MG-149, 2 μM JQ1, or 50 μM MG-149 + 2 μM JQ1 for 24 hr. After spinning down the cells, supernatants (1 ml each) were collected and subjected to HIV-1 RNA quantification with the Roche COBAS® AmpliPrep/TaqMan® HIV-1 Qualitative Test system. Each sample was tested twice, and the average viral copy numbers were normalized to the DMSO group and displayed in a scatter plot.

Stable shRNA knockdown (KD) of KAT5 in Jurkat-based cells

The Jurkat 1G5(146) and 1G5+Tat cells(147) (both kind gifts from Melanie Ott lab, Gladstone Institutes, San Francisco) were infected with the pLKO.1-puro-based lentiviral vector containing shScramble 5'-CCTAAGGTTAAGTCGCCCTCG-3', or shKAT5 5'-CCTTGACCATAAGACACTGTA-3' sequences. Two days after infection, the cells were selected by 1 μg/ml puromycin for 5 days until the stable pools were obtained. The KD efficiencies of the pools were examined by Western blot.

Luciferase reporter assay

Two days before the assay, HEK 293T cells (from American Type Culture Collection) at ~60% confluency in 6-well plates were transfected using Polyethylenimine in triplicates by 0.1 μg HIV-1 LTR-luciferase construct combined with 1.85 μg pcDNA3-FLAG-KAT5(148) and/or 0.05 μg pRK5-Tat-HA. The total amount of DNA in each transfection was brought to 2 μg by empty pcDNA3 vector when necessary. For luciferase assays in WT Jurkat 1G5 or 1G5+Tat cells, 1 ml cells at the concentration of 0.5 million/ml were aliquoted into 12-well plates in triplicates and treated with the indicated concentrations of MG-149 for 18 hr. For luciferase assays in 1G5-/+Tat stable shRNA cell pools, the cells were counted on a haemocytometer and about 1.7 million cells from each pool were aliquoted in triplicates. The cells were harvested and lysed in 200 μl 1 × Reporter Lysis Buffer (Promega), and centrifuged at maximum speed on a benchtop centrifuge for 30 seconds. The supernatants were subjected to luciferase activity measurement by using the Luciferase Assay System (Promega) on a Lumat LB 9501 luminometer. For each group, 10 μl cell lysate was aliquoted before centrifugation from each repeat and pooled for Western blots to check the indicated protein levels.

Chromatin immunoprecipitation (ChIP) assay

The assay was based on Nelson *et al.*(149) with some modifications. Briefly, 10 million cells were fixed by 1% formaldehyde for 10 min at room temperature, and then quenched for 5 min by adding glycine to 125 mM final concentration. After washing with PBS and lysed in the IP buffer(149), the chromatin was sheared using the Covaris™ S220 System with 200 Watt peak energy for 30 cycles (30 sec ON, 20 sec OFF) to an average size of 0.5–1 kb DNA fragments. The sheared chromatin was centrifuged at 20,800 × g for 10 min at 4 ℃. Each ChIP reaction was carried out with 300 μl supernatant and 1 μg each of the following antibodies: anti-Ac-H3 (Millipore, 06-599), anti-Ac-H4 (Millipore, 06-598), anti-H3 (Invitrogen, PA5-31954), anti-H4 (Invitrogen, 720166), anti-FLAG (Sigma, F1804), anti-Brd4 (105), normal rabbit total IgG (Santa Cruz, sc-2027), and normal mouse total IgG (Santa Cruz, sc-2025). After overnight incubation with rotation at 4 ℃, the reactions were centrifuged at 20,800 × g for 10 min, and 90% of each supernatant was combined with 20 μl Salmon sperm DNA (Invitrogen)-blocked Protein A Agarose (Invitrogen). After 45 min rotation, the beads were washed 6 times with 1 ml IP buffer and DNA fragments were extracted by boiling in Chelex (Bio-Rad). qPCRs were carried out with the following primers:
HIV-nuc1-F (5'-CTGGGAGCTCTCTGGCTAACTA-3'),
HIV-nuc1-R (5'-TTACCAGAGTCACACAACAGACG-3');
HIV-env-F (5'-TGAGGGACAATTGGAGAAGTGA-3'),
HIV-env-R (5'-TCTGCACCACTCTTCTCTTTGC-3');
MYC-C-F (5’-GCGCGCCCATTAATACCCTTCTTT-3’),
MYC-C-R: (5’-ATAAATCATCGCAGGCGGAACAGC-3’);
IκBα 5’end-F (5'-AAGAAGGAGCGGCTACTGGAC-3'),
IκBα 5’end -R (5'-TCCTTGACCATCTGCTCGTACT-3');
HERVK-LTR-F (5'-GGGCAGCAATACTGCTTTGT-3'),
HERVK-LTR-R (5'-CAATAGTGGGGAGAGGGTCA-3');
intergenic-F (5'-CTCCCAAATTGCTGGGATTA-3'),
intergenic-R (5'-ATTCCAGGCACCACAAAAAG-3').

For ChIP in NH1 cells (previously generated by Zhou lab based on human HeLa cell line (85)) containing an integrated HIV-1 LTR-luciferase reporter construct, the cells seeded in 6-well plates were first transfected in duplicate by either 2 μg empty vector or pCMV2-based vectors containing N-terminally FLAG-tagged Brd4 long isoform (Brd4L, isoform A, amino acids [aa] 1–1,362), or Brd4 short isoform (Brd4S, isoform C, aa 1–722). Both Brd4 vectors were kind gifts from Melanie Ott lab (Gladstone Institutes, San Francisco, (150)). 31 hours after transfection, DMSO or MG-149 were added to the medium to the final concentrations of 0.1% and 30 μM respectively. After 18 hr of drug treatment, about 10^6 cells/well were subjected to ChIP as described above. The ChIP was conducted using anti-FLAG beads (Sigma, A2220), and the qPCRs were carried out with the following primers: LTRS-1 (5’-GTTAGACCAGATCTGAGCCT-3’), and LTRS-2 (5’-GTGGGTTCCCTAGTTAGCCA-3’).

Signals obtained by qPCR were normalized to those of input DNA, and the averages from triplicated qPCR reactions were shown with the error bars representing standard deviations. Two-tailed Student's *t*-tests were conducted and the different significance levels were marked by 1 to 3 asterisks.

HIV-1 latency establishment assay

The HIV-1 infection and progressive latency establishment assay were based on Pearson *et al.*(119) with some modifications. Briefly, HIV-1 virions were produced by transfecting HEK 293T cells with the wild-type pHR'-p-d2EGFP plasmid(119) using a 3rd generation lentiviral packaging system and then used to spin-infect wild-type Jurkat (from American Type Culture Collection) or Jurkat pools expressing the indicted shRNAs in the presence of 6 μg/ml polybrene (Santa Cruz). Two days post infection (d.p.i.), GFP(+) cells (of the HIV-infected Jurkat cells described above) were enriched by flow cytometry and allowed to propagate in culture. The percentages of GFP(+) cells in this population (called the total pool in Fig. 3-1) were monitored continuously until the indicated d.p.i. On 29 d.p.i., a population of GFP(-) cells were enriched by flow cytometry from the original GFP(+) cells selected on 2 d.p.i. and maintained as the latent pool in Fig. 3-1. On 43 d.p.i., the latent pool was subjected to latency reversal assays as described above with the indicated concentrations of LRAs, and both the total and latent pools were subjected to Western blots and ChIP assays for the indicated proteins.

Results

Silenced HIV proviruses contain elevated amounts of AcH4 and Brd4 but drastically decreased levels of AcH3

Given the importance of Brd4 in modulating HIV latency, we determined the precise histone acetylation pattern on the viral LTR, which is targeted by Brd4 to sequester P-TEFb away from the Tat-SEC complex. Toward this goal, we first examined the levels of AcH3 and AcH4 on the LTR of latent HIV proviruses.

The original observations indicating the importance of Brd4 in HIV latency were made by using isolated clones of Jurkat T cells (e.g. the J-Lat cell lines and the 2D10 system(106,108)) that contain only a single viral integration site within each cell population. To rule out site-specific integration effects, we created a pool of latently infected cells that contain a diverse array of all possible integration sites. This was achieved by adapting a protocol from Pearson *et al.* (119) to progressively establish HIV latency in Jurkat cells that were first infected on day 0 with a GFP-encoding HIV virus (Fig. 3-1A). The freshly infected cells containing actively replicating HIV were then sorted by fluorescence-activated cell sorting (FACS) on day 2 into a GFP(+) population, which was then cultured for additional 6 weeks (Fig. 3-1A). This population of cells, called the total pool, was examined for the percentages of GFP(+) cells on various days post infection (d.p.i.). The results showed that on 43 d.p.i., 95.3% of the cells still remained GFP(+), while the rest have reverted to the GFP(-) state (Fig. 3-1B and 3-1C).

To enrich the latently infected cells, a portion of the GFP(+) cells that was originally isolated by FACS on 2 d.p.i. was subjected to sorting again on 29 d.p.i. to isolate the GFP(-) cells, which were then allowed to propagate until 43 d.p.i. (Fig. 3-1A). This population, called the latent pool, had 89.8% of cells that remained GFP(-) on 43 d.p.i., while the rest had undergone spontaneous reactivation to become GFP(+) again (Fig. 3-1C). It is important to point out that the HIV proviruses in the latent pool could readily be reactivated by conventional LRAs such as JQ1 and prostratin, demonstrating that the pool retained transcriptionally functional proviruses (Fig. 3-1D).

Western analysis of cell lysates indicates no major difference in the overall levels of AcH3, AcH4, total H3 and total H4 between the total and latent pools (Fig. 3-1E). However, examination by chromatin immunoprecipitation (ChIP) demonstrates a 2 to 3-

fold increase in the levels of total H3 and H4 on the HIV LTR in the latent pool compared to the total pool (Fig. 3-1F). This is consistent with the previous finding that the latent, transcriptionally silent HIV proviruses are more likely to be occupied by nucleosome 1 (nuc-1) situated immediately downstream of the transcription start site(151). Despite the increased total H3 level on the viral LTR in the latent pool, the acetylation of H3 decreased by 2-fold (Fig. 3-1F). This observation agrees with the general view that deacetylated H3 provides a marker for repressed and compact chromatin structure(152) as well as the result obtained previously using the Jurkat 2D10 cells, a widely used post-integrative HIV latency model(119).

In contrast to AcH3, the AcH4 level on the LTR increased when the pool of proviruses entered latency (Fig. 3-1F). In fact, AcH4 increased at about the same extent as total H4 during this process. Similarly, more Brd4 was found on the LTR in the latent pool than in the total pool (Fig. 3-1F), likely due to the increased AcH4 level. Collectively, these data indicate that during the establishment of HIV latency, the incoming nucleosomes assembled on the viral LTR had very low AcH3 content, but maintained a high AcH4 level, which in turn increased the recruitment of Brd4 to inhibit HIV gene expression.

Antagonizing KAT5 reverses HIV latency and potentiates conventional LRAs

Previously, it has been reported that Brd4 recognizes both AcH3 and AcH4 to interact with a chromatin template(137). However, the surprising finding that AcH4, but not AcH3, exists in high concentration on the silenced HIV LTR raises the possibility that AcH4 is the primary histone modification responsible for recruiting Brd4 onto the LTR.

Lysines 5, 8, 12 and 16 (H4K5/8/12/16) are the primary acetylation sites found at the N-terminus of H4 (153) and acetylation of these sites has been shown to promote the binding of Brd4 to H4 both *in vivo* and *in vitro* (137). Three major histone acetyltransferases (HATs) are known to modify H4. While KAT5 (Tip60) is the only one capable of acetylating all four H4K5/8/12/16 positions, the other KATs are more selective (143,153). For example, KAT7 acetylates H4K5, 8 and 12, whereas KAT8 only acetylates H4K16. We therefore examined the impact of silencing the expression of KAT5, KAT7 or KAT8 on HIV transcription and latency.

We used the doxycycline (Dox)-inducible CRISPRi system(144) to suppress the expression of KAT5, KAT7 or KAT8 in the Jurkat-based 2D10 cell line, a widely used post-integrative HIV latency model containing the GFP-coding sequence in place of the viral *Nef* gene(119). An sgRNA sequence (sg1) that specifically targets the promoter region of the KAT5 gene was found to reduce the KAT5 mRNA level by ~80% in the engineered CRISPRi-KAT5-sg1 cells upon exposure to Dox (Fig. 3-2A, left panel). Western analysis of the cell lysates showed a corresponding decrease in the KAT5 protein level as well as a marked reduction of the AcH4 but not AcH3 level (Fig. 3-2A, right panel). The global AcH4 reduction agrees well with the demonstrated role of KAT5 as a promiscuous acetyltransferase for H4(142).

Using GFP induction as an indicator of latency reversal in the engineered 2D10 cells, the FACS analyses show that the Dox-induced inhibition of KAT5 expression by CRISPRi caused ~15% of the cell population to become GFP(+) (Fig. 3-2B). In addition, CRISPRi against KAT5 also strongly synergized with JQ1, prostratin, and SAHA, the three well-studied conventional LRAs, to enhance GFP production across a broad range

of drug concentrations (Fig. 3-2B). Very similar results were obtained in another 2D10-based CRISPRi-KAT5 cell pool, in which the inhibition of KAT5 expression was achieved by using sgRNA #2 (sg2) that targets a distinct KAT5 promoter sequence (Supplemental Fig. 3-S1), thus effectively ruling out a potential off-target effect caused by CRISPRi. Finally, inhibition of the catalytic activity of KAT5 with a selective inhibitor MG-149(154) also reversed HIV latency and potentiated traditional LRAs in a dosage-dependent manner (Fig. 3-2C).

CRISPRi inhibition of KAT7 or KAT8 failed to reactivate latent HIV

In contrast to the above results showing a key role of KAT5 in silencing HIV transcription, the CRISPRi-mediated inhibition of the KAT7 or KAT8 expression in 2D10 cells (Figs. 2D-2G) neither activated GFP expression by itself nor promoted the effects of the three conventional LRAs (Figs. 2E and 2G). In fact, the inhibition of KAT7 even slightly decreased the levels of both basal and the LRA-induced GFP production (Fig. 3-2G), a result that was also observed in another CRISPRi-KAT7 cell pool generated with a different sgRNA (Supplemental Fig. 3-S2). Thus, unlike KAT5, KAT7 appears to play a small but positive role in HIV transcription.

Consistent with the demonstration of KAT8 as a specific H4K16 acetyltransferase and KAT7 as a HAT for three out of the four lysine positions in the H4 N-terminus(143,153), the global AcH4 level was only slightly decreased in the CRISPRi-KAT8 cells but more prominently decreased in the CRISPRi-KAT7-sg1 cells (Figs. 2D & 2F). Collectively, these data indicate that KAT5, but not its two paralogs KAT7 and KAT8, is required to maintain the HIV provirus in a transcriptionally silent state in latency.

Antagonizing KAT5 activates Tat-dependent HIV transcriptional elongation but inhibits cellular primary response genes

In the majority of cases, acetyltransferases activate gene expression through acetylating histone tails, which de-condenses chromatin to facilitate transcriptional initiation and elongation(152). The Brd4-P-TEFb complex that is recruited to a chromatin template through the interaction between the Brd4 bromodomains and acetyl-histones plays a critical role in promoting transcriptional elongation of many cellular genes, especially those that are involved in primary responses(155,156). In light of our surprising finding that KAT5 did not activate HIV, but rather repressed HIV gene expression to keep the virus in latency, we investigated how antagonizing KAT5 might affect the expression of non-HIV genes such as MYC, FOS and JUNB, which are well-known cellular primary response genes(139,157). In agreement with the expectation that the pan acetyltransferase KAT5 should act to promote gene expression, inhibiting KAT5's expression by CRISPRi (Fig. 3-3A) or activity by MG-149 (Fig. 3-3B) was found to decrease the mRNA levels of all the three genes.

To confirm that the inhibition of HIV gene expression by KAT5 was indeed working through the viral LTR and at the transcription level, we first examined the effect of the shRNA-induced KAT5 knockdown (KD) on the ability of an integrated HIV-1 LTR to drive the expression of the luciferase reporter gene in Jurkat 1G5 cells(146). Interestingly, while the KD slightly decreased the basal LTR activity in the absence of Tat, it significantly increased luciferase expression when Tat was present in the cells (Fig. 3-3C). The differential effect on basal versus Tat-dependent HIV LTR activity was also observed when the catalytic activity of KAT5 was inhibited by MG-149 (Fig. 3-3D). In

contrast to the effects caused by antagonizing KAT5, the overexpression of KAT5 significantly repressed the Tat-dependent, but not -independent LTR activity (Fig. 3-3E). Finally, using a qRT-PCR-based assay that can distinguish between the processes of transcription initiation and elongation(158), the inhibitory effect of KAT5 on Tat-transactivation was deemed to be primarily at the elongation stage (Supplemental Fig. 3-S3). All together, these data strongly suggest that while KAT5 plays a stimulatory role in promoting the expression of cellular Brd4-dependent primary response genes, it can efficiently inhibit the Tat-dependent HIV transcriptional elongation.

Antagonizing KAT5 reduces AcH4, but not AcH3, on both HIV and cellular promoters

To determine whether the global reduction of the AcH4 but not AcH3 level observed in the CRISPRi-KAT5-sg1 cell lysates (Fig. 3-2A) would also result in a decreased AcH4 but not AcH3 level on both HIV and cellular gene promoters, we conducted the anti-AcH4 and -AcH3 ChIP assay. Indeed, suppressing KAT5's expression by CRISPRi (Fig. 3-4A) or activity by MG-149 (Fig. 3-4B) reduced the level of AcH4 detected on the HIV provirus at both the viral LTR and *Env* gene. In addition, a marked reduction in the AcH4 level was also detected at the promoters of two cellular genes, MYC and IκBα, as well as at the endogenous retroviral element HERVK(159) and an intergenic region upon the inhibition of KAT5 (Fig. 3-4A and 3-4B).

In contrast, CRISPRi against KAT5 did not significantly affect the AcH3 levels at these HIV and non-HIV locations, with the only exception seen at the MYC promoter, where a small reduction that could be a secondary effect of the diminished transcription was detected (Fig. 3-4C). Furthermore, on the silent HIV provirus in 2D10 cells, the overall levels of AcH3 relative to total H3 were lower than those detected on the two cellular genes MYC and IκBα (Fig. 3-4C), a result that echoes the observation made in a whole population of latently infected Jurkat cells in Fig. 3-1F. Finally, the poorly transcribed HERVK and the intergenic genomic region displayed generally low levels of AcH3 and AcH4 when compared with the robustly expressed HIV, MYC and IκBα genes (Fig. 3-4C & 3-4B).

While the relatively low level of AcH3 on the latent HIV LTR has been reported previously (119,160) and is likely due to a diminished recruitment of H3 acetyltransferase p300 (127), the unusually high level of AcH4 on the LTR (Figs. 1F, 4A and 4B) is yet to be explained. To this end, we compared the levels of KAT5 on the HIV LTR and the MYC promoter in infected cells. The ChIP data demonstrate that the LTR had a mildly higher level of KAT5 than did the MYC promoter in the total pool of infected cells. However, the difference between the two became more pronounced and statistically significant upon the establishment of viral latency (Figs. 4D and 4E). Thus, the unbalanced loadings of p300 and KAT5 likely contribute to the unusually low AcH3 but high AcH4 level on the latent HIV LTR.

Inhibition of KAT5 selectively removes Brd4 from and increases SEC binding to the HIV provirus

Since inhibition of KAT5 led to an overall reduction of the AcH4 level at both the HIV and non-HIV gene promoters, we asked how the reduced AcH4 level could promote Tat-dependent HIV transcription while at the same time suppress the expression of cellular primary response genes. To answer this question, we investigated the

consequence of inhibiting KAT5 on the binding of Brd4 and the human Super Elongation Complex (SEC) to the HIV and non-HIV loci.

The ChIP assay conducted in the inducible CRISPRi-KAT5-sg1 cells indicates that upon the Dox-induced down-regulation of KAT5, the Brd4 level significantly decreased at the HIV LTR, HIV *Env*, and the MYC promoter region (Fig. 3-5A). This implicates AcH4 as the primary route of recruitment for Brd4 at these locations. In contrast, although the Brd4 level was quite high at the IκBα gene promoter before the Dox treatment, it displayed little change after CRISPRi silencing of KAT5 (Fig. 3-5A), probably because Brd4 is recruited to this locus by recognizing mostly AcH3 but not AcH4. The Brd4 levels at the poorly transcribed HERVK and the intergenic region were relatively low and remained fairly constant upon CRISPRi silencing of KAT5 (Fig. 3-5A). Importantly, a very similar change in the Brd4 distribution pattern was also observed when the catalytic activity of KAT5 was inhibited by MG-149 (Fig. 3-5B).

A recent study by the Ott laboratory demonstrates that both the long and short isoforms of Brd4 can promote HIV latency, albeit through distinct mechanisms (140). To assess the roles of the two Brd4 isoform in transducing the signal downstream of the KAT5-AcH4 axis, we compared the effect of MG-149 on the bindings of the long (simply labeled as Brd4 throughout the current study) and short form of Brd4 (Brd4S) to the integrated HIV-1 LTR. The ChIP data show that when expressed at a similar level, more Brd4 bound to the LTR than did Brd4S (Supplemental Fig. 3-S4). Furthermore, compared to Brd4S, the binding of Brd4 to the LTR was also more sensitive to the MG-149-induced AcH4 reduction. Thus, between the two Brd4 isoforms, the long form appears to be more responsive to changes in the level of AcH4 on the LTR and thus more likely to be a key target of the KAT5-AcH4 axis.

Because the abundant Brd4 long isoform containing the C-terminal P-TEFb-interacting domain is a direct competitor of HIV Tat for the limited cellular supply of P-TEFb(105,106), the decreased Brd4 occupancy on the HIV provirus in KAT5-inhibited cells is expected to free up P-TEFb for its incorporation into the Tat-SEC complex, which is very efficiently recruited to the provirus through the TAR RNA route (108,161). Consistent with this mechanism, the ChIP analysis showed that inhibiting KAT5's expression by CRISPRi (Fig. 3-5C) or activity by MG-149 (Fig. 3-5D) significantly increased the level of AFF1, the scaffolding subunit of the SEC, on both the HIV LTR and *Env* gene. In addition, MG-149 also significantly enhanced the loading of another key SEC subunit ELL2 onto the HIV provirus in an engineered Jurkat cell line ΔE2-R2 (Fig. 3-5E), in which the endogenous ELL2 gene has been knocked out and ELL2-FLAG is expressed at a similar level from an integrated vector(158).

By contrast, the inhibition of KAT5 decreased the SEC level on the MYC promoter (Fig. 3-5C-E), which agrees with the diminished MYC expression in the KAT5-inhibited cells (Fig. 3-3A & 3-3B). Although the precise function of SEC in MYC transcription is yet to be revealed, our data suggest a likely role for Brd4 in recruiting SEC to this important primary response gene. Finally, very low levels of AFF1 and ELL2-FLAG were detected at the IκBα gene promoter, HERVK, and the intergenic region (Fig. 3-5C-E), implicating that the SEC plays little role in their transcription.

KAT5 depletion prevents HIV from efficiently establishing latency

The data presented thus far are consistent with the hypothesis that abundant AcH4 on the HIV provirus is used to locally recruit Brd4, which then competes with Tat for

host P-TEFb. KAT5 enhances the levels of AcH4, and consequently it behaves as an inhibitor of the Tat-SEC formation on HIV LTR to suppress Tat-transactivation and enforce viral latency. Based on this notion, we hypothesized that silencing the expression of KAT5 would therefore make it more difficult for HIV to establish latency in the progressive latency establishment assay outlined in Fig. 3-6A.

To test this hypothesis, we generated stable pools of Jurkat cells that express either a non-targeting scrambled shRNA (shScramble) or the KAT5-specific shRNA (shKAT5). The latter was shown to cause ~70% reduction in the cellular level of KAT5 (Fig. 3-6B). When tested in the progressive latency establishment assay, the shKAT5 pool displayed a significantly delayed dynamics in reverting to the GFP(-) status, i.e. transcriptionally silent or latent state, when compared with the shScrambled pool (Fig. 3-6C & D). This result confirms the prediction that KAT5 and its acetylation of H4 play a critical role in allowing HIV to efficiently establish latency.

Inhibiting KAT5 potentiates proviral reactivation by JQ1 in a primary T cell-based latency model

In primary T-cells, P-TEFb levels are dramatically reduced when the cells enter quiescence, and this in turn, forces HIV into latency. To evaluate the role of KAT5 in maintaining HIV in a transcriptionally silent state in primary CD4+ T cells, we used our recently described Th17 cell latency model (145). Briefly, polarized and expanding Th17 cells were infected with a VSVG-pseudotyped HIV-1 virus HIV-Nef-CD8a/eGFP and then forced to enter quiescence by culturing in a restrictive cytokine environment (Fig. 3-7A). Proviral gene expression, as assessed by immunofluorescence staining for Nef, was low in the quiescent cells, but could be induced ~4 to 6-fold upon activation of the T-cell receptor (TCR) by antibodies to CD3 and CD28 (Supplemental Fig. 3-S5 and Fig. 3-7C). In each of these experiments, the EGFP signal remained high in Th17 cells containing latent HIV due to the prolonged stability of the membrane-bound CD8a-EGFP fusion protein.

As expected, MG-149 significantly and preferentially decreased the AcH4 level in primary CD4+ T cells (Fig. 3-7B). In comparison, the levels of AcH3 and total H4 were only mildly reduced, probably due to an indirect effect of global inhibition of gene expression in the treated cells. When used alone, MG-149 (at 10 or 50 μM) and JQ1 (at 1 or 5 μM) produced no, or only very modest, stimulatory effects on proviral gene induction in our Th17 cell latency model (Figs. 3-7C-D). However, exposure of the cells to 1 μM JQ1 plus 10 μM MG-149 for 48 hr increased the HIV-expressing cell population by more than 2-fold (Fig. 3-7C). Similarly, while the treatment with 5 μM JQ1 alone slightly elevated HIV expression, the addition of 50 μM MG-149 further enhanced the stimulatory effect of 5 μM JQ1 by ~1.8-fold (Fig. 3-7D). At 10 to 50 μM, MG-149 produced very little enhancing effect on HIV reactivation in cells that were treated with SAHA, the PKC agonist Ingenol (111,112), or TCR-activating signals (Supplemental Fig. 3-S5 and Fig. 3-7C). Thus, the enhancing effect of MG-149 appears to be restricted to JQ1 in this primary T cell model of latency. Of note, both MG-149 alone and in combination with other LRAs did not cause global T-cell activation as indicated by minimal changes in CD25 and CD69 immunostaining after the treatment (Supplemental Fig. 3-S6).

Inhibition of KAT5 by MG-149 stimulates release of virions from primary T cells isolated from ART-treated patients

To further investigate the impact of KAT5 inhibition by MG-149 in a more clinically relevant setting, we performed an *ex vivo* experiment to test the effect of MG-149 alone or in combination with JQ1 to release virions from primary T cells that are isolated from ART-treated patients (Fig. 3-7E and Supplemental Table 3-1). The data reveal a statistically significant positive effect displayed by MG-149 alone (6.5-fold increase on average of HIV RNA released into supernatant) as well as by the JQ1 plus MG-149 combination (5.3-fold increase on average). In comparison, JQ1 alone failed to produce a statistically significant effect.

It is interesting to note that a previous report shows that both the PKC-agonist and PMA plus ionomycin (PMA/I), but not JQ1 or HDACi alone, could efficiently increase virion release from latently infected primary cells (136). Our *ex vivo* data confirm these observations about PMA/I and JQ1, and more importantly, show that MG-149 was almost as effective as PMA/I to single-handedly increase the virion release (Fig. 3-7E). This effect of MG-149 could be important for maximally exposing the latently infected cells for immuno-recognition and clearance and thus implicate the potential utility of KAT5 inhibition as an effective latency reversal strategy.

Discussion

In contrast to the well-characterized positive effects of histone H3 acetyltransferases p300/CBP and P/CAF on HIV transcription (45), the roles played by the major H4 acetyltransferases in this process are unknown. In this study, we report that KAT5, but not KAT7 and KAT8, is a host factor that promotes HIV latency establishment, and inhibits latency reversal, by acetylating H4 on the viral LTR. The unique pattern of histone acetylation found at the LTR permits recruitment of Brd4 to the HIV promoter where it competes with Tat for P-TEFb, blocks Tat-SEC formation, and ultimately inhibits Tat-transactivation (Fig. 3-7F). When KAT5 is antagonized by either CRISPRi or MG-149, the loss of AcH4 on the LTR dissociates Brd4 and allows P-TEFb to join Tat in the Tat-SEC complex to enhance HIV transcriptional elongation and latency reversal (Fig. 3-7F).

Importantly, the strong correlation between the shutdown of HIV transcription during latency establishment and elevated levels of AcH4 and Brd4 on the LTR was demonstrated not only with the extensively characterized Jurkat clone 2D10 cell model, but also in a pool of latently infected cells with diverse integration sites. Thus, the negative effects exerted by the KAT5-Ac-H4-Brd4 axis on HIV transcription are independent of the proviral integration site and the cellular chromatin context.

Although inhibitory to Tat-induced HIV transactivation, the KAT5-AcH4-Brd4 axis appears to play a positive role in stimulating the expression of cellular genes, especially those involved in primary response. The differential effects of KAT5 on transcription of the HIV versus host genes implicate this histone acetyltransferase as a promising candidate that can be selectively targeted to reactivate latent HIV without globally activating numerous host genes at the same time. The high selectivity toward HIV is likely to be an important attribute for LRAs used in the “Shock and Kill” strategy for eradicating latent HIV reservoirs (53).

In contrast to KAT5, KAT7 and KAT8 produced no inhibitory effects on HIV transcription and latency reversal (Figs. 2D-2G). We ascribe this to KAT5’s broader substrate specificity toward four H4 lysines (K5, K8, K12, and K16) versus KAT8’s sole

targeting of H4K16 and KAT7's more restrictive target specificity (142,143,153). It has been shown that the poly-acetylated K5, K8, K12 is essential for Brd4's binding to H4, whereas the acetylation of K16 only minimally increases Brd4's affinity to H4 peptides already acetylated at K5, K8, and K12 (137).

Interestingly, KAT5 was first identified as an HIV Tat-interacting protein of 60 kDa, hence originally named as Tip60 (162). It was subsequently found to be inhibited by Tat (163). Thus, in addition to the inhibition of KAT5 by MG-149, which functions as a LRA to kick-start the initial rounds of HIV transcription to produce viral proteins including Tat, the accumulated Tat protein may further inhibit KAT5 to decrease AcH4 and antagonize Brd4's action, thus fueling another positive feedback loop besides the Tat-SEC axis to expedite the reversal of latency.

Proviral transcription of latent HIV is silenced by multiple mechanisms including heterochromatinization of the LTR (164). In the present study, we found that the AcH3 level is very low on the LTR in 2D10 cells as well in a diverse population of latently infected Jurkat cells. In contrast, the AcH4 level on the LTR is relatively high and comparable to those on the cellular genes. The activity of AcH4 is therefore distinct from that of AcH3, which is an activating signal since it prevents H3K9/K27-methylations that recruit the chromatin-compacting proteins HP1 and Polycomb (152). By contrast, AcH4 is compatible with heterochromatin (165) and can even induce heterochromatinization in certain cases (166). Thus, our data point to a plausible scenario where latent HIV proviruses are low in AcH3 but high in AcH4, which helps keep the LTR heterochromatinized but still capable of retaining Brd4 to suppress Tat-transactivation. This also resolves an apparent paradox concerning how histone acetylation, which is generally considered pro-euchromatin and promote HIV transcription (141), can be exploited by Brd4 to further silence Tat-transactivation.

Finally, it is worth noting that prior to the current study, the KAT5-AcH4-Brd4 axis has already been reported as a restriction mechanism for papillomaviral and adenoviral gene transcription through retaining or interacting with negative transcription factors on the viral promoters (167,168). In light of these findings, our current work adds HIV to the growing list of viral infections that employ KAT5 as a crucial regulator. Due to the presence of multiple additional restrictions imposed on proviral transcription in quiescent primary T cells, it is considerably more difficult to reverse HIV latency in these cells than in transformed cell lines (169). Nevertheless, the observation that the KAT5 inhibitor MG-149 cooperates with JQ1 to promote HIV latency reversal not only in activated cell lines but also in quiescent primary T cells derived from ART-treated HIV patients underscores the clinical relevance of targeting the KAT5-AcH4-Brd4 axis. Future studies are necessary to explore this potential for therapeutic intervention and eventual eradication of HIV/AIDS.

Figure 3-1. Establishment of HIV latency correlates with elevated amounts of AcH4 and Brd4 but drastically decreased AcH3 content on viral LTR. A. A schematic diagram showing the procedure and timeline of experiments to progressively establish HIV latency in the total infected Jurkat cell pool (total pool) as well as to enrich the latently infected cell pool (latent pool). **B.** The total pool was checked by fluorescence-activated cell sorting (FACS) for the percentages of GFP(+) or (-) cells on the indicated days post infection (d.p.i.) and the average of three measurements at each time point is shown. **C.** Representative FACS plots of total and latent pools at the indicated time points. **D.** The latent pool was treated in triplicates on 43 d.p.i. by JQ1 or prostratin at the indicated concentrations for 24 hr and subjected to FACS to determine the percentage of GFP(+) cells in each cell population. The error bars indicate mean +/- SD from three independent measurements. **E.** Western analysis of the total and latent pools on 43 d.p.i. for the various proteins labeled on the left. **F.** The total and latent pools on 43 d.p.i. were subjected to ChIP-qPCR analyses to determine the levels of the indicated proteins bound to HIV LTR. The ChIP signals were normalized to those of input DNA and shown as an average of three independent reactions, with the error bars representing mean +/- SD and the asterisks indicating the levels of statistical significance calculated by two-tailed Student's *t*-test.

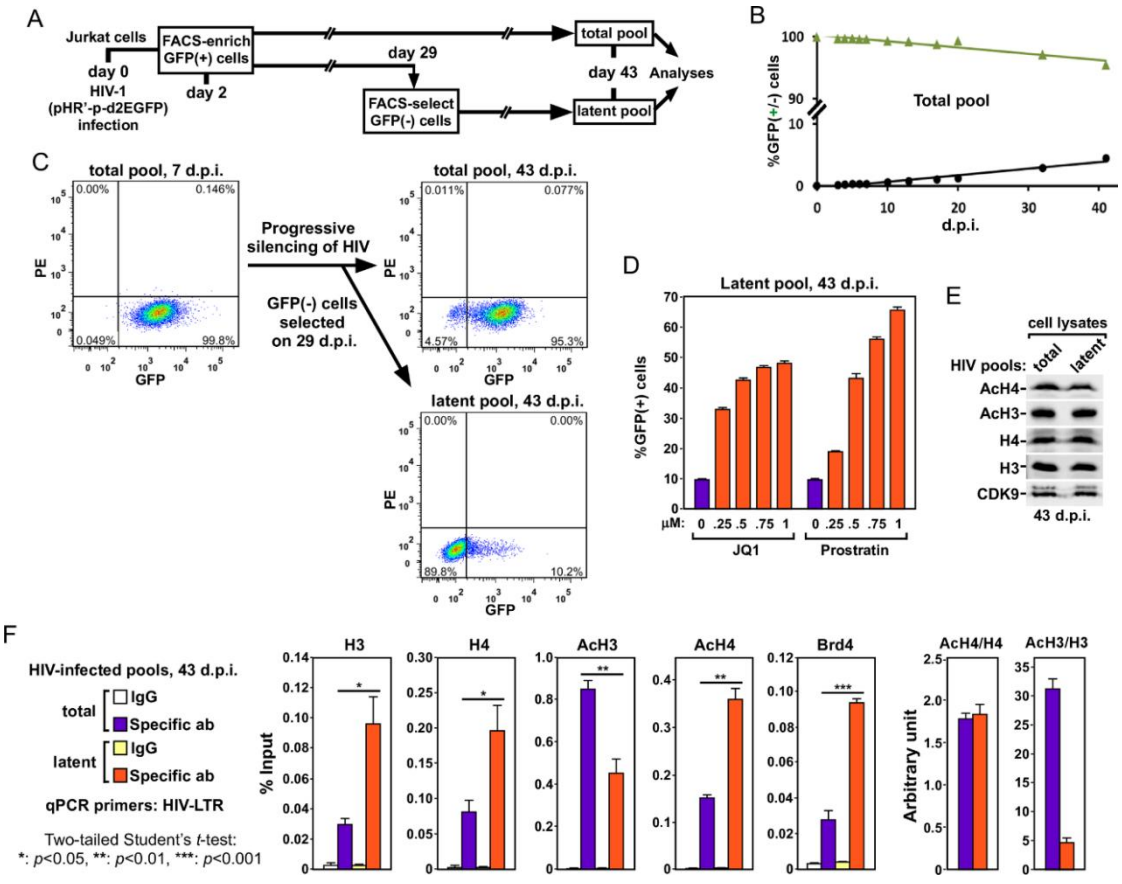

Figure 3-1

Figure 3-2. Antagonizing KAT5 but not KAT7 or KAT8 reverses HIV latency and potentiates conventional LRAs. A. D. & **F.** The Jurkat 2D10-based inducible CRISPRi-KAT5-sg1, CRISPRi-KAT7-sg1, and CRISPRi-KAT8 cells were treated with (+) or without (-) doxycycline (Dox) and analyzed by RT-qPCR for the KAT5/7/8 mRNA levels, which were normalized to those of ActB, and by Western blotting for the indicated proteins. **B. E.** & **G.** CRISPRi-KAT5-sg1, CRISPRi-KAT7-sg1, and CRISPRi-KAT8 cells were treated with or without Dox (1 μl/ml) and the various LRAs at the indicated concentrations. The treated cells were subjected to FACS analysis to determine the percentage of GFP(+) cells in each cell population. **C.** Wild-type 2D10 cells were treated with combinations of MG-149 and DMSO or the various LRAs at the indicated concentrations and subjected to FACS analysis as in B. Each column in all panels represents the average of three independent measurements, with the error bars indicating mean +/- SD.

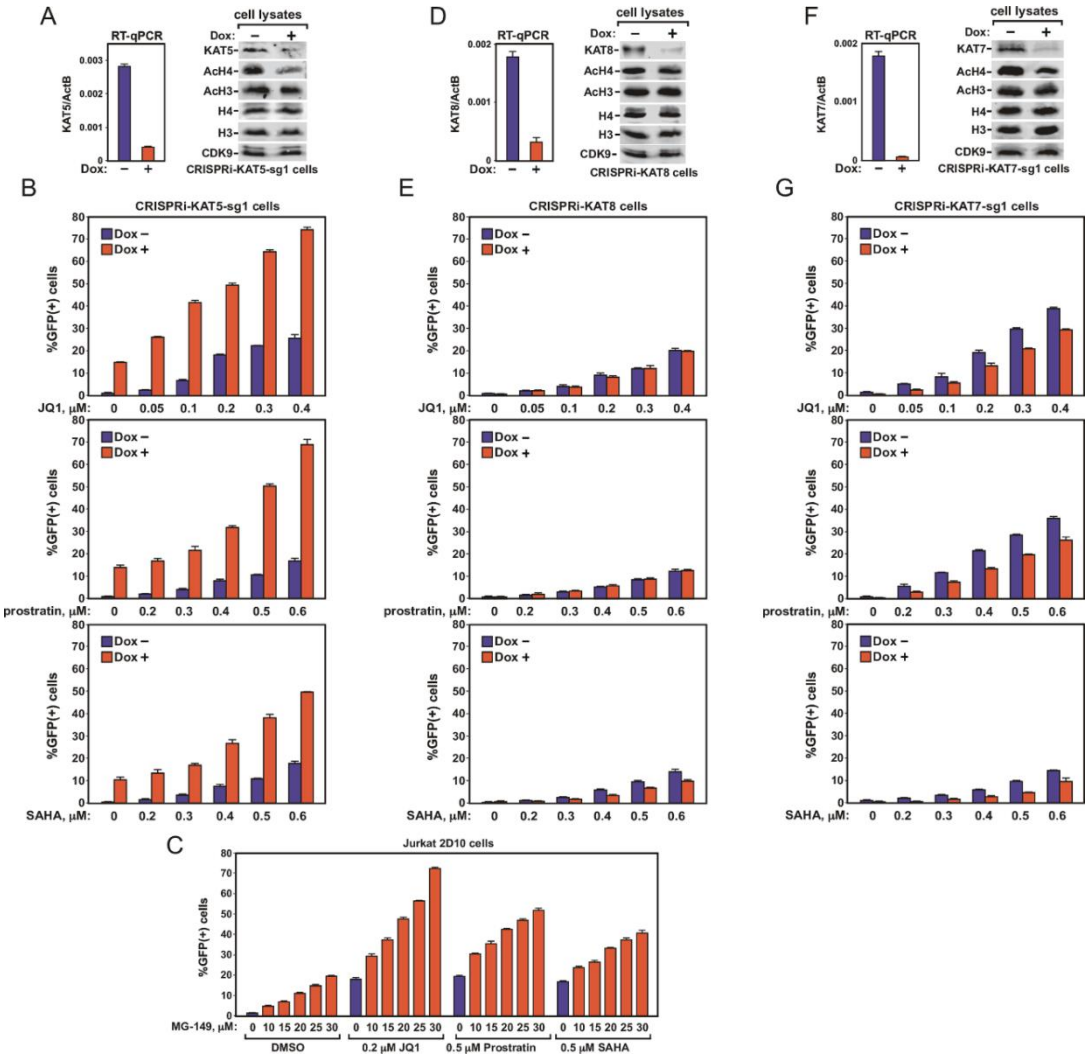

Figure 3-2

Figure 3-3. Antagonizing KAT5 activates Tat-dependent HIV transcription but inhibits cellular primary response genes. A. & **B.** Jurkat 2D10-based CRISPRi-KAT5-sg1 (A) and parental 2D10 (B) cells were treated with (+) or without (-) Dox (A) or MG-149 (B). The mRNA levels of the indicated genes were measured by RT-qPCR and normalized to those of ActB and shown as averages of three independent measurements. The error bars indicate mean +/- SD and the asterisks denote levels of statistical significance calculated by two-tailed Student's *t*-test (*: $p<0.05$, **: $p<0.01$, and ***: $p<0.001$). **C.** & **D.** Luciferase activities were measured in extracts of Jurkat 1G5 or Jurkat 1G5+Tat cells containing an integrated HIV-1 LTR-luciferase reporter construct and stably expressing the indicated shRNA (C) or treated with the indicated concentrations of MG-149 (D). **E.** Luciferase activities were measured in extracts of 293T cells that were transfected with the HIV-1 LTR-luciferase reporter construct together with the vector expressing FLAG-KAT5- and/or Tat-HA as indicated. All experiments in C to E were performed in triplicates with the error bars representing mean +/- SD and the activities in the first column set to 1.0. An aliquot of each cell extract was examined by Western blotting for the proteins labeled on the left.

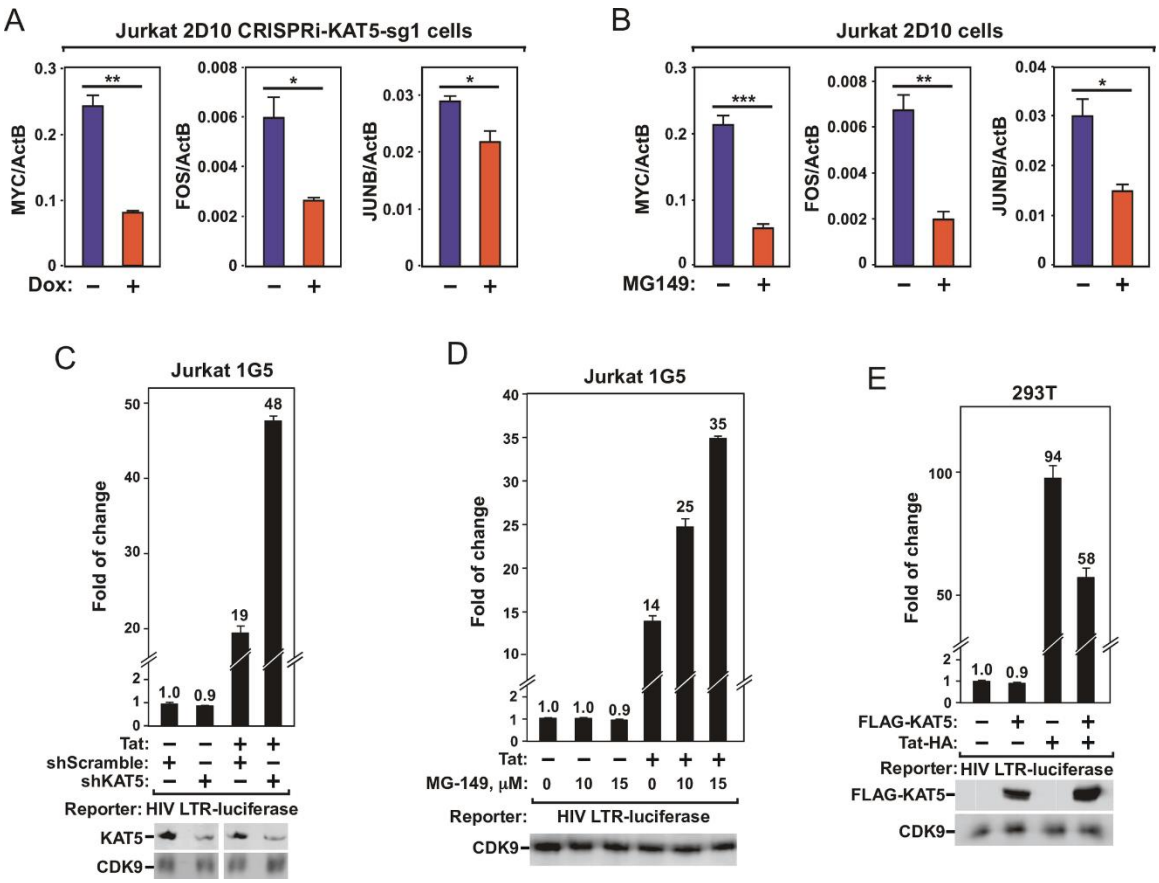

Figure 3-3

Figure 3-4. Antagonizing KAT5 reduces AcH4 but not AcH3 level on both HIV and non-HIV gene promoters and a higher level of KAT5 exists on the viral LTR than on the cellular MYC gene promoter in latently infected cells. A., B., & C. The 2D10-based CRISPRi-KAT5-sg1 (A & C) and parental 2D10 (B) cells were treated with the indicated drugs and subjected to ChIP-qPCR assays to determine the levels of AcH3, AcH4, total H3 and total H4 bound to the various genomic locations labeled at the bottom. The ChIP-qPCR signals were normalized to those of input DNA for each genomic location and the ratios of AcH3 over H3 and AcH4 over H4 were shown. The error bars represent mean +/- SD from three independent qPCR reactions. The asterisks (*: $p<0.05$, **: $p<0.01$, and ***: $p<0.001$) indicate different levels of statistical significance as calculated by two-tailed Student's t-tests. **D.** The total and latently infected Jurkat cell pools generated in Fig. 3-1A were analyzed by FACS to determine the percentage of GFP(+) cells in each population. The error bars indicate mean +/- SD from three independent measurements. **E.** The indicated cell pools from D were subjected to ChIP-qPCR analysis with the anti-KAT5 antibody to determine the levels of KAT5 bound to the various genomic locations labeled at the bottom. The ChIP-qPCR signals were normalized to those of input DNA for each location and shown as an average of three independent reactions, with the error bars representing mean +/- SD and the asterisks indicating the levels of statistical significance calculated by two-tailed Student's *t*-test.

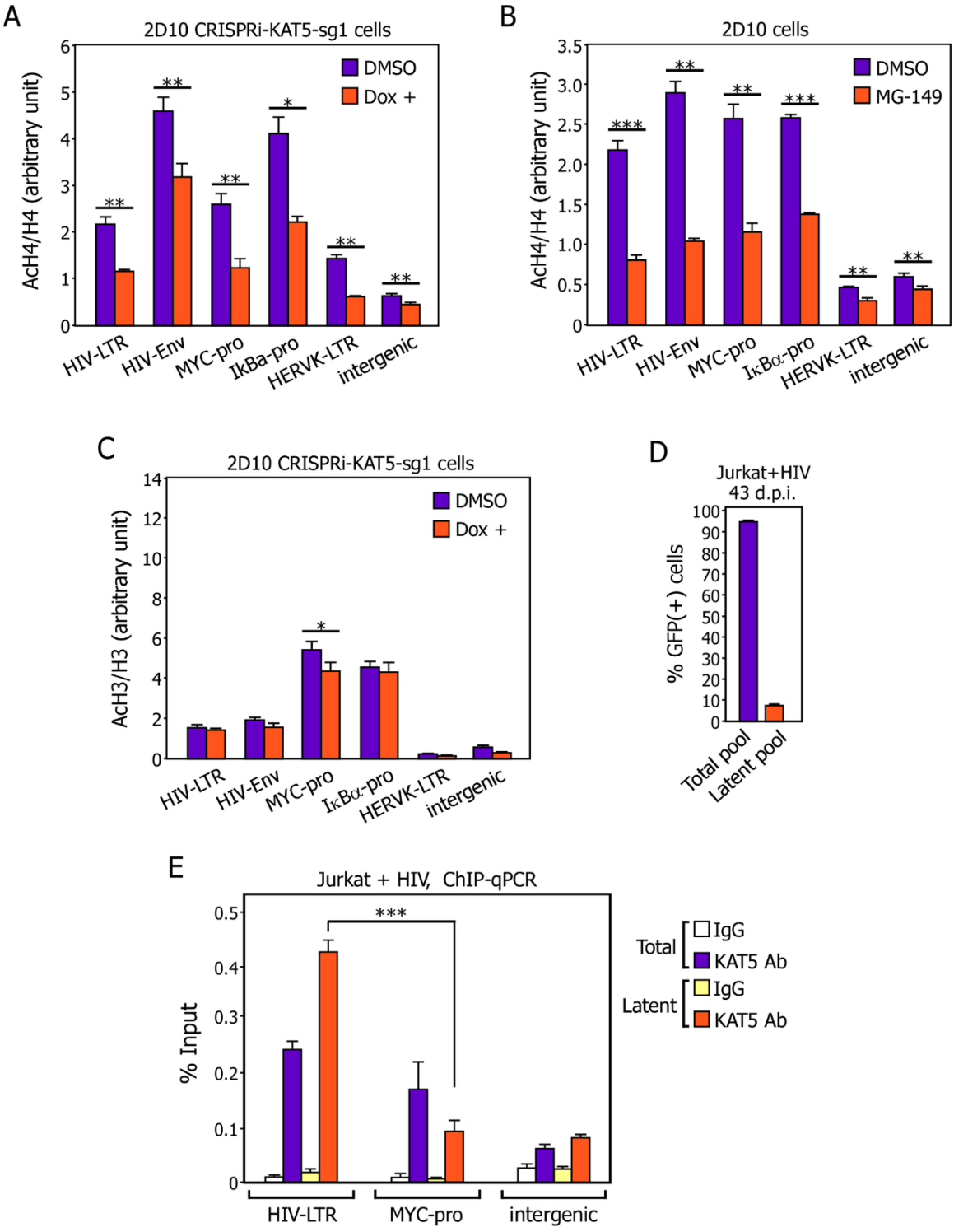
A
2D10 CRISPRi-KAT5-sg1 cells
AcH4/H4 (arbitrary unit)
DMSO
Dox +
HIV-LTR
HIV-Env
MYC-pro
IkBa-pro
HERVK-LTR
intergenic
B
2D10 cells
AcH4/H4 (arbitrary unit)
DMSO
MG-149
HIV-LTR
HIV-Env
MYC-pro
IκBα-pro
HERVK-LTR
intergenic
C
2D10 CRISPRi-KAT5-sg1 cells
AcH3/H3 (arbitrary unit)
DMSO
Dox +
HIV-LTR
HIV-Env
MYC-pro
IκBα-pro
HERVK-LTR
intergenic
D
Jurkat+HIV
43 d.p.i.
% GFP(+) cells
Total pool
Latent pool
E
Jurkat + HIV, ChIP-qPCR
% Input
Total
IgG
KAT5 Ab
Latent
IgG
KAT5 Ab
HIV-LTR
MYC-pro
intergenic

Figure 3-4

Figure 3-5. Inhibition of KAT5 selectively removes Brd4 from and increases SEC binding to the HIV provirus. A., B., C., D., & E. CRISPRi-KAT5-sg1 (A & C), 2D10 (B & D), and ΔE2-R2 (E) cells were treated with DMSO or the indicated drugs and subjected to ChIP-qPCR assays using the antibodies (Ab) that specifically recognize the indicated proteins bound to the various genomic regions as labeled at the bottom. The ChIP-qPCR signals were normalized to those of input DNA for each genomic location. The error bars represent mean +/- SD from three independent qPCR reactions. The asterisks indicate different levels of statistical significance as calculated by two-tailed Student's t-tests.

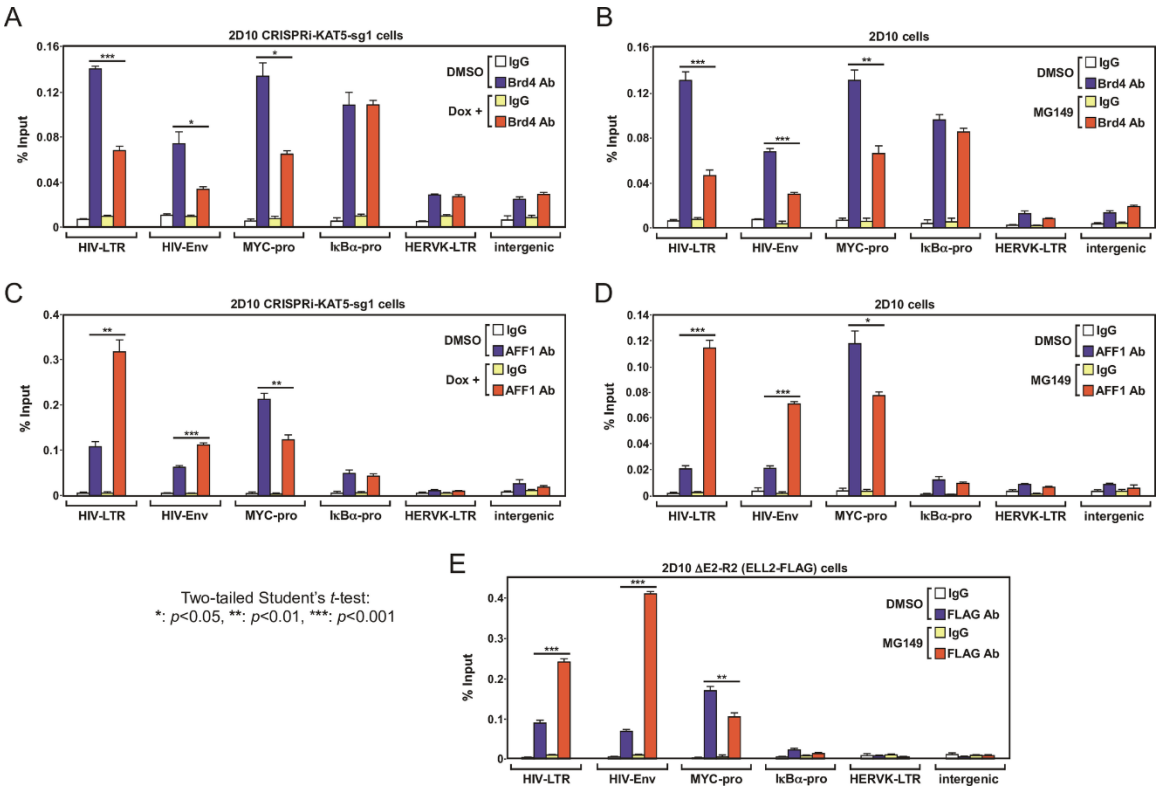

Figure 3-5

Figure 3-6. KAT5 depletion prevents HIV from efficiently establishing latency. A. A schematic diagram showing the procedure and timeline of experiments to progressively establish latency in Jurkat cell pools stably expressing either shKAT5 or shScramble. d.p.i.: Days post infection. **B.** Lysates of the cell pools expressing the indicated shRNA were examined by Western blotting for the proteins labeled on the left. **C.** The GFP(+) cells that were selected by FACS on 2 d.p.i from each cell pool were checked by flow cytometry for the percentages of GFP(+) cells on the indicated d.p.i. and the average of three measurements at each time point is shown. **D.** Representative immunofluorescence flow cytometry analysis of shScramble- and shKAT5-expressing cells that were either uninfected or infected with HIV and harvested at the indicated d.p.i.

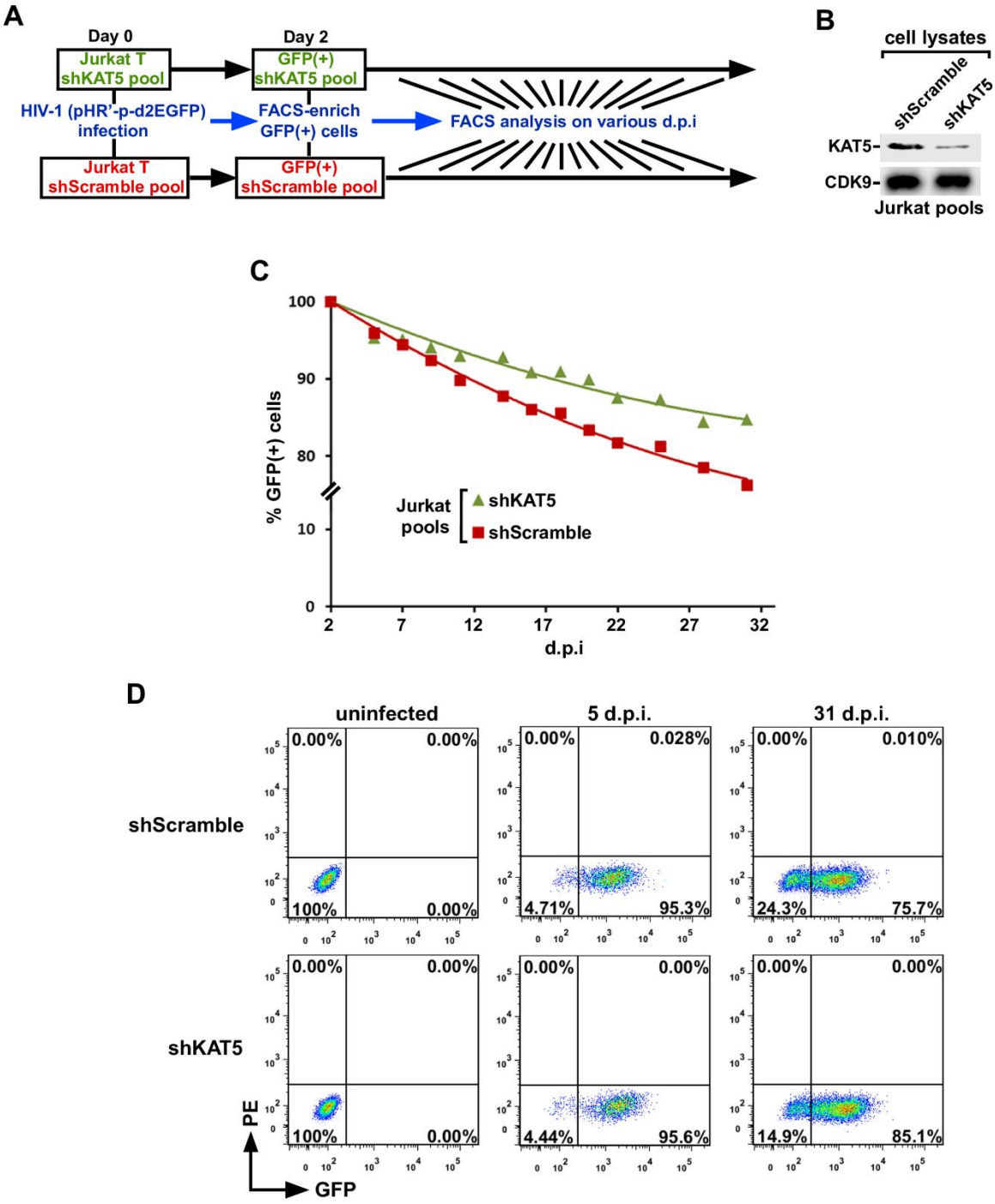
A
Day 0
Day 2
Jurkat T shKAT5 pool
GFP(+) shKAT5 pool
HIV-1 (pHR'-p-d2EGFP) infection
FACS-enrich GFP(+) cells
FACS analysis on various d.p.i
Jurkat T shScramble pool
GFP(+) shScramble pool
B
cell lysates
shScramble
shKAT5
KAT5-
CDK9-
Jurkat pools
C
% GFP(+) cells
d.p.i
Jurkat pools
shKAT5
shScramble
D
uninfected
5 d.p.i.
31 d.p.i.
shScramble
shKAT5
PE
GFP
0.00%
0.028%
0.010%
100%
4.71%
95.3%
24.3%
75.7%
4.44%
95.6%
14.9%
85.1%

Figure 3-6

Figure 3-7. Inhibition of KAT5 in a primary cell latency model and ART-suppressed patient cells enhances HIV latency reversal and virion release. A. Scheme showing the procedure followed to generate latently infected resting Th17 cells. **B.** Memory CD4+ T cells from a healthy donor were pretreated with 1 μM SAHA overnight and then incubated with the indicated concentrations of MG-149 for 24 hr. Western blotting analyses were conducted to detect the levels of AcH4, AcH3, and total H4 in whole cell lysates. The AcH4:AcH3 ratio in each lane was measured by densitometry and shown on the right. **C.** Representative immunofluorescence flow cytometry analysis of Nef-Cy5 and CD8a-EGFP expression in latently infected primary Th17 cells that were either TCR-activated or treated with 1 μM JQ1 for 48 hr in the presence or absence of 10 μM MG-149. EGFP reporter used for positive selection remained high in the latently infected cells due to prolonged stability of the membrane-bound CD8a-EGFP fusion protein. **D.** Representative immunofluorescence flow cytometry analysis of Nef-Cy5 and CD8a-EGFP expression in latently infected primary Th17 cells that were either untreated or treated with 5 μM JQ1 with or without MG-149 for 48 hr. **E.** Primary cells from ART-suppressed HIV-1-infected individuals were treated with the indicated drug(s) for 24 hr. HIV-1 RNA in culture supernatant were quantified with the Roche COBAS® AmpliPrep/TaqMan® HIV-1 Qualitative Test system. The viral copy numbers were presented as fold induction relative to the DMSO control. Numbers in parentheses indicate number of individuals used for each treatment. N.S. not significant; *$P < 0.05$; **$P < 0.01$. Error bars represent standard error of the mean (SEM). **F.** Diagram depicting KAT5 but not KAT7 and KAT8 as a host factor for suppressing HIV proviral transcription and promoting viral latency. See text for more details.

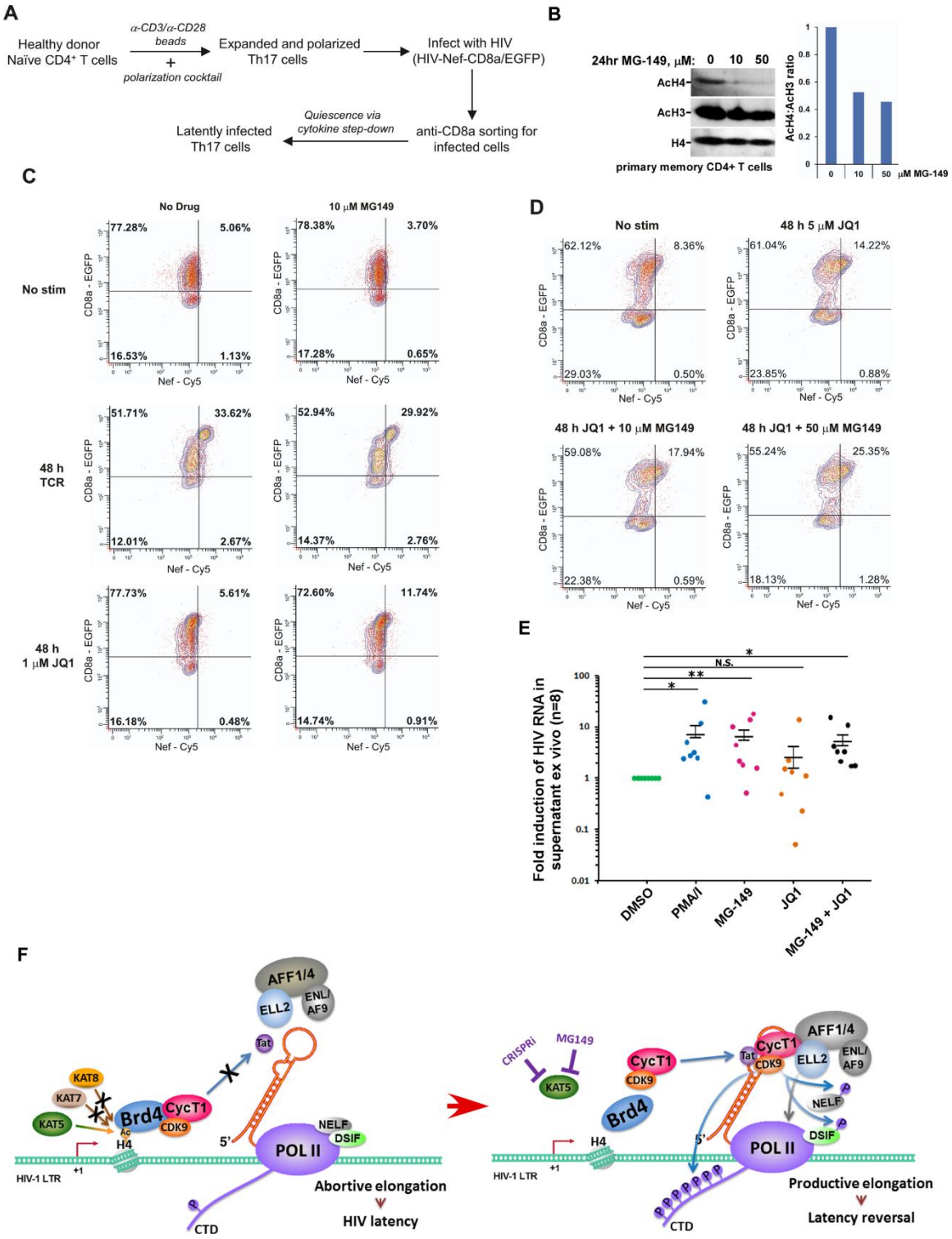
A
Healthy donor
Naïve CD4+ T cells
α-CD3/α-CD28
beads
+
polarization cocktail
Expanded and polarized
Th17 cells
Infect with HIV
(HIV-Nef-CD8a/EGFP)
anti-CD8a sorting for
infected cells
Quiescence via
cytokine step-down
Latently infected
Th17 cells
B
24hr MG-149, μM: 0 10 50
AcH4
AcH3
H4
primary memory CD4+ T cells
AcH4:AcH3 ratio
μM MG-149
C
No Drug
10 μM MG149
No stim
48 h
TCR
48 h
1 μM JQ1
CD8a - EGFP
Nef - Cy5
77.28%
5.06%
16.53%
1.13%
78.38%
3.70%
17.28%
0.65%
51.71%
33.62%
12.01%
2.67%
52.94%
29.92%
14.37%
2.76%
77.73%
5.61%
16.18%
0.48%
72.60%
11.74%
14.74%
0.91%
D
No stim
48 h 5 μM JQ1
48 h JQ1 + 10 μM MG149
48 h JQ1 + 50 μM MG149
62.12%
8.36%
29.03%
0.50%
61.04%
14.22%
23.85%
0.88%
59.08%
17.94%
22.38%
0.59%
55.24%
25.35%
18.13%
1.28%
E
Fold induction of HIV RNA in
supernatant ex vivo (n=8)
N.S.
DMSO
PMA/I
MG-149
JQ1
MG-149 + JQ1
F
AFF1/4
ELL2
ENL/
AF9
Tat
KAT8
KAT7
KAT5
Brd4
CycT1
CDK9
Ac
H4
5'
NELF
DSIF
POL II
HIV-1 LTR
+1
P
CTD
Abortive elongation
HIV latency
CRISPRi
MG149
Productive elongation
Latency reversal

Figure 3-7

Figure 3-S1. CRISPRi inhibition of KAT5 expression by using an alternative sgRNA (sg2) that targets a different KAT5 promoter sequence produces the same result as in CRISPRi-KAT5-sg1 cells. A. The Jurkat 2D10-based inducible CRISPRi-KAT5-sg2 cells were treated with (+) or without (-) Dox and analyzed by RT-qPCR for the KAT5 mRNA levels, which were normalized to those of ActB. **B., C. & D.** CRISPRi-KAT5-sg2 cells were treated with or without Dox (1 μl/ml) and the various LRAs at the indicated concentrations, and then subjected to FACS analysis to determine the percentage of GFP(+) cells in each cell population.

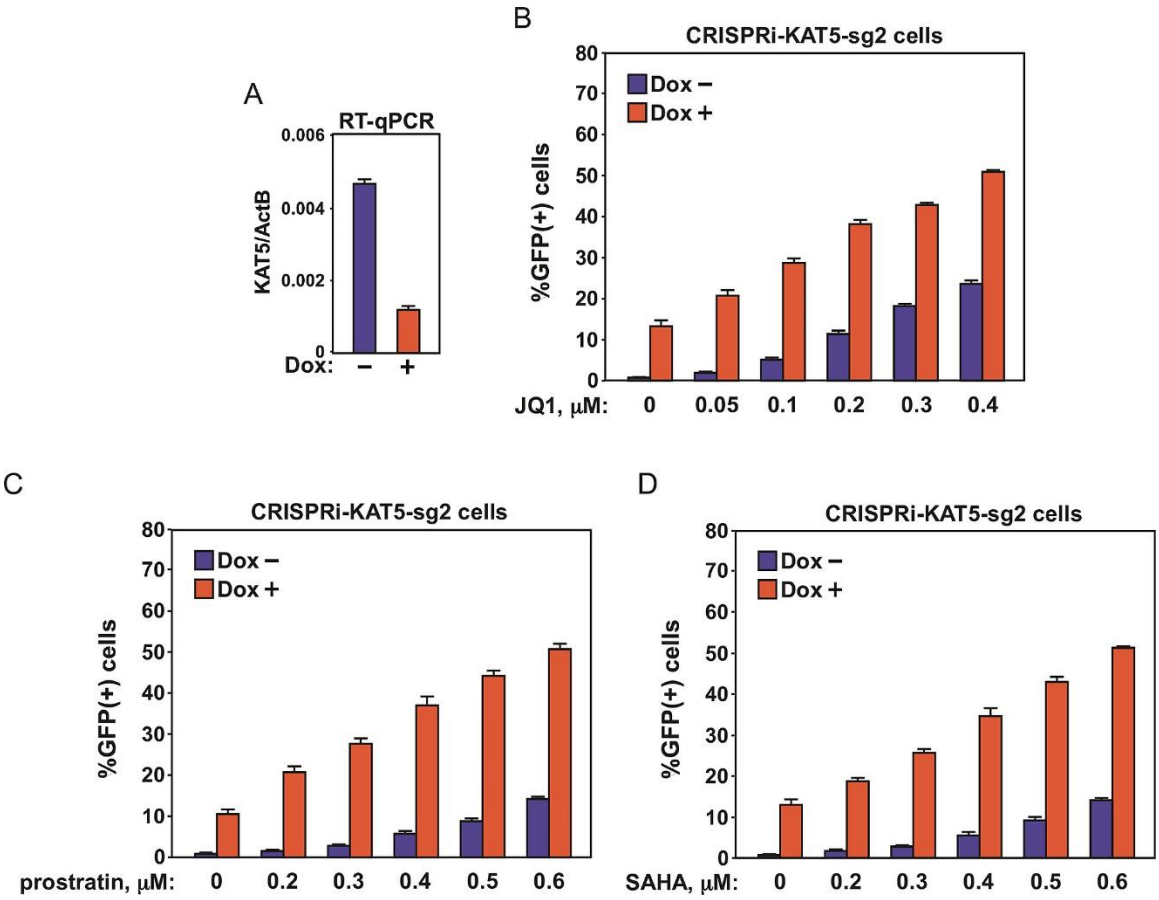

Figure 3-S1

Figure 3-S2. CRISPRi inhibition of KAT7 expression by using an alternative sgRNA (sg2) that targets a different KAT7 promoter sequence produces the same result as in CRISPRi-KAT7-sg1 cells. A. The Jurkat 2D10-based inducible CRISPRi-KAT7-sg2 cells were treated with (+) or without (-) Dox and analyzed by RT-qPCR for the KAT5 mRNA levels, which were normalized to those of ActB. **B., C., & D.** CRISPRi-KAT7-sg2 cells were treated with or without Dox (1 μl/ml) and the various LRAs at the indicated concentrations, and then subjected to FACS analysis to determine the percentage of GFP(+) cells in each cell population.

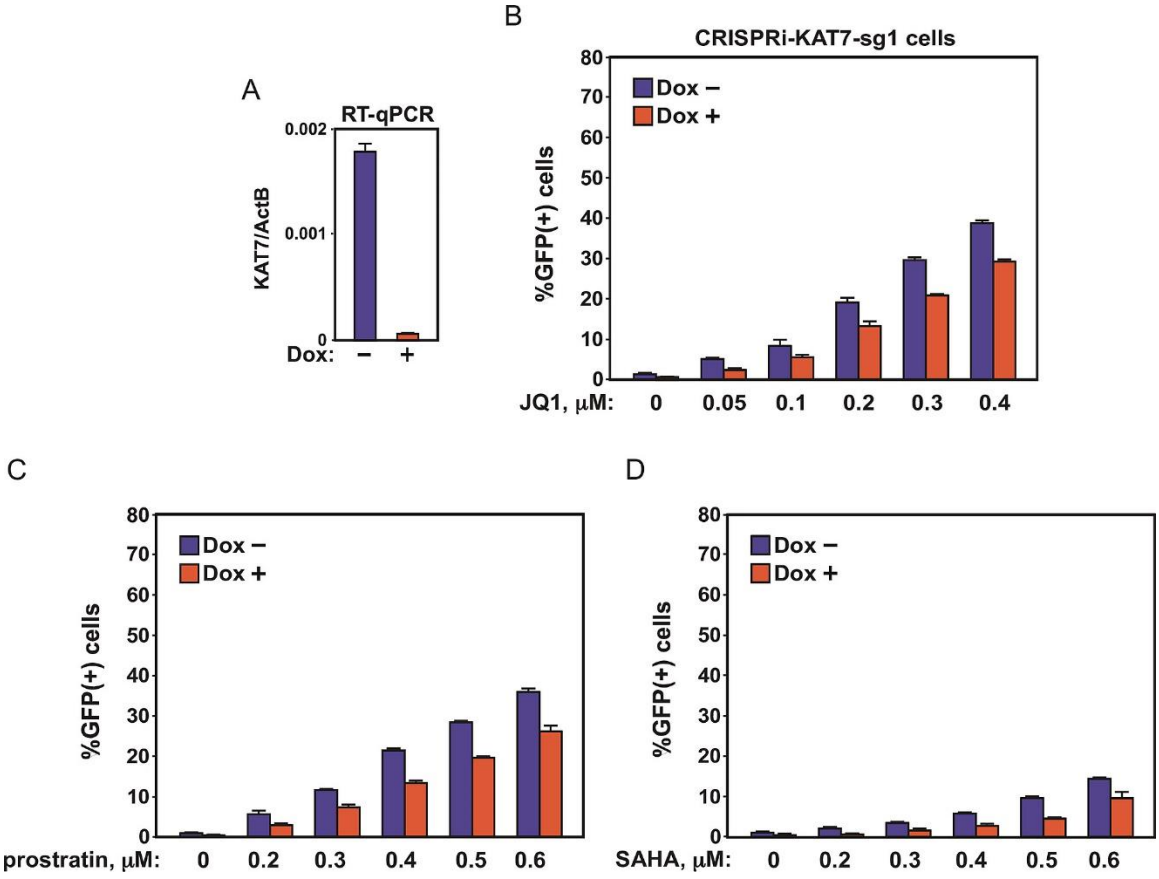

Figure 3-S2

Figure 3-S3. Antagonizing KAT5 synergizes with JQ1 to promote HIV transcription at largely the elongation stage. Top: a schematic diagram showing the elements of HIV-1 5' LTR and the positions of transcription start site (TSS) and the primer pairs used in RT-qPCR reactions to quantify the short 59-nucloetide (nt) and long 190-nt HIV-1 transcripts. Bottom: CRISPRi-KAT5-sg1 and the parental 2D10 cells were treated with the indicated drugs. Total RNAs extracted from these cells were subjected to RT-qPCR quantifications to determine the short and long HIV-1 transcripts using the indicated specific primers. The qPCR signals were normalized to those of ActB. Each column represents the average of three independent RT-qPCR reactions, with the error bars indicating mean +/- SD.

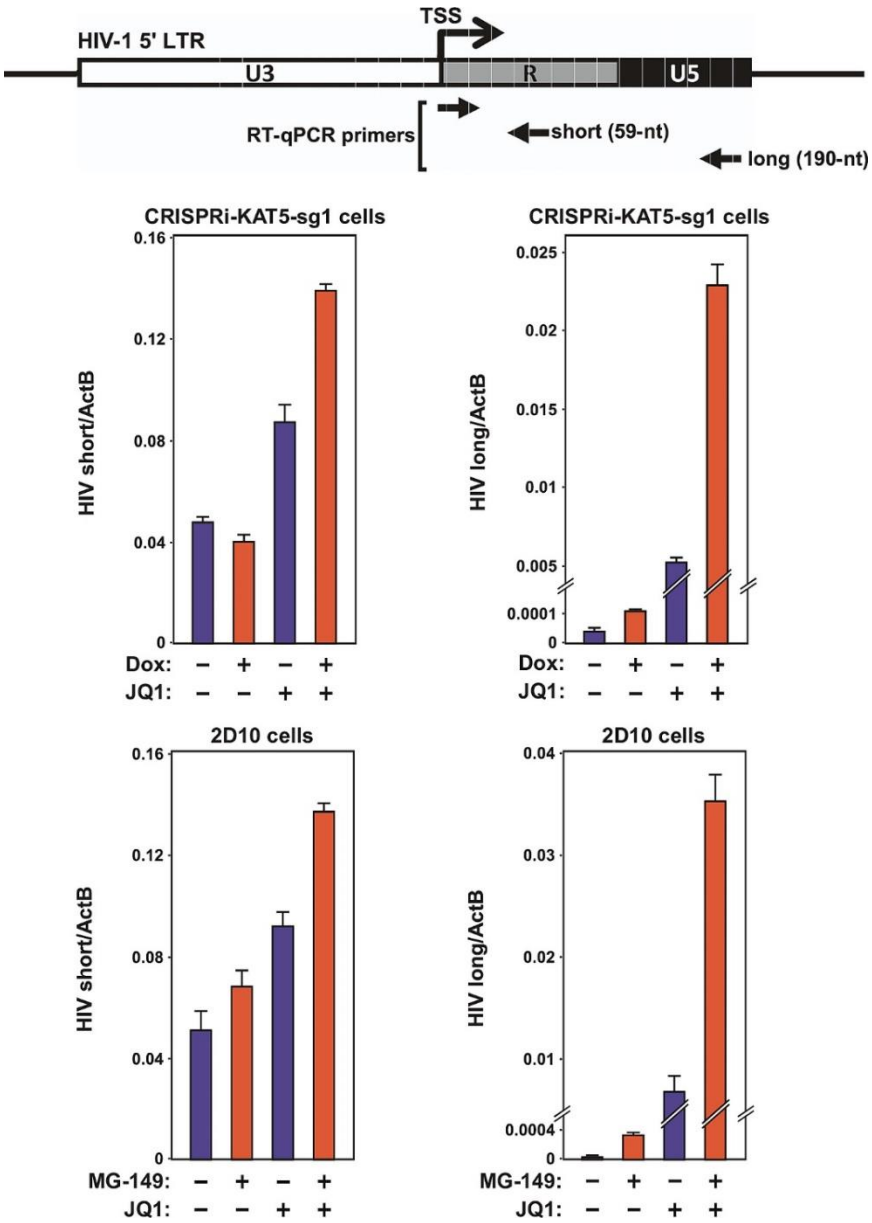

Figure 3-S3

Figure 3-S4. On a per-molecule basis, more Brd4 binds to HIV LTR than does Brd4S and the Brd4-LTR binding is also more sensitive to MG-149-induced AcH4 reduction. NH1 cells containing an integrated HIV-1 LTR were transfected with either an empty vector or vectors expressing the indicated FLAG-tagged Brd4 isoforms, treated by either 0.1% DMSO or 30 μM MG-149 for 18 hr, and subjected to ChIP-qPCR analysis using the anti-FLAG beads to determine the levels of the Brd4 isoforms bound to HIV LTR. The ChIP-qPCR signals were normalized to those of input DNA. The error bars represent mean +/- SD from three independent qPCR reactions. An aliquot of each cell sample was also examined by Western blotting for the proteins labeled on the left.

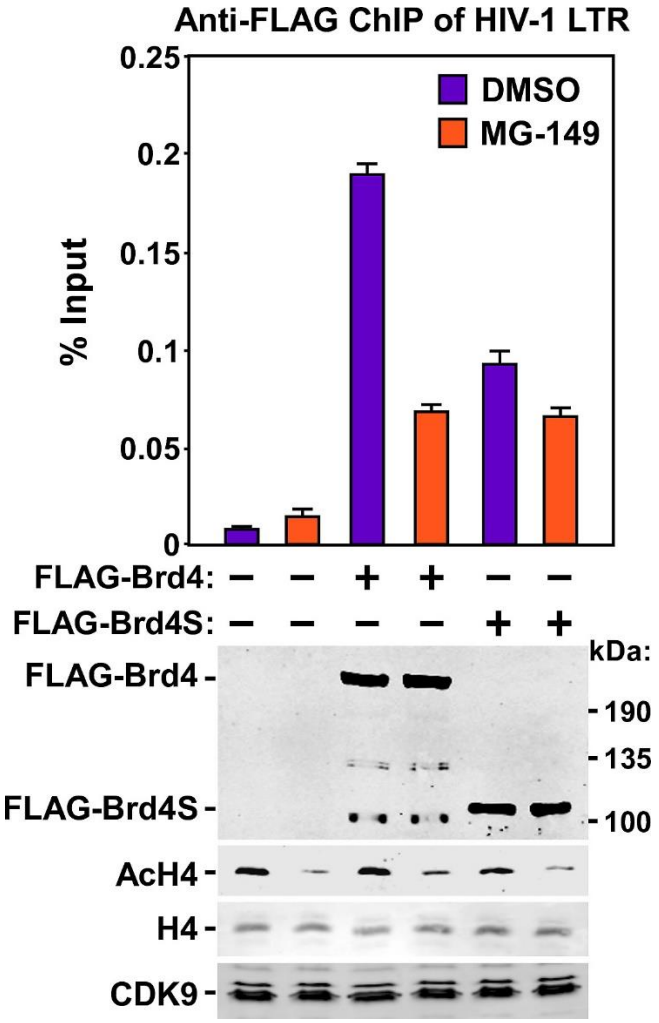

Figure 3-S4

Figure 3-S5. MG-149 fails to potentiate the effect of SAHA, Ingenol or T-cell receptor activation on proviral reactivation in a primary T cell model of latency. A. Latently infected Th17 cells (No stim) were placed in media containing 60 IU/ml IL-2 and then challenged with MG-149 for 24 hr in the presence or absence of SAHA (500 nM), ingenol (20 nM), or α-CD3 antibody (500 ng/ml). Proviral HIV expression was determined by flow cytometry measurements of the percentage of cells that were positive for both Nef and EGFP. Graphed data are from two independent experiments. **B.** Latently infected Th17 cells were stimulated or not with an antibody cocktail of α-CD3/α-CD28 for 24 or 48 hr in the absence or presence of the indicated concentrations of MG-149. Proviral HIV expression was determined by flow cytometry measurements of the percentages of cells positive for both Nef and EGFP. Graphed data for the 24 hr treatment are from four independent experiments and the 48 hr treatment from two experiments.

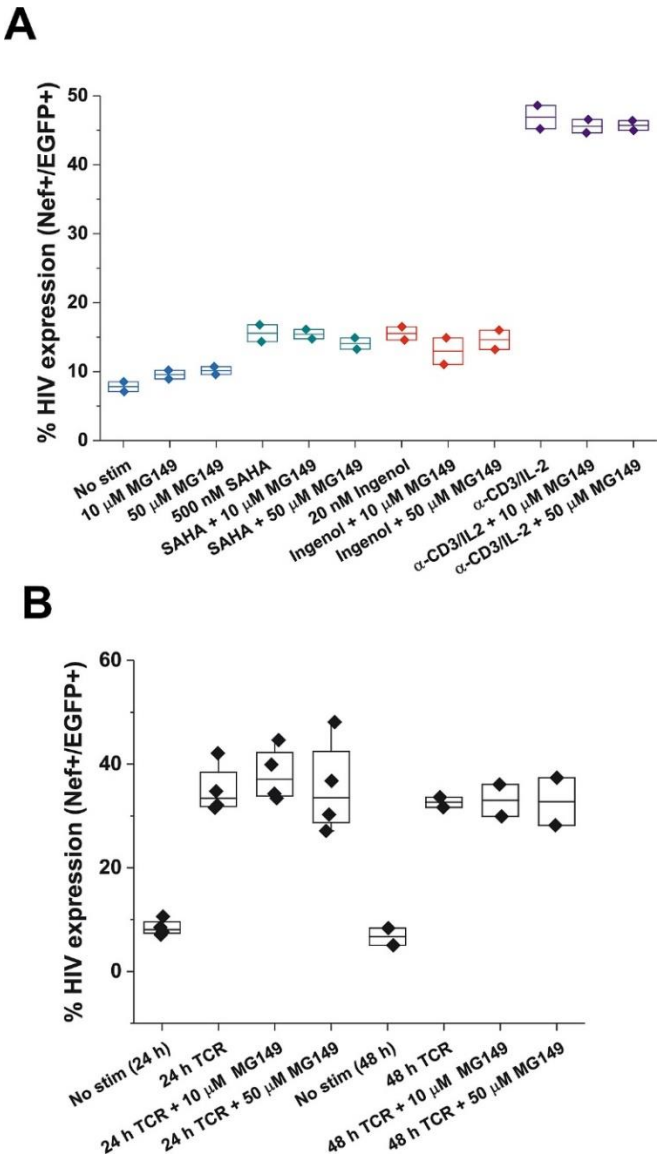

Figure 3-S5

Figure 3-S6. MG-149 does not induce global T cell activation. Primary resting $CD4^+$ T cells were treated for 24 hr with the indicated drugs or their combinations. The levels of T cell activation were accessed by immunostaining of CD25 and CD69, which was then analyzed by flow cytometry.

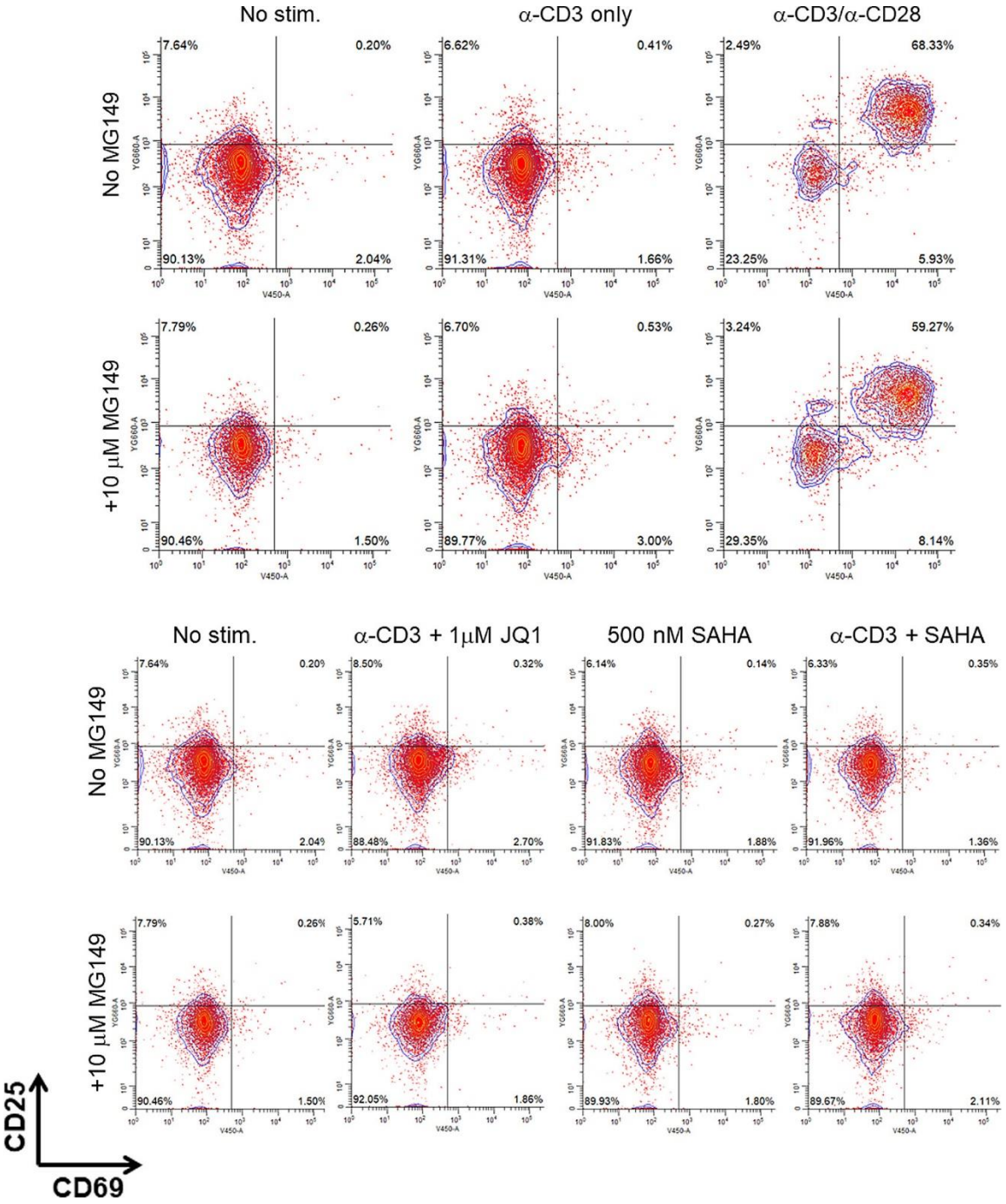

Figure 3-S6

Supplemental Table 3-1. Characteristics of HIV-1–infected study participants.

ID	Age	Sex	Race	Duration of infection (months)	ART regimen	Time on ART (months)	Time on suppressive ART (months)	CD4 count (cells/mm^3)	Peak reported viral load (copies ml^{-1})
1	29	M	A	24	EFV/3TC/TDF	24	21	543	3.55×10^4
2	37	M	A	24	EFV/3TC/TDF	24	15	179	9.19×10^5
3	35	M	A	38	EFV/3TC/TDF	13	9	697	3.52×10^5
4	39	F	A	90	EFV/3TC/TDF	65	33	819	Unknown
5	35	M	A	7	EFV/3TC/TDF	6	3	536	1.42×10^5
6	34	M	A	7	EFV/3TC/TDF	6	3	517	2.56×10^4
7	47	F	A	38	EFV/3TC/TDF	36	26	440	2.42×10^4
8	52	M	A	119	EFV/3TC/AZT	118	81	620	unknown

M, male; F, female; A, Asian; 3TC, lamivudine; TDF, tenofovir disoproxil fumarate; EFV, efavirenz; AZT, azidothymidine.

Chapter 4

Reiterative Enrichment and Authentication of CRISPRi Targets (REACT) identifies the proteasome as a key contributor to HIV-1 latency

Summary

The establishment of HIV-1 latency gives rise to persistent chronic infection that requires life-long treatment. To reverse latency for viral eradiation, the HIV-1 Tat protein and its associated ELL2-containing Super Elongation Complexes (ELL2-SECs) are essential to activate HIV-1 transcription. Despite efforts to identify effective latency-reversing agents (LRA), avenues for exposing latent HIV-1 remain inadequate, prompting the need to identify novel LRA targets. Here, by conducting a CRISPR interference-based screen to reiteratively enrich loss-of-function genotypes that increase HIV-1 transcription in latently infected $CD4^+$ T cells, we have discovered a key role of the proteasome in maintaining viral latency. Downregulating or inhibiting the proteasome promotes Tat-transactivation in cell line models. Furthermore, the FDA-approved proteasome inhibitors bortezomib and carfilzomib strongly synergize with existing LRAs to reactivate HIV-1 in $CD4^+$ T cells from antiretroviral therapy-suppressed individuals without inducing cell activation or proliferation. Mechanistically, downregulating/inhibiting the proteasome elevates the levels of ELL2 and ELL2-SECs to enable Tat-transactivation, indicating the proteasome-ELL2 axis as a key regulator of HIV-1 latency and promising target for therapeutic intervention.

Introduction

Transcriptional silence of integrated HIV-1 proviruses in a minority of infected $CD4^+$ T cells is a key signature of the latent viral reservoirs that necessitate a lifelong antiretroviral therapy (ART) to maintain their silence (48,49). Strategies to expose the latently infected cells for immune recognition and clearance in individuals on ART rely on latency reversing agents (LRAs) to reactivate proviral transcriptions (45,53,54). To date, multiple clinical trials have tested a variety of LRAs that are dominated by histone deacetylase (HDAC) inhibitors and NF-κB agonists (170). However, only modest increases in viral transcription with little to no reservoir reduction are induced by these drugs, which often also produce serious adverse effects (118).

Compared with the mechanisms used by the HDAC inhibitors and NF-κB agonists to relax chromatin and recruit RNA polymerase (Pol) II to the HIV-1 promoter, respectively, a less leveraged but arguably more specific and prominent feature of the HIV-1 transcriptional control is the Tat-dependent transition of Pol II from promoter-proximal pausing to productive elongation (46,65). This rate-limiting step fuels a potent positive-feedback circuit to activate viral transcription without causing T cell activation (72).

Mechanistically, Tat stimulates HIV-1 transcriptional elongation by recruiting a specific host co-activator, the human Super Elongation Complex (SEC) (90,91), to the paused Pol II through forming the Tat-SEC complex on the TAR RNA, a stem-loop structure located at the 5' end of the nascent viral transcript (101,103). The two critical components of the SEC, P-TEFb and ELL2, stimulate Pol II elongation by different mechanisms and can thus synergistically induce the production of full-length viral transcripts (65). In addition to residing in the SEC, P-TEFb also interacts with the bromodomain protein Brd4, which competitively inhibits the Tat-SEC interaction (105,106). The small molecule suppressor JQ1 binds to Brd4 to antagonize its inhibitory action on Tat-SEC, leading to the activation of HIV-1 transcription and latency reversal (108,109,171). Notably, JQ1 is shown to synergize with other LRAs to reactivate latent HIV-1 in a number of pre-clinical trials involving CD4+ T cells from the ART-suppressed individuals (110-112,136,172).

A typical SEC contains P-TEFb, as well as one of each of the three pairs of homologous proteins: ELL1/ELL2, AFF1/AFF4, and ENL/AF9. Owing to the ability of these proteins to create multiple different combinations among them, a family of related SEC complexes exists in cells. Our recent study shows that a low-abundance subset of SECs containing ELL2 and AFF1 play a predominant role in cooperating with Tat to reverse HIV-1 latency (158). In fact, by simply increasing the cellular level of ELL2, a highly unstable protein due to its polyubiquitination by the E3 ubiquitin ligase Siah1 and subsequent degradation by the proteasome (90,96,173), it was possible to activate latent HIV-1 without using any drugs (158).

The complexity of the mechanisms that contribute to HIV-1 latency suggests that combinatorial LRAs from distinct mechanistic classes are necessary to expose the hidden viruses (53). To identify novel classes of LRAs that cooperate well with the existing ones, we developed a genetic screen based on CRISPR interference (CRISPRi) (174) to look for additional host restriction factors that may represent previously unrecognized drug targets. By selecting authentic and effective CRISPRi targets through reiterative enrichments, we have identified several subunits of the proteasome as novel host factors that strongly inhibit HIV-1 transcription and promote latency. Our data indicate that the proteasome preferentially inhibits the Tat-dependent HIV-1 transcription by decreasing the cellular level of ELL2, which in turn prevents formation of the ELL2-containing SECs. Furthermore, several FDA-approved proteasome inhibitors are shown to act synergistically with the existing LRAs to activate HIV-1 without inducing cell activation or proliferation in both cell line-based latency models and primary T cells from HIV-1-infected and ART-suppressed individuals. Collectively, our data indicate that targeting the proteasome-ELL2 axis provides a new avenue to expose the latent HIV-1 proviruses.

Experimental Procedures

Reiterative Enrichment and Authentication of CRISPRi Targets (REACT)

All the Jurkat-based cells were maintained in RPMI 1640 medium with L-glutamine, 10% fetal bovine serum (FBS), 100 IU/ml penicillin, and 100 μg/ml streptomycin in 5% CO_2 at 37℃. To prepare the CRISPR interference (CRISPRi) platform, Jurkat 2D10 cells (119) were transduced by pHR-TRE3G-Krab-dCas9-P2A-mCherry (144) and pLVX-advanced-TetOn (from IGI, UC Berkeley). A clone (named "2D10-CRISPRi") expressing KRAB-dCas9-HA-P2A-mCherry in response to doxycycline (Dox) was first selected by fluorescence-activated cell sorting (FACS) and then verified by Western blotting.

To start REACT, a genome-wide CRISPRi sgRNA library in pSico-based vector with BFP marker and puromycin-resistance (144) were packaged using a 3rd generation lentiviral packaging system and transduced into 2×10^8 2D10-CRISPRi cells at an efficiency of ~40%. Two days after transduction, the non-transduced cells were killed by adding puromycin into the medium to a final concentration of 1 μg/ml for 3 days, at which time more than 95% of the surviving cells were BFP-positive as confirmed by FACS. About 5×10^7 of the cells were pooled and treated with 1 μg/ml Dox for 3 days in 400 ml medium. The Dox-treated cells were then selected by FACS for the GFP/mCherry/BFP triple-positive phenotype.

Then sgRNA cassettes were PCR-amplified from the genomes of the selected cells using the primer pair: REACT-5F (5'-GCACAAAAGGAAACTCACCCT-3')/ REACT-3R (5'-CGACTCGGTGCCACTTTTTC-3'). After digestion with BstXI and BlpI, the cassettes were cloned into the empty library vector pSico-BFP-puro (144) and then amplified in *E. coli* and extracted as an enriched library, which was then transduced into the original 2D10-CRISPRi cells for the next round of REACT. Upon repeating the procedure 4 times, the sgRNA sequences from the round 4-enriched library and original

library were subjected to deep-sequencing by using the index primer pairs CRISPRi_TSS_12_P5/CRISPRi TSS_12_P7 for round 4-enriched library, and CRISPRi_TSS_6_P5/CRISPRi TSS_6_P7 for the original library, and sequenced by using the primer CRISPRi TSS_seq V2. The sequences of the primers were listed in Table 4-S2. The deep-sequencing results were then converted into sgRNA counts by using the ScreenProcessing tool (175). The fold of enrichment for each sgRNA sequence was calculated based on its reads per million in the round 4-enriched library divided by those in the original library and presented on a scatter plot.

Cell line-based latency reversal assay

The Jurkat-based HIV-1 latency models 2D10 and J-Lat A2 (129) were first treated in triplicates with 0.1% DMSO, 1 μg/ml Dox or the various concentrations of proteasome inhibitors, and then re-suspended in cold phosphate-buffered saline (PBS). Quantification of the GFP+ cells was conducted on a BD Bioscience LSR Fortessa X20 cytometer. The data were analyzed with the Flowjo™ software and plotted as bar graphs.

CRISPRi in 1G5-/+Tat cells and luciferase reporter assay

The preparations of the CRISPRi platform in Jurkat 1G5 (146) and 1G5+Tat cells (147) (both kind gifts from Dr. Melanie Ott in the Gladstone Institutes, San Francisco) were the same as in 2D10 cells described above. DNA oligos containing the sgRNA sequences identified by REACT and a negative control (5'-GCAGCATGCTCGCCTGGCTGC-3') were synthesized and cloned into the pSico-BFP-puro vector and stably transduced into the 1G5-/+Tat-CRISPRi cells. For the luciferase assay, $1x10^6$ of the cells were treated with 0.1% DMSO or 1 μg/ml Dox in triplicates for three days, and then lysed in 200 μl 1 × Reporter Lysis Buffer (Promega), frozen-thawed once, and centrifuged at 20,800 × g for 1 min at 4 ℃. Luciferase activities in the supernatants were measured by using the Luciferase Assay System (Promega) on a Lumat LB 9501 luminometer. The relative luciferase units in the Dox-treated cells were normalized to those of the DMSO-treated cells and plotted as bar graphs.

Reverse transcription and real-time quantitative PCR (RT-qPCR) assay

Total cellular RNAs were extracted by using the RNeasy kit (Qiagen) and reverse transcribed by M-MLV Reverse Transcriptase (VWR, M1701) with random hexamers (Invitrogen, 48190-011). The cDNAs were subjected to qPCR using DyNAmo HS SYBR Green qPCR kit (Fisher, F-410L) on a CFX96 system (Bio-Rad) with the primer pairs listed in Table 4-S2. All reactions were carried out in triplicates. The PCR signals were normalized to those of ActB and displayed as bar graphs.

Stable shRNA knockdown (KD) in Jurkat 2D10 cells

Jurkat 2D10 cells were transduced with the pLKO.1-puro lentiviral vectors containing shScramble (5'-CCTAAGGTTAAGTCGCCCTCG-3'), shPSMA1 (5'-AATGATTATACAGACCCTTTC-3'), or shPSMB1 (5'-AAGACATCTTTCACCAGCCGC-3') sequences. Two days after transduction, puromycin was added to the medium to a final concentration of 1 μg/ml to obtain and maintain the stable KD pools. The KD efficiencies of the pools were examined by RT-qPCR and Western blot.

Proteasome inhibitor treatment *in vitro*

Jurkat 2D10 or J-Lat A2 cells were aliquoted into 24-well plates in 1 ml medium at the density of 5×10^5 cells/ml. Each of the following drugs was added to the cells in triplicate at the indicated concentrations: MG132 (Sigma, M7449), Bortezomib (Millennium, Velcade, PS-341, from Selleckchem, S1013), Carfilzomib (ONYX, PR171, from Selleckchem, S2853), Ixazomib (Millennium, MLN2238, from Selleckchem, S2180), Ixazomib citrate (MLN9708, from Selleckchem, S2181), Oprozomib (ONYX, ONX0912, from Selleckchem, S7049), and Delanzomib (CEP18770, from Selleckchem, S1157). For control groups, 0.1% DMSO was used. After 16~20 hours treatment, the cells were subjected to FACS to measure the percentages of GFP+ cells as described above. Cell viabilities were determined by Forward Scatter vs. Side Scatter gating using untreated cells as the control.

Co-immunoprecipitation followed by Western blotting

Approximately 2×10^8 2D10 cells maintained in 400 ml RPMI medium were treated with 10 nM bortezomib or 0.1 % DMSO for 18 hours. The following operations were all carried out at 4 ℃ or on ice unless stated otherwise. The cells were harvested and swollen in 4 ml hypotonic buffer A [10 mM HEPES-KOH (pH 7.9), 1.5 mM $MgCl_2$ and 10 mM KCl] for 5 min and then centrifuged at 362 g for 5 min. The cells were then disrupted by grinding 20 times with a Dounce tissue homogenizer (Fisher K8853000007) in 4 ml buffer A, followed by centrifugation at 3,220 g for 10 min to collect the nuclei. The nuclei were then extracted in 450 μl buffer C [20 mM HEPES-KOH (pH 7.9), 0.42 M NaCl, 25 % glycerol, 0.2 mM EDTA, 1.5 mM $MgCl_2$, 0.4 % NP-40, 1 mM dithiothreitol and 1 × protease inhibitor cocktail] for 30 min and then subjected to centrifugation at 20,800g for 10 min. The supernatant (nuclear extracts or NE) was mixed with 4 μg anti-CDK9 antibody (90) for 45 min, and then with 15 μl Protein A agarose (Invitrogen 15918-014) for 1 hr with rotation. After being washed three times with 1 ml buffer D [20 mM HEPES-KOH (pH 7.9), 0.3 M KCl, 15 % glycerol, 0.2 mM EDTA and 0.4 % NP-40], the beads were eluted with 30 μl 0.1 M glycine-HCl (pH 2.0) at room temperature for 15 min. For western blot, 3% of the NE input and 50% of the immunoprecipitation eluate from each treatment condition were analyzed.

The primary antibodies used for Western blots are listed in Table 4-S3. The primary antibodies were diluted to 1 μg/ml and the secondary antibodies were diluted 10,000-fold.

Isolation of resting $CD4^+$ T cells from ART-suppressed individuals and measurement of intracellular HIV-1 mRNA after drug treatment

This part of the study was approved by the UCSF Committee on Human Research. All research participants were recruited from the UCSF SCOPE cohort after obtaining written informed consent, and all subject data and specimens were coded to protect confidentiality. The participants met strict selection criteria and had well-documented persistent viral suppression for over 7 years (Table 4-S1). Fresh blood (100 ml) was collected and peripheral blood mononuclear cells (PBMCs) were isolated from whole blood using Lymphocyte Separation Medium (Corning 25-072-CI). $CD4^+$ T cells

were isolated from PBMCs using negative selection by EasySep kit (STEMCELL 19052) according to the manufacturer's instructions.

Isolated $CD4^+$ T cells were aliquoted at a density of 1×10^6 cells per well in 1 mL RPMI medium plus 10% FBS in a 48-well flat-bottom plate. The cells were treated with 0.2% DMSO, 25 μl (1:1 bead:cell ratio) αCD3 + αCD28-conjugated beads (Dynal 11131D), 50 ng/ml (81 nM) PMA + 1 μM Ionomycin, 1 μM vorinostat, 1 μM JQ1, 40 nM romidepsin, or 10 nM bryostatin alone or in combination with 10 nM or 100 nM bortezomib or carfilzomib for 24 hr. All drugs were prepared in the culture medium from stock solutions dissolved in DMSO. After the treatment, total RNAs from the cells were extracted by 1 ml TRIzol™ Reagent (Invitrogen 15596026). The RNAs were reverse-transcribed using M-MLV Reverse Transcriptase (VWR, M1701) with random hexamers (Invitrogen, 48190-011). The HIV-1 RNA was quantified by qPCR using DyNAmo HS SYBR Green qPCR kit (Fisher, F-410L) with the HIV-1-specific primers F522-43 (5'-GCCTCAATAAAGCTTGCCTTGA-3') and R626-43 (5'-GGGCGCCACTGCTAGAGA-3') (172) on a CFX96 system (Bio-Rad). All reactions were carried out in triplicates. The PCR signal from each drug combination was normalized to the DMSO group for each individual to calculate the fold induction and displayed in scatter plots.

Quantitative analysis of synergy of latency reversing agent combinations

We adapted the Bliss independence model (176) as implemented by previous studies (112,136,172) to test for synergy when different concentrations of bortezomib and carfilzomib were combined with JQ1 or romidepsin *ex vivo*.(112,136,172) to test for synergy when different concentrations of bortezomib and carfilzomib were combined with JQ1 or romidepsin *ex vivo*. For drugs x and y, we used the equations $fa_{xyP} = fa_x + fa_y - (fa_x)(fa_y)$, and $\Delta fa_{xy} = fa_{xyO} - fa_{xyP}$. Here, fa_x and fa_y represent the observed effects of drug x and drug y respectively, fa_{xyP} represents the predicted fraction affected by the combination of drug x and drug y if there is no synergy or antagonism between drug x and drug y; fa_{xyO} represents the observed effect when x and y were tested together. Calculation of fa_x utilized the following approach adapted from the above cited publications: fa_x = (HIV RNA copies with drug x - background copies with DMSO) / (HIV RNA copies with αCD3-αCD28 stimulation - background copies with DMSO). The copy number of HIV RNA was determined by extrapolation against a 7-point standard curve (1–1,000,000 copies) prepared from a synthetic HIV cDNA fragment. In cases where one or more experimental drug conditions resulted in RNA expression exceeding the αCD3-αCD28 stimulation, we imputed the highest HIV RNA value in that experiment +1 to represent the denominator for calculation of fa_x. Statistical significance was calculated by two-tailed Student's t-test comparing fa_{xyO} and fa_{xyP} (*: $p < 0.05$, **: $p < 0.01$, and ***: $p < 0.001$). With this model, $\Delta fa_{xy} > 0$ with statistical significance ($p < 0.05$) indicates synergy, $\Delta fa_{xy} = 0$ indicates additive effect (Bliss independence), $\Delta fa_{xy} < 0$ with statistical significance indicates antagonism.

$CD4^+$ T cell activation assay

$CD4^+$ T cells isolated from HIV-infected ART-suppressed individuals were treated with 0.2% DMSO, 50 ng/ml (81 nM) PMA and 1 μM Ionomycin, 1 μM vorinostat,

10 nM bortezomib, 100 nM bortezomib, 10 nM carfilzomib, or 100 nM carfilzomib for 24 hours. The cells were stained with LIVE/DEAD Cell Stain Kit (Invitrogen, L34955), and then stained with PE-conjugated mouse anti-Human CD69 antibody (BD Biosciences, 555531), and FITC-conjugated mouse anti-Human CD25 antibody (BD Biosciences, 555431). Flow cytometry was conducted on a BD Bioscience LSR Fortessa X20 cytometer, and data were analyzed using the Flowjo software.

$CD4^+$ T cell proliferation assay

$CD4^+$ T cells isolated from HIV-infected ART-suppressed individuals were stained with 10 μM 5(6)-carboxyfluorescein N-hydroxysuccinimidyl ester (CFSE, Abcam ab113853) for 15 min. The cells were treated subsequently with 0.2% DMSO, 10 nM bortezomib, 100 nM bortezomib, 10 nM carfilzomib, or 100 nM carfilzomib for 24 hr, and then washed and cultured for another 3 days in fresh medium. The cells were stained with LIVE/DEAD Cell Stain Kit (Invitrogen, L34955) and PE-conjugated anti-human CD4 Antibody (BioLegend, 317410). Flow cytometry and data analysis were conducted as described above.

$CD4^+$ T cell viability assay

$CD4^+$ T cells isolated from HIV-infected ART-suppressed individuals were treated with the various drugs for 4 days as described above. On day 1, 2, 3, and 4, an aliquot of cells from each treatment was stained with LIVE/DEAD Cell Stain Kit (Invitrogen, L34955). Untreated cells were used for day 0. Flow cytometry and data analysis were conducted as described above.

Results

Reiterative Enrichment and Authentication of CRISPRi Targets (REACT) identifies novel HIV-1 restriction factors in Jurkat 2D10 cells

To identify novel human genes that inhibit HIV-1 expression, we set up a screen for the loss-of-function genotypes that could lead to the activation of latent HIV-1 provirus in the Jurkat-based 2D10 cell line, a widely used post-integration latency model with the d2EGFP-coding sequence in place of the viral *nef* gene in the proviral genome (119). We first generated a 2D10-based TetOn mCherry-dCas9-KRAB cell line (named 2D10-CRISPRi) by adapting an inducible CRISPRi platform (144). The loss-of-function genotypes were produced in this cell line by stably transducing a whole genome sgRNA library containing a total of ~200,000 sgRNAs at an average of 10 per gene (144). Three days after the doxycycline (Dox)-induced production of the dCas9-KRAB fusion, the cells were subjected to fluorescence-activated cell sorting (FACS) to isolate the GFP+ cells containing activated HIV-1 (Fig. 4-1A).

Because the first round of selection did not yield any positive signals that were above the background (Fig. 4-1B), we decided to repeat the procedure a few more times in the hope of enriching the desired genotypes (Fig. 4-1A). To do this, the sgRNA sequences were PCR-amplified from the genome of GFP+ cells isolated from the previous round of FACS and cloned into the empty vector to generate an enriched

sgRNA library, which was then transduced into the original 2D10-CRISPRi cells for the next round of selection (Fig. 4-1A). This procedure, called the Reiterative Enrichment and Authentication of CRISPRi Targets or REACT, was repeated 4 times.

As expected, the CRISPRi-induced HIV-1 activation began to noticeably increase in the cell population starting from round 3 (1.06% GFP+ cells under Dox+ vs. 0.46% spontaneous reactivation under Dox- conditions) and culminating in round 5 of REACT (4.27% vs. 0.55%; Fig. 4-1B). High-throughput sequencing of the enriched library from round 4 and the original library revealed that the most significant enrichment occurred for 7 sgRNAs that target 6 different genes, PSMD1, NFKBIA, CYLD, GON4L, PSMD3, and PSMD8 (Fig. 4-1C & 4-1D). Among these, NFKBIA (aka. IκBα, an inhibitor of NF-κB) and CYLD (a deubiquitinase for NFKBIA) have been reported to encode suppressors of HIV-1 transcription (177,178). It is thus unsurprising that their silencing caused viral activation. On the other hand, PSMD1, PSMD3, and PSMD8, all encoding the canonical proteasome subunits, and GON4L, which encodes a protein found in a transcriptional co-repressor complex with HDAC1 (179), represent previously unreported and potentially novel host restriction factors for HIV-1.

Proteasomal subunits identified by REACT inhibit Tat-dependent HIV-1 transcription

To verify that the 6 genes identified by REACT indeed encode the restriction factors that promote HIV-1 latency, we synthesized and cloned the top 7 sgRNA hits and a negative control sequence into the empty vector used to generate the library, and stably transduced them into the 2D10-CRISPRi cells. The RT-qPCR and FACS analyses indicate that the 7 sgRNAs but not the negative control downregulated the expression of their respective target genes (Fig 2A) and efficiently activated HIV-1 (Fig. 4-2B). Further RT-qPCR analyses demonstrated that after the 6 genes were downregulated by CRISPRi, the HIV-1 *env* mRNA level increased by one to two orders of magnitude (Fig. 4-2C), whereas the cellular GAPDH transcript remained mostly unchanged (Fig. 4-2D).

To further confirm that the proteasomal subunits can be downregulated to activate latent HIV-1, we used siRNAs to knock down the expression of PSMD1, PSMD3, as well as a non-proteasomal REACT target CYLD in two different HIV-1 latency model cell lines, Jurkat 2D10 (119) and J-Lat A2, which contains an integrated, transcriptionally silent LTR-Tat-Flag-IRES-EGFP cassette (129). Similar to the CRISPRi-induced silencing, the knockdown (KD) by RNA interference (RNAi) significantly reactivated latent HIV-1 and enhanced mRNA production from the HIV-1 LTR but not the GAPDH promoter in both systems (Supplemental Fig. 4-S1A-F).

The latent HIV-1 is kept in a transcriptionally silent state. To determine whether the 6 genes identified by REACT directly affected HIV-1 transcription especially Tat-transactivation, we examined the impact of their CRISPRi-induced downregulation (Fig. 4-2E) on expression of an integrated, HIV-1 LTR-driven luciferase reporter gene in Jurkat-based 1G5 (146) and 1G5+Tat cell lines (147). The data indicate that downregulating PSMD1, PSMD3, PSMD8, NFKBIA and CYLD significantly increased the LTR-driven luciferase expression only in 1G5+Tat cells that constitutively express Tat (Fig. 4-2F). In contrast, targeting GON4L by two different sgRNAs did not increase

the LTR activity in either cell line (Fig. 4-2F). Together, these data implicate the proteasomal subunits PSMD1, PSMD3, and PSMD8 as novel host factors that promote HIV-1 latency through directly inhibiting the Tat-dependent viral transcription.

Downregulating proteasomal core subunits or inhibiting proteasomal activity promotes HIV-1 transcription and latency reversal in cell line models

Since PSMD1, PSMD3 and PSMD8 are all located in the 19S regulatory particle of the 26S proteasome (180), we asked whether subunits in the 20S core particle also restrict HIV-1 activation. To answer this question, we used shRNAs to knock down two core subunits, PSMA1 and PSMB1, in 2D10 cells and discovered that the KD potently reactivated latent HIV-1 and increased the viral *env* but not cellular GAPDH mRNA level (Fig. 4-3A-C).

In light of these results, we further tested whether inhibiting the proteasomal function with drugs could also reactivate latent HIV-1. We treated 2D10 and A2 cells with MG132, which is frequently used in research settings, three FDA approved proteasome inhibitors: Bortezomib (Millennium, Velcade, PS-341), Carfilzomib (ONYX, PR171), Ixazomib (Millennium, MLN2238), as well as three inhibitors in late stage clinical trials: Ixazomib citrate (MLN9708), Oprozomib (ONYX, ONX0912), Delanzomib (CEP18770). The results show that when used at nano- to submicro-molar concentrations, all the inhibitors were able to dose-dependently increase the HIV-1 LTR-driven transcription and reverse viral latency in up to ~80% of 2D10 and ~30% of A2 cells (Fig. 4-3D-I). Notably, these drug concentrations only mildly affected cell viability and no more than 50% cell death was observed even under the highest concentrations used (Supplemental Fig. 4-S2A-D). Together, our data indicate that targeting the proteasome by either gene silencing or drugs can effectively promote HIV-1 transcription and latency reversal.

Proteasome inhibitors cooperate with existing LRAs to reactivate latent HIV-1 *ex vivo* without inducing T cell activation or proliferation

To investigate the impact of inhibiting the proteasome in a more clinically relevant setting, we selected the two FDA-approved proteasome inhibitors, bortezomib and carfilzomib, and assessed their abilities to reactivate latent HIV-1 in $CD4^+$ T cells isolated from 11 HIV-1-infected individuals on suppressive ART (Table 4-S1). While 10 nM bortezomib alone was able to reactivate HIV-1 by ~2-fold, the more significant finding is that both inhibitors potently enhanced the latency-reversing effects of existing LRAs at concentrations (10-100 nM; Fig. 4-4A) that were effective in anti-cancer treatments (181,182).

For example, when used alone, 1 μM JQ1, a BET bromodomain inhibitor and known LRA (108,111), reactivated HIV-1 just 4-fold compared to the DMSO control. However, bortezomib and carfilzomib enhanced this effect up to 19-fold (Fig. 4-4A). Furthermore, 40 nM of the HDAC inhibitor romidepsin reactivated HIV-1 5-fold by itself, but produced up to 27-fold activation together with bortezomib or carfilzomib (Fig 4-4A). Finally, while 1 μM of the HDAC inhibitor vorinostat (aka SAHA;) alone did not activate HIV-1 in a statistically significant manner, its combination with bortezomib or carfilzomib caused up to 11-fold activation (Supplemental Fig. 4-S3). Notably, the PKC

agonist bryostatin (183) produced no obvious effect either alone or together with the two proteasome inhibitors (Supplemental Fig. 4-S3).

Using the Bliss Independence model for assessing drug synergism (136,172,176), we discovered that the co-administration of bortezomib (both 10 and 100 nM) or carfilzomib (10 nM) with JQ1 (1 μM) or romidepsin (40 nM) all exhibited robust synergistic activity ($p<0.05$) (Fig. 4-4B). In addition, after 24 hours of treatment at 10 and 100 nM concentrations, which were the same conditions used in the latency-reversal assay, bortezomib and carfilzomib did not induce the surface expression of CD25 and only marginally induced CD69 in cells from 3 patients (Fig. 4-4C & Fig. 4-S4). This is in contrast to the robust induction of the two activation markers by PMA plus ionomycin as well as the considerable CD69 induction by vorinostat (Fig. 4-4C & Fig. 4-S4).

Furthermore, staining with CellTrace CFSE detected no proliferation of live primary $CD4^+$ T cells after the initial 24-hour exposure to the proteasome inhibitors and then additional 3 days of culture in the absence of the drugs (Fig. 4-4D & Fig. 4-S5). Finally, at least during the initial 24-hour treatment, the two inhibitors were well-tolerated by cells from all 3 patients, with the cells from patient #1 showing only a mild loss of viability in the presence of 10 nM carfilzomib for up to 4 days (Fig. 4-S6). In summary, these data demonstrate that the proteasome inhibitors can synergize with existing LRAs to potently reactivate HIV-1 *ex vivo* without inducing activation or proliferation of the patient-derived primary $CD4^+$ T cells.

Inhibition or downregulation of proteasome increases Tat-transactivation by stabilizing ELL2 to form more ELL2-SECs

Consistent with the CRISPRi result in Fig. 4-2E, the bortezomib inhibition of the proteasome also enhanced the HIV-1 LTR-driven transcription in a Tat-dependent manner (Fig. 4-5A). HIV-1 transcriptional elongation, especially the Tat-activated process, is exquisitely controlled by a network of P-TEFb complexes that include the 7SK snRNP, the SECs and the Brd4-P-TEFb complex (Zhou et al. Annual Rev. Biochem). In light of this revelation, we examined whether the levels of P-TEFb, its major known associated factors as well as the NFκB-inhibitor IκBα, which is believed to be regulated at the protein stability level (ref), would change after the downregulation of the proteasome.

Examination of cell extracts by Western blotting demonstrates that among all the proteins analyzed, downregulating the proteasome in Jurkat cells by CRISPRi against PSMD1, PSMD3, and PSMD8 (Fig. 4-5B), or RNAi against PSMA1 and PSMB1 (Fig. 4-5C) consistently elevated the protein levels of only ELL2 and occasionally ELL1 (e.g. after CRISPRi against PSMD1 & PSMD3), which are two alternative subunits of the SECs (Lu et al. PNAS paper). Notably, the mRNA level of ELL2 was not elevated, but the ELL1 mRNA level was somewhat increased in this process (Fig. 4-S7).

The elevated ELL2 protein level as a result of the proteasomal downregulation is consistent with the previous reports showing that ELL2 is tightly controlled by the E3 ubiquitin ligase Siah1-induced degradation by the proteasome (90,96,173). Of note, inhibiting the proteasome by bortezomib also elevated the ELL2 protein level in Jurkat nuclear extract, which in turn resulted in the formation in the nuclei of more ELL2-

containing SECs as revealed by anti-CDK9 immunoprecipitation followed by Western blotting (Fig. 4-5D).

Since among all the related members of the family of SEC complexes, the ELL2-containg SECs play a predominant role in supporting Tat-transactivation and reversing viral latency (158), we compared the bortezomib-induced HIV-1 activation in three different 2D10-based cell lines: WT (119), ΔELL2 (ELL2-knockout) and ΔELL2-R2 (ΔELL2 cells containing an integrated vector expressing ELL2-Flag to approximately the endogenous level) (158). The FACS analysis demonstrates that compared to WT 2D10 cells, the absence of ELL2 in ΔELL2 cells abolished the bortezomib-induced HIV-1 latency reversal, which was efficiently rescued by expressing ELL2-Flag in the ΔELL2-R2 cells (Fig. 4-5E). Taken together, these results indicate the stabilization of ELL2 and elevated formation of the ELL2-SECs as a key mechanism for promoting HIV-1 Tat-transactivation and latency reversal in CD4+ T cells upon the inhibition/downregulation of the proteasome (Fig. 4-5F).

Discussion

In this study, we have developed a CRISPRi-based genetic screen to reiteratively enrich loss-of-function genotypes that promote HIV-1 transcription in latently infected $CD4^+$ T cells. The identified hits include the not-so-surprising factors that suppress the NF-κB pathway (NFKBIA, CYLD) or interact with the HDAC complex (GON4L), as well as unexpected ones in the form of three proteasomal subunits. Our subsequent experiments employing RNAi to target these three and also two other core subunits of the proteasome and testing multiple proteasome inhibitors in two different cell line-based latency models as well as primary $CD4^+$ T cells from HIV-infected individuals on suppressive ART all support the notion that targeting the proteasome can be an effective strategy to expose latent HIV-1.

Interestingly, a study published in 2004 has shown that the mRNA levels of multiple genes encoding the various proteasome subunits are upregulated in latently-infected cell lines and that treating these cell lines with a proteasome inhibitor CLBL stimulated lytic viral replication (184). Based on these early revelations and our current study, which employs multiple proteasome inhibitors and also extends the analysis to the patient-derived primary $CD4^+$ T cells, we propose that the elevated proteasome level in HIV-infected cells is a key mechanism that is used to silence transcription and drive the virus into latency.

Consistent with a previous report showing that the proteasome inhibitors can enhance the P-TEFb-mediated HIV-1 transcriptional elongation (185), our current mechanistic studies pinpoint ELL2, which joins P-TEFb, AFF1 and ENL/AF9 to form the ELL2-SECs especially important for Tat-transactivation (90,158), as the target of the proteasome inhibitors. This mechanistic insight as well as the observation that the Tat-dependent HIV-1 transcription is preferentially affected by downregulating/inhibiting the proteasome (Figs. 2E, 2F & 5A) allow us to propose a model in Fig. 4-5F. According to this model, in latently infected cells, the elevated proteasome level keeps the ELL2 concentration low through polyubiquitination and proteasomal degradation (96). This

prevents the assembly of the ELL2-SECs and blocks HIV-1 transcription. Upon downregulating/inhibiting the proteasome, this blockage is removed to increase the cellular ELL2 level. This results in the formation of more ELL2-SECs to stimulate Tat-transactivation, which in turn generates more Tat to fuel a robust positive feedback loop for HIV to exit latency.

The proteasome has been extensively characterized as a therapeutic target for treating both hematologic and solid tumors; and a number of inhibitors have been developed and approved for this purpose (186,187). Our present study indicates that in addition to their anti-cancer effects, the two FDA-approved proteasome inhibitors, bortezomib and carfilzomib, can also synergize with existing LRAs such as JQ1 and romidepsin to reverse HIV latency in resting $CD4^+$ T cells from ART-suppressed individuals without inducing T cell activation or proliferation (Fig. 4-5). Future studies will inform us whether this effect can also be detected in real clinical settings involving HIV patients. Moreover, the safety and efficacy of combining the two proteasome inhibitors with other LRAs to expose the latent HIV-1 reservoirs for eradication also await further evaluation.

Methodologically, the REACT protocol described here represents a significantly improved strategy to identify authentic genotypes that are hidden in a noisy background. Due to the stochastic nature of HIV-1 transactivation (71,188), the GFP-based HIV-1 latency models always display a small percentage of GFP-positive cells due to a low level of spontaneous viral activation (119,129). This background noise could potentially mask and overwhelm the real signals in any genome-wide screens that must start with a pooled library. The complexity of such libraries causes each genotype to have an extremely low representation in the whole population. Therefore, the phenotypic change induced by a to-be-identified genotype in only a few cells, even though genuine and significant, could easily be lost in a noisy background as exemplified by the first two rounds of REACT in our study. Only through repeated cycles of enrichment, the desired genotypes can eventually emerge and become prominent in the population as demonstrated by the results in rounds 3 to 5 of REACT (Fig. 4-1B). Thus, although this strategy may under-sample genotypes that inhibit cell growth, it can be very useful for identifying the genetic basis of other noisy phenotypes that are not amenable to the single-round genome-wide screens.

Figure 4-1. Reiterative Enrichment and Authentication of CRISPRi Targets (REACT) identifies novel HIV-1 restriction factors in Jurkat 2D10 cells. A. A diagram showing the procedure of REACT that involves repeated cycles of CRISPRi, FACS-selection of GFP+ cells, and subcloning of the sgRNA library to enrich the sgRNA sequences that target host HIV-1 restriction factors. The 2D10-based TetOn mCherry-dCas9-KRAB cell line (called 2D10-CRISPRi) was used. **B.** Representative FACS plots of 2D10-CRISPRi cells non-transduced or transduced by original or enriched sgRNA libraries. The cells were first treated with either DMSO (Dox-) or doxycycline (Dox+) to induce the expression of the KRAB-dCas9-HA-P2A-mCherry fusion protein and then selected by FACS for the GFP+ cells harboring activated HIV-1. **C.** The round 4-enriched and original sgRNA libraries were subjected to high throughput sequencing and the fold of enrichment for each sgRNA was calculated based on its reads per million in the round 4-enriched library divided by those in the original library and presented on a scatter plot, with the 7 most significantly enriched sequences highlighted in green. **D.** Shown are the sequences of the 7 sgRNA highlighted in C and their target genes.

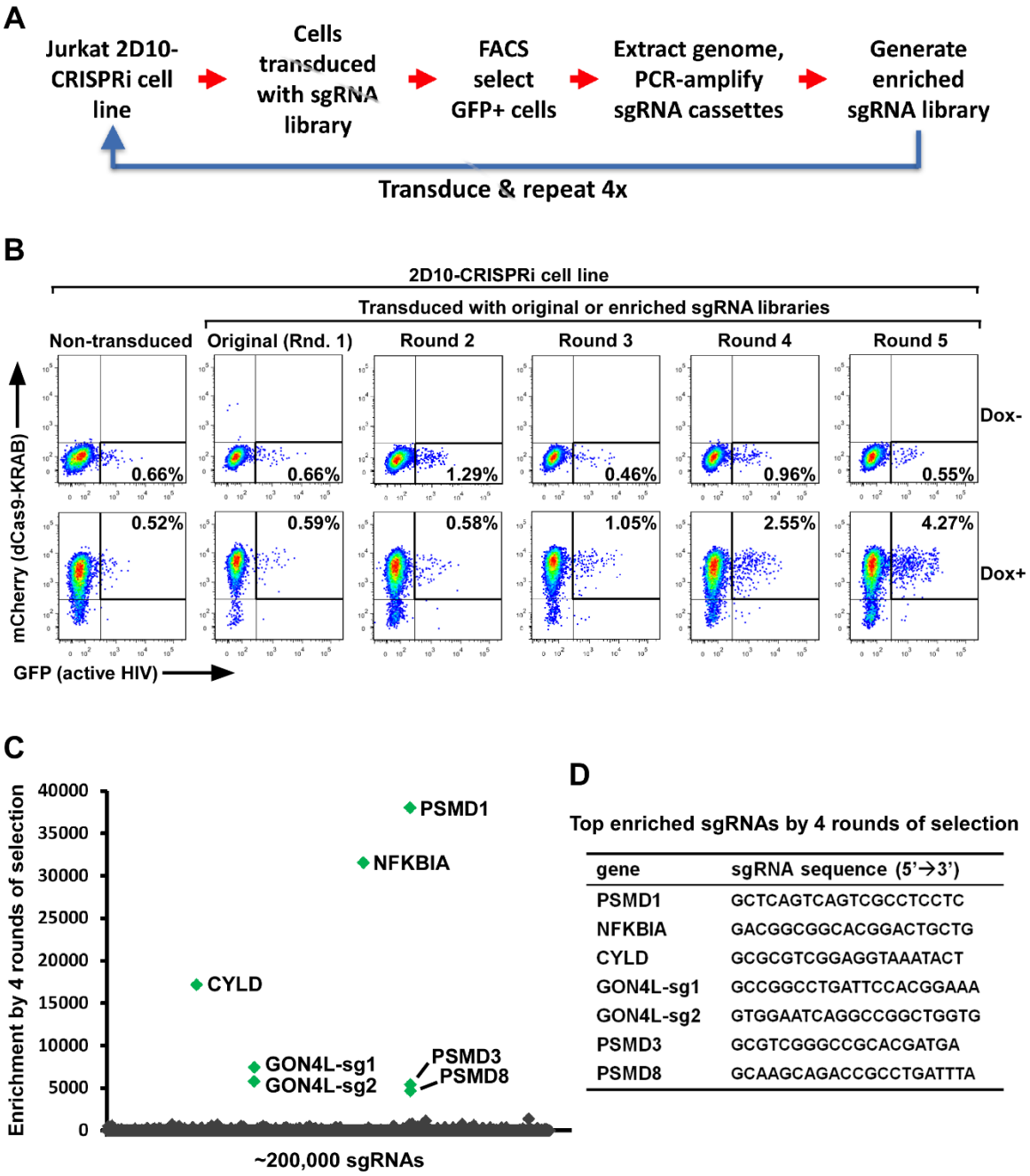
A
Jurkat 2D10-CRISPRi cell line
Cells transduced with sgRNA library
FACS select GFP+ cells
Extract genome, PCR-amplify sgRNA cassettes
Generate enriched sgRNA library
Transduce & repeat 4x
B
2D10-CRISPRi cell line
Transduced with original or enriched sgRNA libraries
Non-transduced
Original (Rnd. 1)
Round 2
Round 3
Round 4
Round 5
Dox-
Dox+
0.66%
0.66%
1.29%
0.46%
0.96%
0.55%
0.52%
0.59%
0.58%
1.05%
2.55%
4.27%
mCherry (dCas9-KRAB)
GFP (active HIV)
C
Enrichment by 4 rounds of selection
40000
35000
30000
25000
20000
15000
10000
5000
0
PSMD1
NFKBIA
CYLD
GON4L-sg1
GON4L-sg2
PSMD3
PSMD8
~200,000 sgRNAs
D
Top enriched sgRNAs by 4 rounds of selection
gene | sgRNA sequence (5'→3')
PSMD1 | GCTCAGTCAGTCGCCTCCTC
NFKBIA | GACGGCGGCACGGACTGCTG
CYLD | GCGCGTCGGAGGTAAATACT
GON4L-sg1 | GCCGGCCTGATTCCACGGAAA
GON4L-sg2 | GTGGAATCAGGCCGGCTGGTG
PSMD3 | GCGTCGGGCCGCACGATGA
PSMD8 | GCAAGCAGACCGCCTGATTTA

Figure 4-1

Figure 4-2. Verification of target specificity and HIV-1 activation potential of the 7 sgRNAs identified by REACT in 2D10 and 1G5-/+Tat cells. A., C., D., & E. The Jurkat-based 2D10-CRISPRi cells (A, C & D) or Jurkat-based 1G5-CRISPRi and 1G5+Tat-CRISPRi cells (E) were stably transduced with the indicated sgRNA expression vectors and then treated with DMSO or Dox. Aliquots of the cells were subjected to RT-qPCR analysis of the mRNA levels of the genes that are denoted by their corresponding qPCR primers. For each gene, the mRNA level detected in the DMSO-treated cells was set to 1. **B.** Results of FACS analysis of the percentages of GFP+ cells within the various cell populations obtained in A. **F.** Results of luciferase activities measured in extracts of the cells described in E. In all panels, error bars represent mean +/- standard deviation (SD) from three experimental replicates. In A, C, E, & F, asterisks denote levels of statistical significance calculated by two-tailed Student's *t*-test (*: $p<0.05$, **: $p<0.01$, and ***: $p<0.001$).

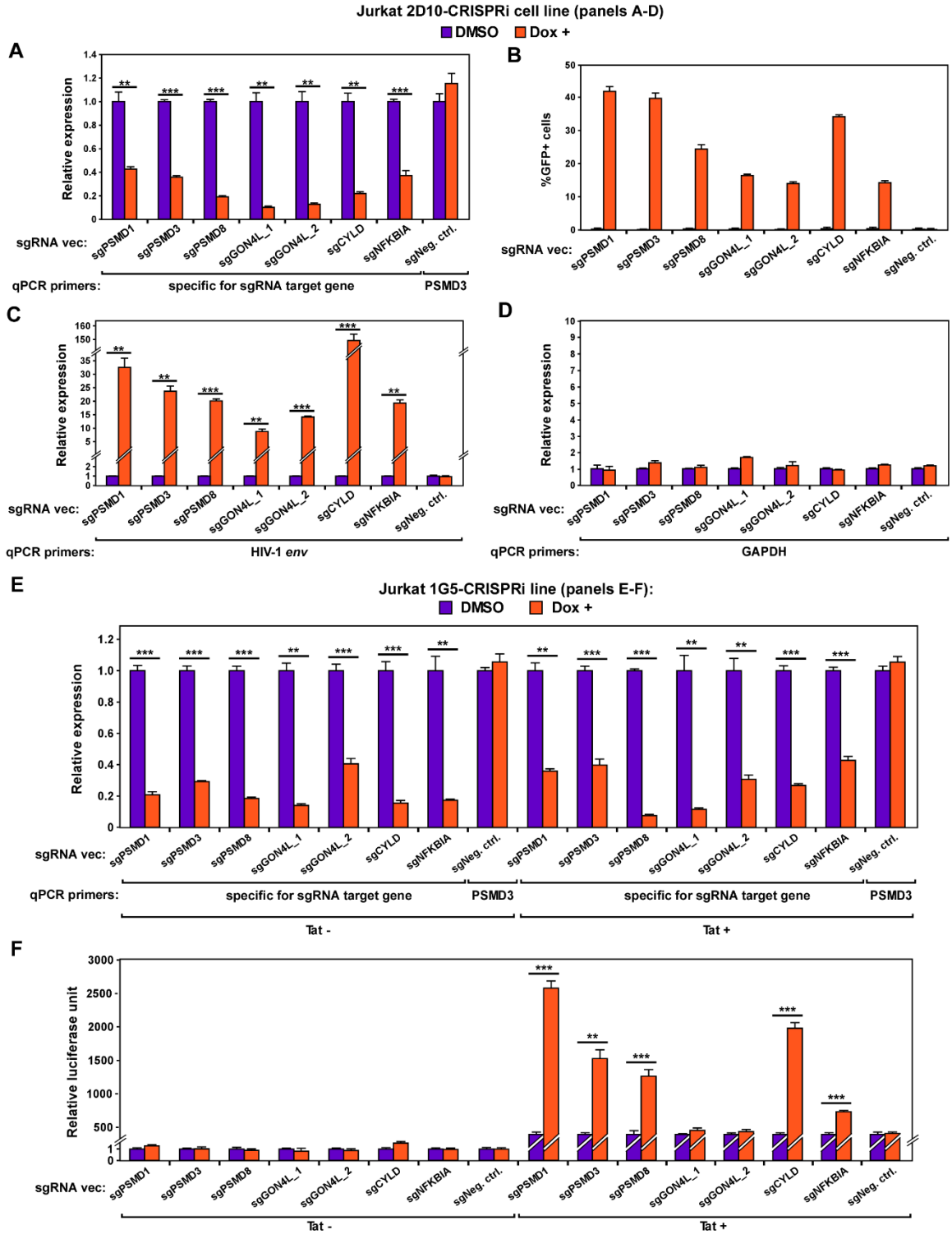
Jurkat 2D10-CRISPRi cell line (panels A-D)
DMSO
Dox +
A
Relative expression
sgRNA vec:
sgPSMD1
sgPSMD3
sgPSMD8
sgGON4L_1
sgGON4L_2
sgCYLD
sgNFKBIA
sgNeg. ctrl.
qPCR primers:
specific for sgRNA target gene
PSMD3
B
%GFP+ cells
C
HIV-1 env
D
GAPDH
Jurkat 1G5-CRISPRi line (panels E-F):
Tat -
Tat +
F
Relative luciferase unit

Figure 4-2

Figure 4-3. Downregulating proteasomal core subunits or inhibiting proteasomal activity promotes HIV-1 transcription and latency reversal in cell line models. A., B., & C. Jurkat 2D10 cells were nucleofected with the indicated siRNAs. Aliquots of the cells were subjected to FACS analysis to detect the percentages of GFP+ cells in each population (A) or RT-qPCR analysis of the mRNA levels produced by the genes labeled at the bottom (B & C). **D., E., F., G., H., & I.** Jurkat 2D10 (D, E, & H) or J-Lat A2 cells (F, G, & I) were treated with the indicated proteasome inhibitors at the indicated concentrations for either 16 or 20 hours as labeled. The treated cells were then subjected to FACS analysis to determine the percentages of GFP+ cells in each population (D, F, H, & I) or RT-qPCR analysis to examine the mRNA levels from the genes denoted by their specific qPCR primer (E & G). In all panels, error bars represent mean +/- SD from three experimental replicates. In B, E, & G, asterisks denote levels of statistical significance calculated by two-tailed Student's *t*-test (*: $p<0.05$, **: $p<0.01$, and ***: $p<0.001$).

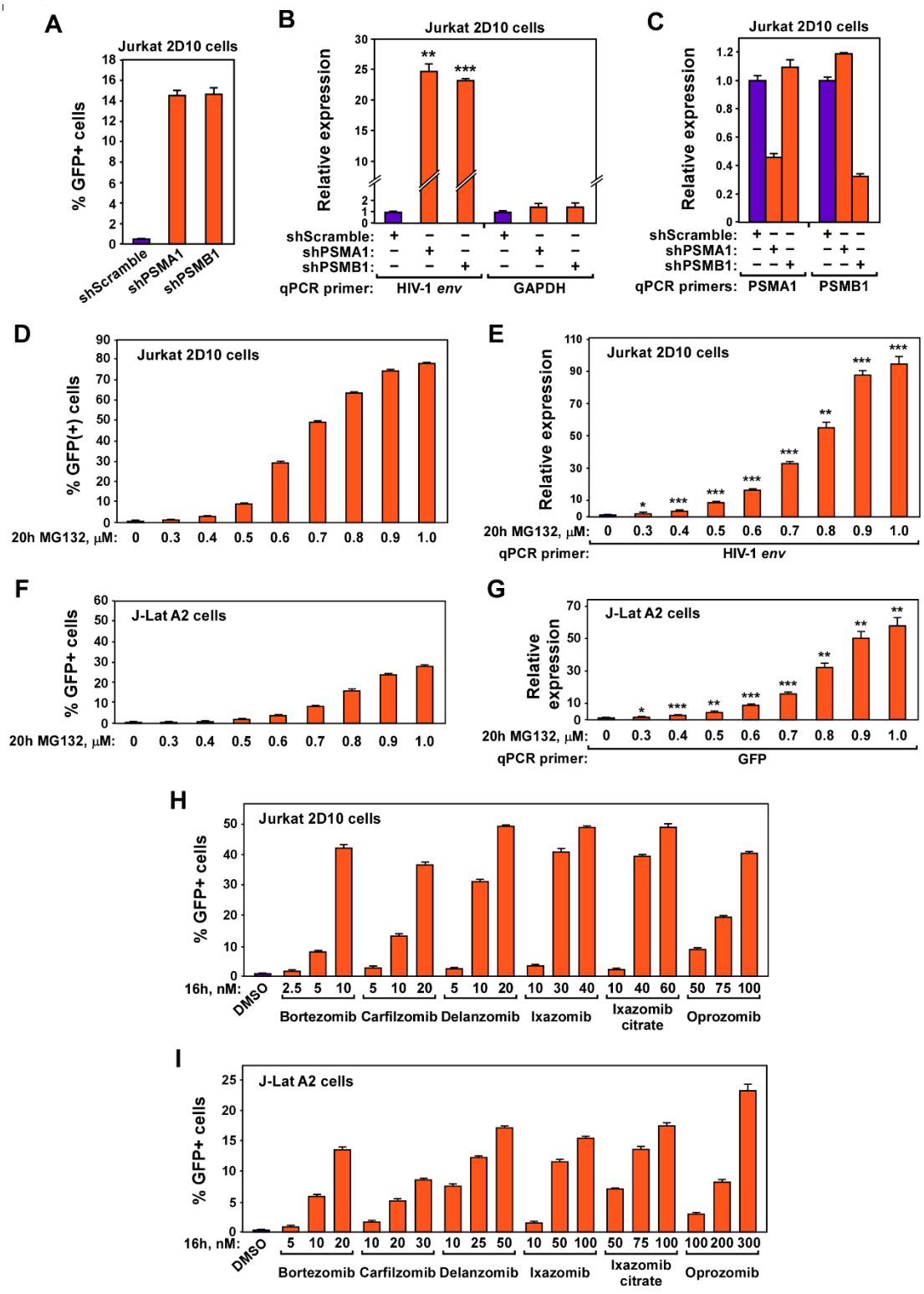
A
Jurkat 2D10 cells
% GFP+ cells
shScramble
shPSMA1
shPSMB1
B
Jurkat 2D10 cells
Relative expression
shScramble:
shPSMA1:
shPSMB1:
qPCR primer:
HIV-1 env
GAPDH
C
Jurkat 2D10 cells
Relative expression
shScramble:
shPSMA1:
shPSMB1:
qPCR primers:
PSMA1
PSMB1
D
Jurkat 2D10 cells
% GFP(+) cells
20h MG132, μM:
E
Jurkat 2D10 cells
Relative expression
20h MG132, μM:
qPCR primer:
HIV-1 env
F
J-Lat A2 cells
% GFP+ cells
20h MG132, μM:
G
J-Lat A2 cells
Relative expression
20h MG132, μM:
qPCR primer:
GFP
H
Jurkat 2D10 cells
% GFP+ cells
16h, nM:
DMSO
Bortezomib
Carfilzomib
Delanzomib
Ixazomib
Ixazomib citrate
Oprozomib
I
J-Lat A2 cells
% GFP+ cells
16h, nM:
DMSO
Bortezomib
Carfilzomib
Delanzomib
Ixazomib
Ixazomib citrate
Oprozomib

Figure 4-3

Figure 4-4. Proteasome inhibitors cooperate with existing LRAs to reactivate latent HIV-1 *ex vivo* without inducing T cell activation or proliferation. A. Freshly isolated $CD4^+$ T cells from ART-suppressed HIV-1-infected individuals were treated with the indicated drug(s) for 24 hr. HIV-1 RNAs in the cells were quantified with RT-qPCR. The PCR signal from each drug combination was normalized to the DMSO group for each individual to calculate the fold induction displayed in the scatter plot. Mean ± standard error of the mean (SEM) is displayed, and the asterisks indicate the levels of statistical significance calculated by two-tailed unpaired t-tests (*: $p<0.05$, **: $p<0.01$, and ***: $p<0.001$). **B.** The Bliss independence model was used to assess drug synergism displayed by the indicated drug combinations. The mean ± standard deviation (SD) is shown for each combination. The asterisks indicate the levels of statistical significance calculated by two-tailed unpaired t-tests to compare between the predicted and observed drug combination effects (*: $p<0.05$, **: $p<0.01$, and ***: $p<0.001$). The dotted horizontal line denotes pure additive effect ($\Delta fa_{xy} = 0$). $\Delta fa_{xy} > 0$ indicates synergy, whereas $\Delta fa_{xy} < 0$ indicates antagonism. **C.** Primary $CD4^+$ T cells isolated from patient #1 were treated with the indicated drugs for 24 hr. The cell surface expression of the T cell activation markers CD69 and CD25 was examined by immunostaining and flow cytometry. **D.** Primary $CD4^+$ T cells from patient #1 were stained with CellTrace CFSE, treated with the indicated drugs for 24 hr, cultured under drug-free conditions for 3 additional days, stained with the anti-CD4 fluorescent antibody, and then analyzed by flow cytometry.

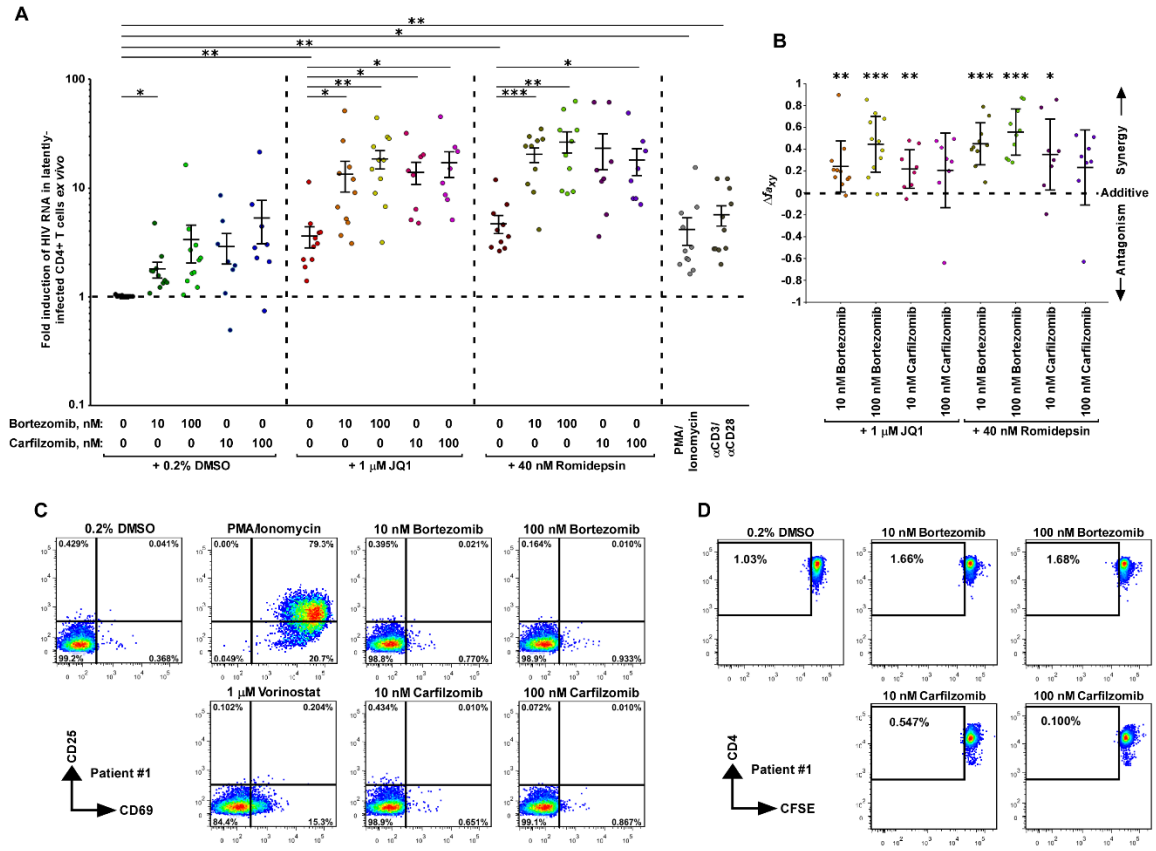
A
Fold induction of HIV RNA in latently-infected CD4+ T cells ex vivo
Bortezomib, nM:
Carfilzomib, nM:
+ 0.2% DMSO
+ 1 μM JQ1
+ 40 nM Romidepsin
PMA/Ionomycin
αCD3/αCD28
B
Δfbxy
Synergy
Additive
Antagonism
10 nM Bortezomib
100 nM Bortezomib
10 nM Carfilzomib
100 nM Carfilzomib
+ 1 μM JQ1
+ 40 nM Romidepsin
C
0.2% DMSO
PMA/Ionomycin
10 nM Bortezomib
100 nM Bortezomib
1 μM Vorinostat
10 nM Carfilzomib
100 nM Carfilzomib
CD25
CD69
Patient #1
D
0.2% DMSO
10 nM Bortezomib
100 nM Bortezomib
1.03%
1.66%
1.68%
10 nM Carfilzomib
100 nM Carfilzomib
0.547%
0.100%
CD4
CFSE
Patient #1

Figure 4-4

Figure 4-5. Inhibition or downregulation of proteasome increases Tat-transactivation by stabilizing ELL2 to form more ELL2-SECs. A. The Jurkat-based 1G5 and 1G5+Tat cells containing an integrated HIV-1 LTR-luciferase reporter construct were treated with the indicated concentrations of bortezomib or 0.1 % DMSO for 20 hr. Luciferase activities in cell extracts were measured and shown. **B. & C.** Results of Western blot analyses of the effects of CRISPRi- or RNAi-induced downregulation of the indicated proteasome subunits in 2D10 cells on levels of the various proteins labeled on the left. **D.** Nuclear extracts (NE) were prepared from 2D10 cells treated with 10 nM bortezomib or 0.1% DMSO (-) for 18 hr and then subjected to immunoprecipitation (IP) with the anti-CDK9 antibody or rabbit total IgG as a control (ctl.). The NE and IP eluates were examined by Western blotting for the indicated proteins. **E.** Result of FACS analysis of the effects of treatment with 7.5 nM bortezomib or 0.1 % DMSO for 18 hr on HIV-1 activation in three different 2D10-based cell lines: WT, ΔELL2 (ELL2-knockout) and ΔELL2-R2 (ΔELL2 cells containing an integrated vector expressing ELL2-Flag to about the endogenous level). **F.** A model showing the proposed mechanism by which the inhibition or downregulation of the proteasome stabilizes ELL2 to form more ELL2-SECs for HIV-1 Tat-transactivation and latency reversal. In A and E, error bars represent mean +/- SD from three experimental replicates.

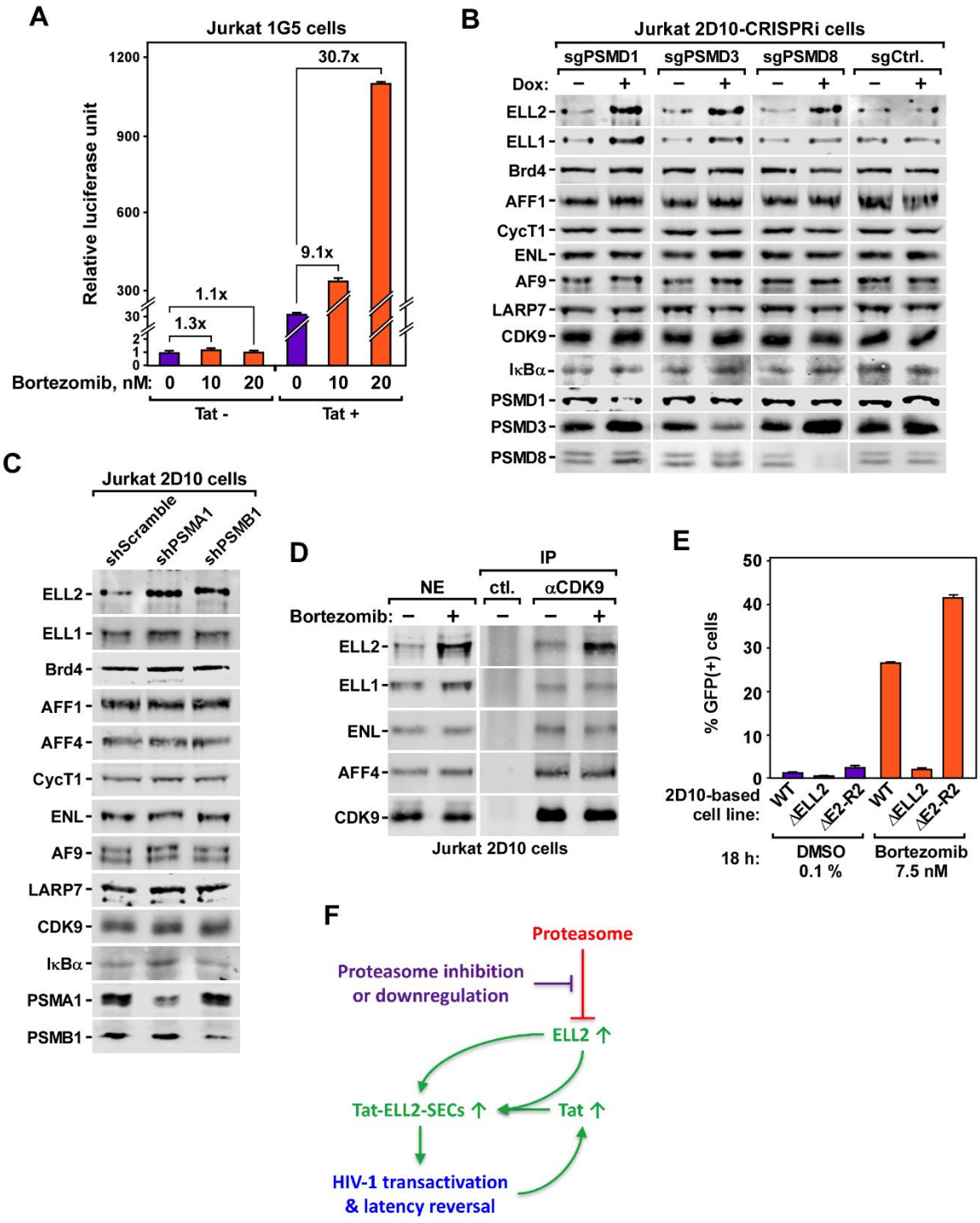
A
Jurkat 1G5 cells
Relative luciferase unit
1200
900
600
300
30
2
1
0
30.7x
9.1x
1.1x
1.3x
Bortezomib, nM: 0 10 20 0 10 20
Tat -
Tat +
B
Jurkat 2D10-CRISPRi cells
sgPSMD1
sgPSMD3
sgPSMD8
sgCtrl.
Dox: – + – + – + – +
ELL2
ELL1
Brd4
AFF1
CycT1
ENL
AF9
LARP7
CDK9
IκBα
PSMD1
PSMD3
PSMD8
C
Jurkat 2D10 cells
shScramble
shPSMA1
shPSMB1
ELL2
ELL1
Brd4
AFF1
AFF4
CycT1
ENL
AF9
LARP7
CDK9
IκBα
PSMA1
PSMB1
D
IP
NE
ctl.
αCDK9
Bortezomib: – + – – +
ELL2
ELL1
ENL
AFF4
CDK9
Jurkat 2D10 cells
E
% GFP(+) cells
50
40
30
20
10
0
2D10-based cell line:
WT
ΔELL2
ΔE2-R2
WT
ΔELL2
ΔE2-R2
18 h:
DMSO 0.1 %
Bortezomib 7.5 nM
F
Proteasome
Proteasome inhibition or downregulation
ELL2 ↑
Tat-ELL2-SECs ↑
Tat ↑
HIV-1 transactivation & latency reversal

Figure 4-5

Figure 4-S1. Verification of target specificity and HIV-1 activation potential of 3 selected REACT-identified genes by RNAi in Jurkat 2D10 and J-Lat cells. A., B., C., D., E., & F. Jurkat 2D10 (A, B, & C) or J-Lat A2 (D, E, & F) cells were nucleofected with siRNAs targeting the indicated genes or nothing (NT). Shown were results of FACS analyses of the GFP-expressing 2D10 (A) or J-Lat A2 (D) cells containing activated HIV-1. Results of RT-qPCR analyses of expression levels of the genes indicated by their corresponding qPCR primers in aliquots of 2D10 (B & C) or J-Lat A2 (E & F) cells were also shown. Error bars in all panels represent mean +/- SD from three experimental replicates. Asterisks denote levels of statistical significance calculated by two-tailed Student's t-test (*: $p<0.05$, **: $p<0.01$, and ***: $p<0.001$).

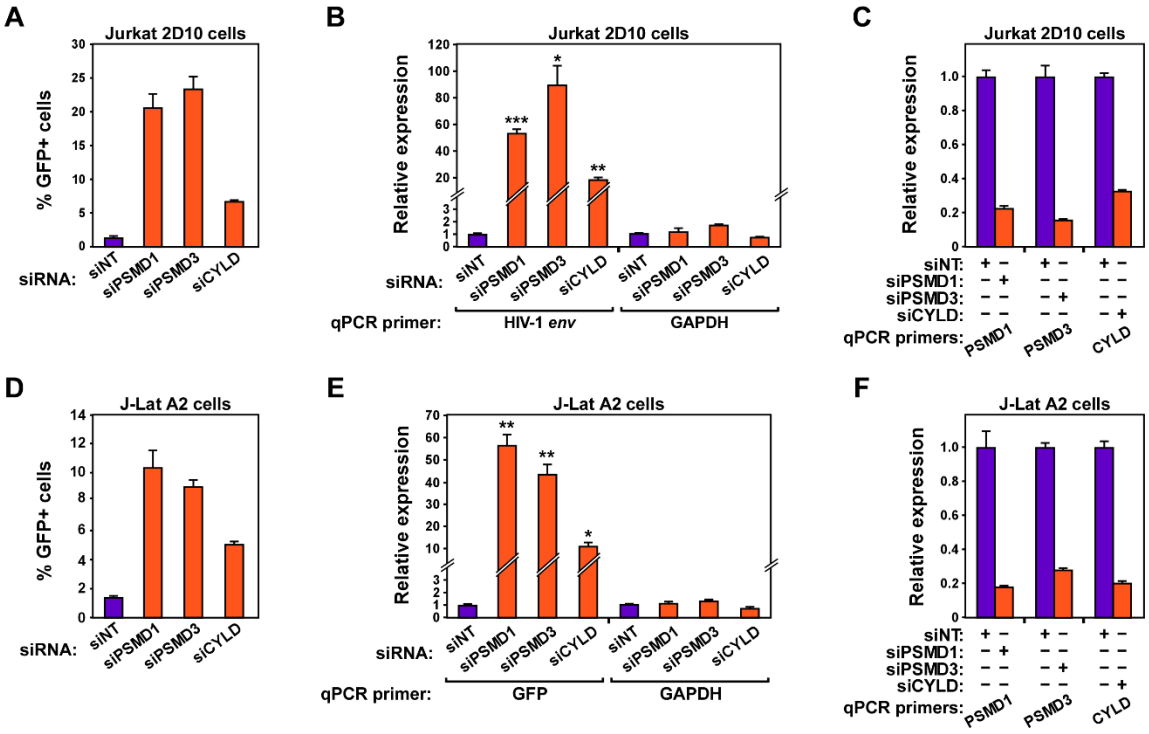

Figure 4-S1

Figure 4-S2. Effects of proteasome inhibitors on viability of Jurkat 2D10 and J-Lat cells. Jurkat 2D10 (A & C) or J-Lat A2 (B & D) cells were treated with the indicated proteasome inhibitors at the indicated concentrations. Cell viabilities were determined by Forward Scatter vs. Side Scatter gating using untreated cells as the control Error bars represent mean +/- SD from three experimental replicates.

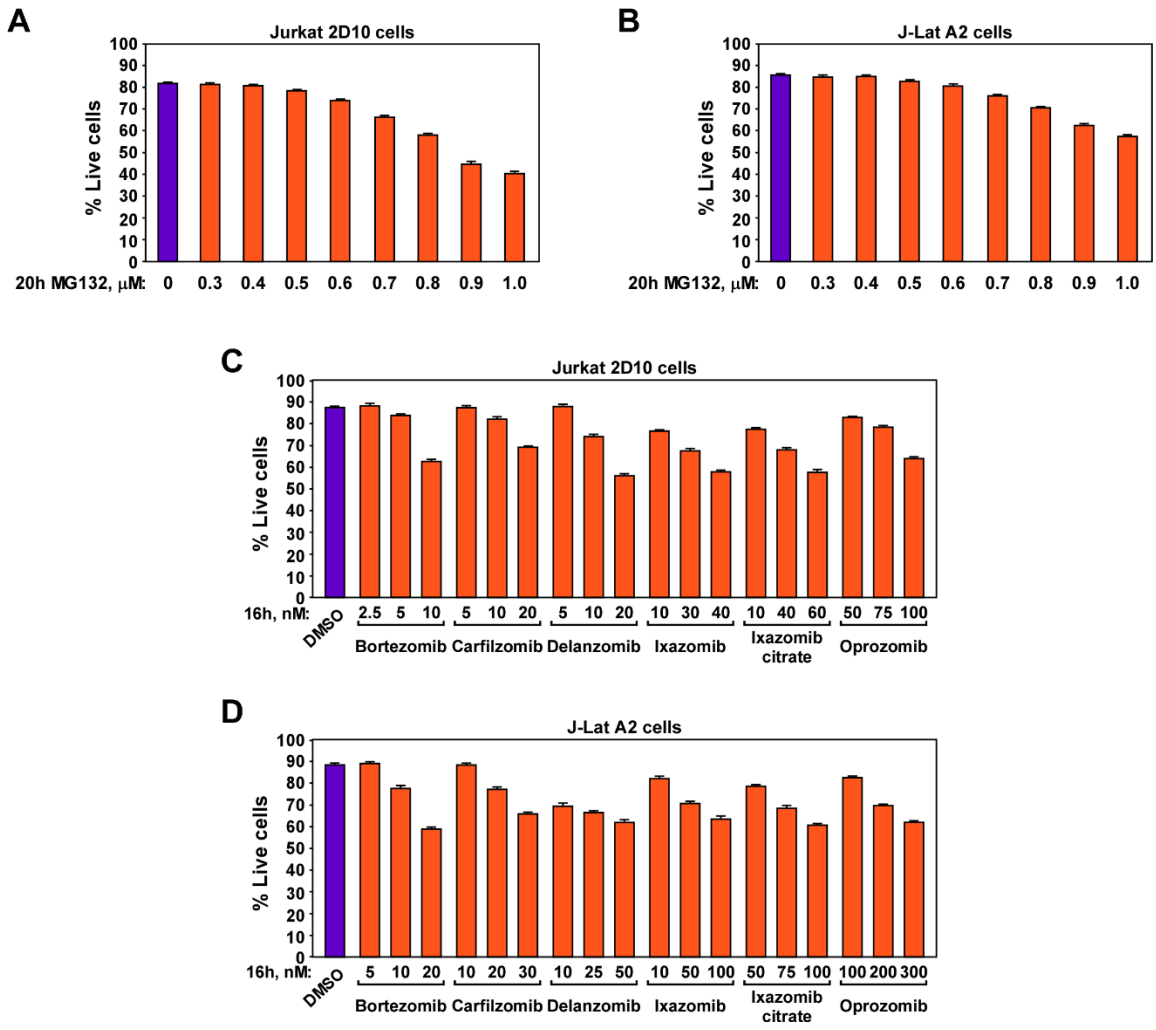

Figure 4-S2

Figure 4-S3. Effect of combining bortezomib or carfilzomib with vorinostat and bryostatin on HIV-1 transcriptional activation in latently infected CD4$^+$ T cells from ART-suppressed individuals. Freshly isolated CD4$^+$ T cells (same as in Figure 4) from ART-suppressed HIV-1-infected individuals were treated with the indicated drug(s) for 24 hr. HIV-1 RNAs in the cells were quantified with RT-qPCR. The PCR signal from each drug combination was normalized to that of the DMSO group (not shown here but same as in Figure 4) for each individual to calculate the fold induction displayed in the scatter plot. Mean ± SEM is displayed, with the asterisks indicating the levels of statistical significance compared with the DMSO group calculated by two-tailed unpaired t-tests (*: p<0.05, **: p<0.01, and ***: p<0.001).

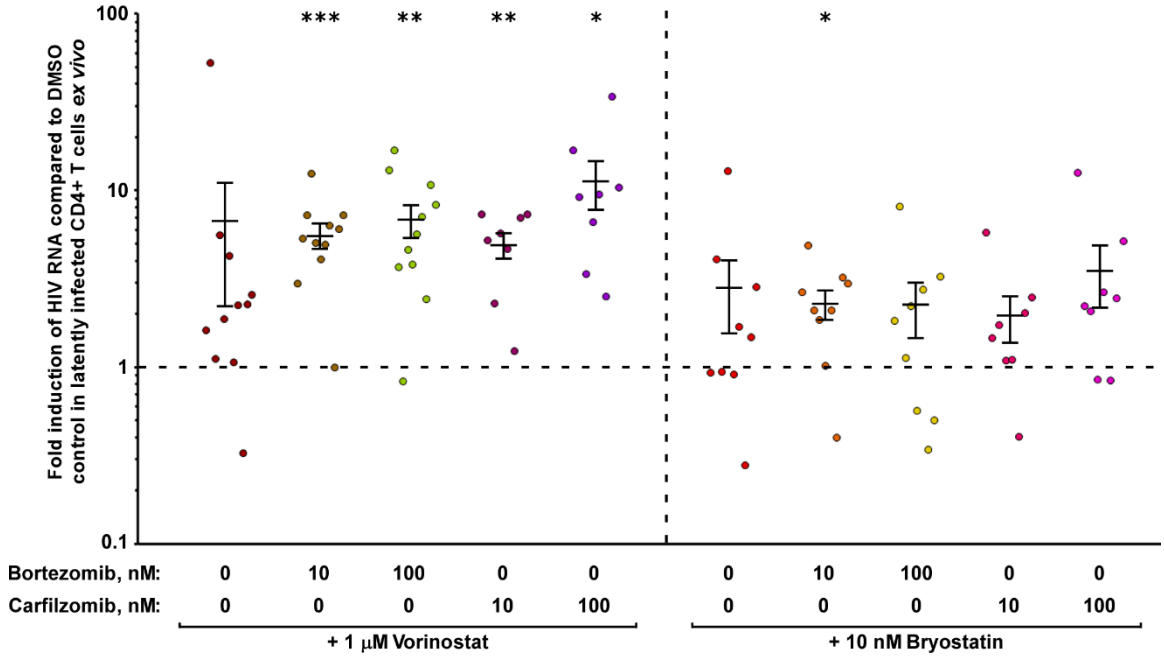

Figure 4-S3

Figure 4-S4. Effects of proteasome inhibitors on T cell activation. A. & B. Primary $CD4^+$ T cells isolated from ART-suppressed HIV-1-infected patient #2 (A) and #3 (B) were treated with the indicated drugs for 24 hr. The cell surface expression of CD69 and CD25 was examined by immunostaining and flow cytometry.

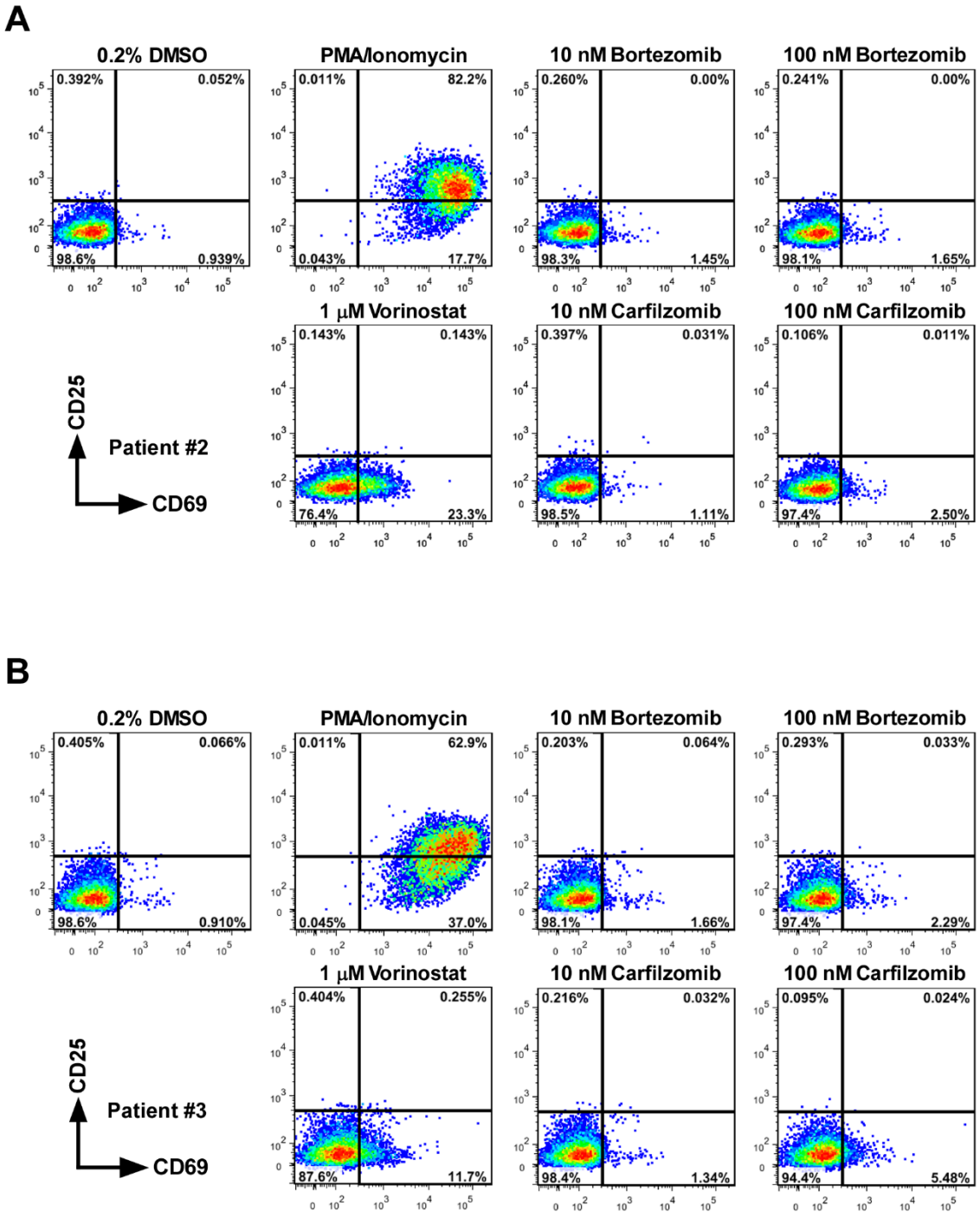

Figure 4-S4

Figure 4-S5. Effects of proteasome inhibitors on proliferation of primary CD4$^+$ T cells. A. & B. Primary CD4$^+$ T cells from ART-suppressed HIV-1-infected patient #2 (A) and #3 (B) were stained with CellTrace CFSE, treated with the indicated drugs for 24 hr, cultured under drug-free conditions for 3 additional days, stained with the anti-CD4 fluorescent antibody, and then analyzed by flow cytometry.

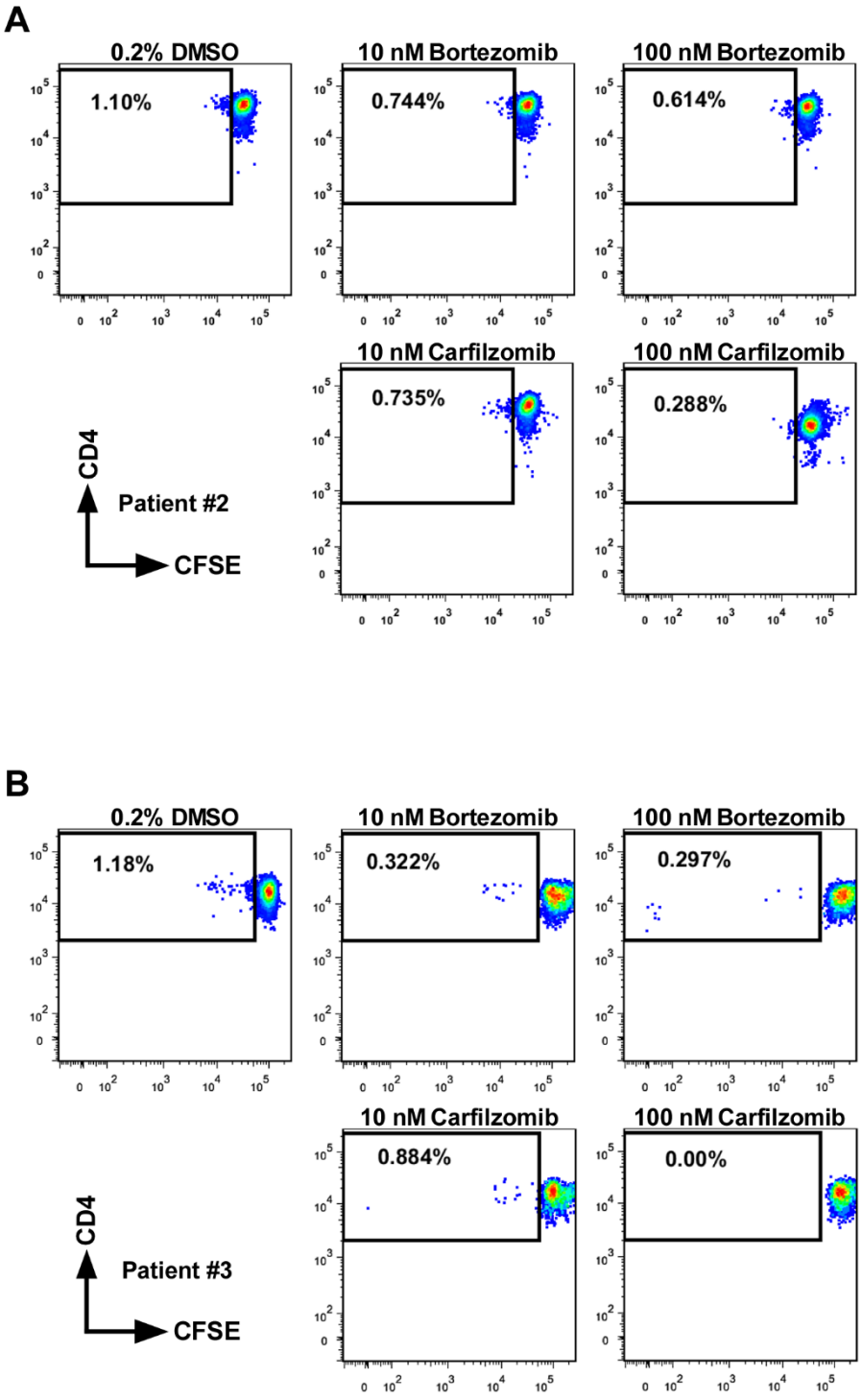
A
0.2% DMSO
1.10%
10 nM Bortezomib
0.744%
100 nM Bortezomib
0.614%
10 nM Carfilzomib
0.735%
100 nM Carfilzomib
0.288%
CD4
Patient #2
CFSE
B
0.2% DMSO
1.18%
10 nM Bortezomib
0.322%
100 nM Bortezomib
0.297%
10 nM Carfilzomib
0.884%
100 nM Carfilzomib
0.00%
CD4
Patient #3
CFSE

Figure 4-S5

Figure 4-S6. Effects of proteasome inhibitors on CD4$^+$ T cell viability. A., B., & C. Primary CD4$^+$ T cells isolated from ART-suppressed HIV-1-infected patient #1 (A), #2 (B) and #3 (C) were treated with the indicated drugs for 4 days. An aliquot of cells from each treatment was collected on the indicated days, stained with LIVE/DEAD Cell Stain Kit (Invitrogen, L34955), and subjected to flow cytometry to quantify the percentages of live cells.

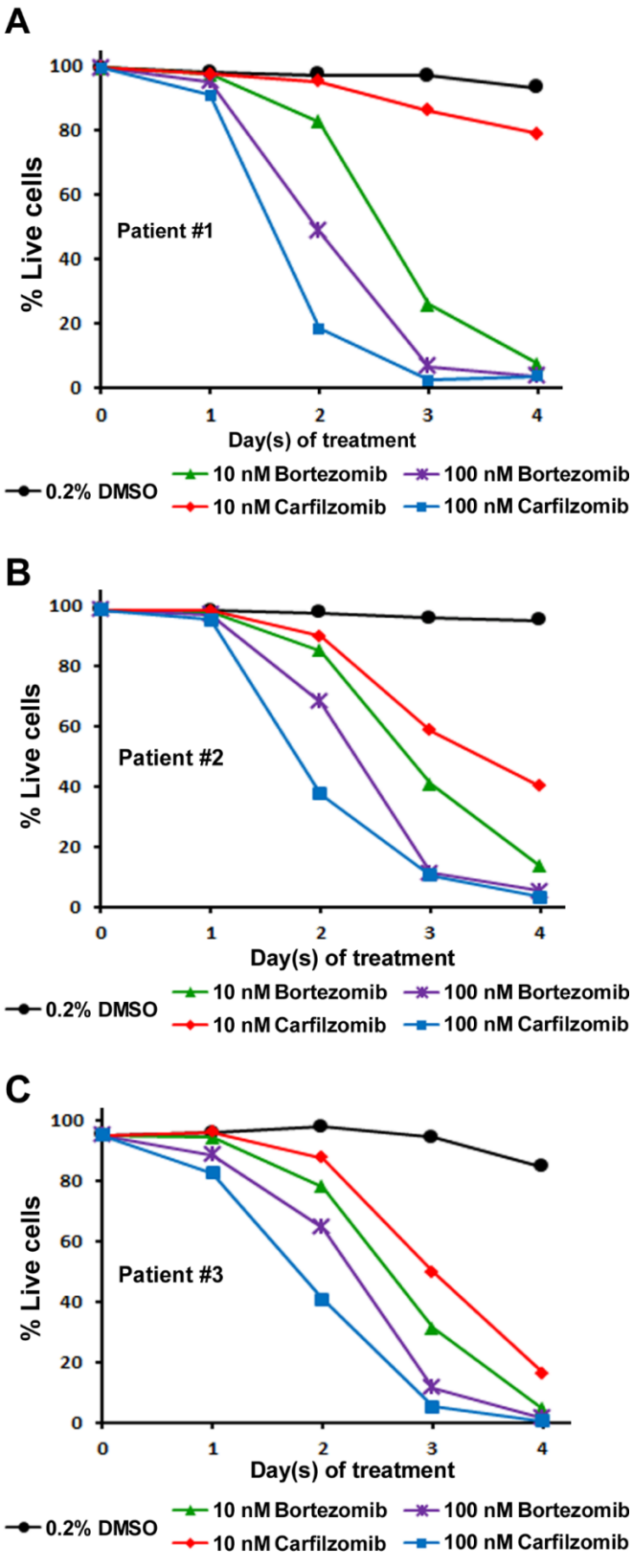
A
% Live cells
Patient #1
Day(s) of treatment
0.2% DMSO
10 nM Bortezomib
100 nM Bortezomib
10 nM Carfilzomib
100 nM Carfilzomib
B
% Live cells
Patient #2
Day(s) of treatment
0.2% DMSO
10 nM Bortezomib
100 nM Bortezomib
10 nM Carfilzomib
100 nM Carfilzomib
C
% Live cells
Patient #3
Day(s) of treatment
0.2% DMSO
10 nM Bortezomib
100 nM Bortezomib
10 nM Carfilzomib
100 nM Carfilzomib

Figure 4-S6

Figure 4-S7. Effect of downregulation of proteasome subunits on mRNA levels of ELL1 and ELL2. A. & B. Results of RT-qPCR analyses of the mRNA levels of ELL1 and ELL2 in aliquots of the cells treated and examined in Figure 6A (A) & 6B (B). For each group, the mRNA level in the DMSO-treated cells was set to 1. Error bars represent mean +/- SD from three experimental replicates. Asterisks denote levels of statistical significance calculated by two-tailed Student's t-test (*: $p<0.05$, **: $p<0.01$, and ***: $p<0.001$).

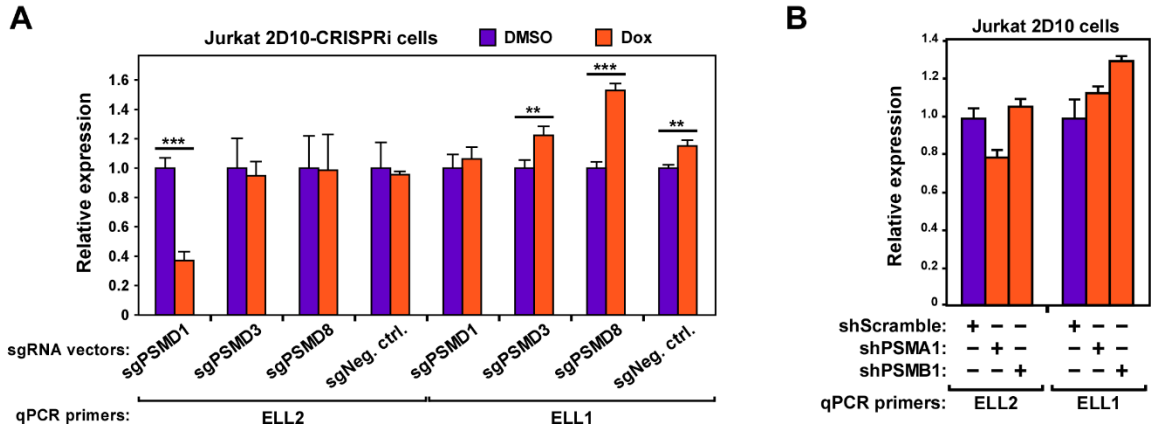

Figure 4-S7

Supplemental Table 4-S1. Characteristics of HIV-1–infected study participants

Patient ID	Age (years)	Gender	Ethnicity	Duration of infection (years)	ART regimen	Time on ART (years)	Time on suppressive ART (years)	CD4 count (cells/mm^3)	CD8 count (cells/mm^3)	Viral load (copies/ml)	Peak viral load (copies/ml)	CD4_Nadir (cells/mm3)
1	72	Male	White	23	TCV, FTC/TAF	12	10	725	1024	<40	28699	223
2	62	Male	Hispanic/Latino	25	ABC/TCV/3TC	16.4	10.9	606	407	<40	119870	4
3	58	Male	Black/African American	37	ABC/TCV/3TC	18.4	16.6	235	729	<40	unknown	185
4	50	Male	White	17	TCV/RPV	13	12	380	304	<40	495912	129
5	66	Male	White	34	TCV, FTC/TAF	19	19	489	619	<40	unknown	40
6	67	Male	White	18	ABC/TCV/3TC	12	11	522	544	<40	376658	378
7	57	Male	White	31	RTV, DRV, ABC/TCV/3TC	20	11	615	804	<40	171000	147
8	57	Male	Black/African American	21	EFV/TDF/FTC	10	9	466	555	<40	150000	211
9	60	Male	Black/African American	13	EFV/TDF/FTC	11	10	687	237	<40	312938	153
10	34	Male	White	7	EVG/TDF/FTC/COBI	7	7	293	642	<40	694195	50
11	49	Male	Black/African American	13	FTC/TDF, RTV, DRV	8	8	639	921	<40	286924	208
12	47	Male	Hispanic/Latino	25	ABC/TCV/3TC, ATV	14	10	351	466	<40	357000	56
13	70	Male	White	33	DRV, RTV, TCV, 3TC	24	7	836	889	<40	80410	98

Abbreviations: 3TC, lamivudine (Epivir); ABC, abacavir (Ziagen); ATV, atazanavir (Reyataz); COBI, cobicistat; DRV, darunavir (Prezista); EFV, efavirenz (Sustiva, Stocrin); EVG, elvitegravir; FTC, emtricitabine (Emtriva); RPV, rilpivirine (Edurant); RTV, ritonavir (Norvir); TAF, tenofovir alafenamide; TCV, dolutegravir (Tivicay); TDF, tenofovir (Viread).

Supplemental Table 4-S2. List of DNA oligonucleotide primers used in this study

Primer	Sequence (5' → 3')
For deep-sequencing:	
CRISPRi_TSS_12_P5	AATGATACGGCGACCACCGAGATCTACACTTGTAGGAAGAGCACACGTCTGAACTCCAGTCACGCACAAAAGGAAACTCACCCT
CRISPRi TSS_12_P7	CAAGCAGAAGACGGCATACGAGATCTTGTAGTGACTGGAGTTCAGACGTGTGCTCTTCCGATCACGACTCGGTGCCACTTTTTC
CRISPRi_TSS_6_P5	AATGATACGGCGACCACCGAGATCTACAGCCAATGGAAGAGCACACGTCTGAACTCCAGTCACGCACAAAAGGAAACTCACCCT
CRISPRi TSS_6_P7	CAAGCAGAAGACGGCATACGAGATGCCAATGTGACTGGAGTTCAGACGTGTGCTCTTCCGATCACGACTCGGTGCCACTTTTTC
CRISPRi TSS_seq V2	GTGTGTTTTGAGACTATAAGTATCCCTTGGAGAACCACCTTGTTGG
For qPCR:	
qActB-F	AGAGCTACGAGCTGCCTGAC
qActB-R	AGCACTGTGTTGGCGTACAG
qGAPDH-F	AATCCCATCACCATCTTCCAG
qGAPDH-R	AAATGAGCCCCAGCCTTC
qEnv-F	GAGACAGAGACAGATCCATTCG
qEnv-R	CCAGAAGTTCCACAATCCTCG
qGFP-F	CAGTGCTTCAGCCGCTACCC
qGFP-R	AGTTCACCTTGATGCCGTTCTT
qPSMD1-F	CTGAGCTGACAGATACACTGC
qPSMD1-R	GTGCAAATTCCTTAAGCTGTGG
qPSMD3-F	CGCCTCAACCACTATGTTCTG
qPSMD3-R	AATCAGCCTCTGTGTCCATG
qPSMD8-F	GAACCGTAAAAGCCCCAATC
qPSMD8-R	CCCGATCTCCAGTATGTCAC
qGON4L-F	GAAGTCAAGGAAGAAGGAGGG
qGON4L-R	AGGAGAGGCACAAACATCTG
qCYLD-F	TGGGATGGAAGATTTGATGGAG
qCYLD-R	CATAAAGGCAAGTTTGGGAGG
qNFKBIA-F	GTCTACACTTAGCCTCTATCCATG
qNFKBIA-R	AGGTCAGGATTTTGCAGGTC
qPSMA1-F	GGTTGCATTGAAAAGGGCG
qPSMA1-R	ATCCAAACACTCCTGACGC
qPSMB1-F	GCTGCAATGCTGTCTACAATC
qPSMB1-R	TCTCTGGTAAGACCCTACTGG
qELL1-F	CCTTCTACCTCTCCAACATCG
qELL1-R	ACCGTGATCTTGTCCTGTATG
qELL2-F	GAGACTTACCAGAGCCACAAG
qELL2-R	TTGTCTTTGCCCACATTTGAC

Supplemental Table 4-S3. List of antibodies used in this study

Antibody	Source
rabbit anti-human ELL2	Bethyl A302–505A
rabbit anti-human ELL1	Bethyl A301–645A
rabbit anti-human ENL	Bethyl A302-268A
mouse anti-human AFF4	Abcam ab57077
rabbit anti-human AFF1	Bethyl A302–344A
rabbit anti-human CycT1	Santa Cruz sc-10750
rabbit anti-human AF9	Bethyl A300-595A
rabbit anti-human LARP7	(He et al., 2008)
mouse anti-human IκBα	Santa Cruz sc-1643
rabbit anti-human PSMD1	Bethyl A303-852A
rabbit anti-human PSMD3	Bethyl A303-826A
mouse anti-human PSMD8	Santa Cruz sc-514053
rabbit anti-human PSMA1	Bethyl A303-845A
rabbit anti-human PSMB1	Abcam ab135830
rabbit anti-human Brd4	(Yang et al., 2005)
rabbit anti-human CDK9	(He et al., 2010)
goat anti-mouse-680 nm	Invitrogen A-21057
goat anti-rabbit-680 nm	Invitrogen A-21076

References cited in this table

He, N., Jahchan, N.S., Hong, E., Li, Q., Bayfield, M.A., Maraia, R.J., Luo, K., and Zhou, Q. (2008). A La-related protein modulates 7SK snRNP integrity to suppress P-TEFb-dependent transcriptional elongation and tumorigenesis. Mol Cell 29, 588-599.

He, N., Liu, M., Hsu, J., Xue, Y., Chou, S., Burlingame, A., Krogan, N.J., Alber, T., and Zhou, Q. (2010). HIV-1 Tat and host AFF4 recruit two transcription elongation factors into a bifunctional complex for coordinated activation of HIV-1 transcription. Mol Cell 38, 428-438.

Yang, Z., Yik, J.H., Chen, R., He, N., Jang, M.K., Ozato, K., and Zhou, Q. (2005). Recruitment of P-TEFb for stimulation of transcriptional elongation by the bromodomain protein Brd4. Mol Cell 19, 535-545.

Chapter 5

Conclusions and Perspectives

Conclusions

The results presented in this dissertation prove that HIV-1 latency could be reversed through enhancing the activity of the Super Elongation Complex (SEC). This could be achieved by directly introducing more SEC into the cells, modulating histone modification, or targeting other cellular mechanisms that inhibit SEC.

As demonstrated in Chapter 2, two subunits of SEC (ELL2 and AFF1) play predominant roles in HIV-1 transcription in $CD4^+$ T cells (Fig. 2-2, 2-3 & 2-5). Compared with their orthologs, ELL2 and AFF1 constitute only a minor subset of the SECs (Fig. 2-6), but are the preferred functional partners for the HIV Tat protein (Fig. 2-4). When the levels of ELL2 and AFF1 are elevated in the cells through ectopic expression, latent HIV could be efficiently reactivated (Fig. 2-5). As a proof of concept, these results suggest that SEC is a promising targeting for therapeutic intervention.

The bromodomain protein Brd4 has been previously reported to promote HIV latency by binding to the viral LTR to inhibit Tat-induced transcription (108,110). As demonstrated in Chapter 3, the LTR of latent HIV has low acetylated histone H3 (AcH3) but high AcH4 content (Fig. 3-1 & 3-4), which recruits Brd4 to inhibit Tat-transactivation (Fig. 3-3 & 3-5). Furthermore, the lysine acetyltransferase KAT5 but not the paralogs KAT7 and KAT8 promotes HIV latency through acetylating H4 on the provirus (Fig. 3-2, 3-4 & 3-7). More important, antagonizing KAT5 by either CRISPRi or a small molecule MG149 reverses HIV-1 latency by removing AcH4 and Brd4 from HIV LTR, enhancing loading of the Super Elongation Complex (Fig. 3-5), and interferes with the establishment of latency (Fig. 3-6). These results suggest that the KAT5-AcH4-Brd4 axis is a key regulator of HIV latency and a potential therapeutic target for eradicating latent HIV reservoirs.

Inhibition of active HIV replication requires a combination of medicines that target multiple steps in its lifecycle. Likewise, reversal of HIV latency requires combined therapeutic interventions to remove multiple blocks in cell that inhibit active HIV transcription. The CRISPRi-based screening strategy developed in Chapter 4 provides an efficient and high throughput platform to identify novel cellular factors that could be targeted. As a proof of concept, using this platform, I identified 6 cellular genes, including 4 genes (PSMD1, PSMD3, PSMD8, and GON4L) that haven't been reported yet as inhibitors for HIV-1 transcription (Fig. 4-1). Three of them (PSMD1, PSMD3, PSMD8) are proteasome subunits. Using the available drugs to inhibit the activity of proteasome, I confirmed that the hits identified through this screening platform could indeed be translated into targets for drugs that efficiently reverse HIV-1 latency (Fig. 4-4). Mechanistically, proteasomes inhibit HIV-1 transcription through reducing the cellular levels of ELL2 (Fig. 4-5). These results further underline the importance of ELL2-containing SECs in HIV-1 transcription and latency reversal.

Perspectives

Based on the discoveries in this dissertation, one probable avenue to reverse HIV-1 latency is to artificially elevate the cellular levels of active SEC in latently infected cells

in vivo. As ELL2 plays a predominant role in HIV-1 transcription, and is the key limiting factor due to its high proneness to protein degradation, it is pivotal to stabilize ELL2 by increasing its assembly into SEC. To achieve this, more detailed knowledge about the assembly of SEC is required. Future studies, including detailed crystallography studies (189), will shed light on how to stabilize SEC in resting $CD4^+$ T cells, which is the major reservoir for latent HIV-1. Base on crystal structures, rational drug design and screen could be conducted for the purpose of increasing the ELL2-SEC assembly *in vivo*.

Besides the direct elevation of the levels of SECs, targeting the KAT5-AcH4-Brd4 axis discovered in this dissertation represents a promising avenue to enhance the loading of SEC on HIV provirus. At the current stage, a major limitation of this strategy is the inefficiency of KAT5 inhibitors. For example, under *ex vivo* conditions, MG-149's working concentration is 50 μM, which is not likely to be achievable *in vivo*. Therefore, future studies are needed to develop more potent KAT5 inhibitors to fully leverage this KAT5-AcH4-Brd4 axis.

Proteasome inhibitors represent a new class of LRAs that merits further investigation. A major drawback of using proteasome inhibitors in the treatment of chromic HIV-1 infection is the severe cytotoxicity resulting from global shutdown of the proteasomal protein degradation. Different from cancer, being chronically infected by HIV-1 is no longer a life-threatening situation thanks to the combined anti-retroviral therapy. Therefore, the benefit-risk ratio may not be high enough to warrant the usage of proteasome inhibitors in individuals chronically infected by HIV-1. However, doctors treating HIV-infected individuals who also receive proteasome inhibitors as cancer treatment should monitor the size of their latent HIV reservoir, so that we can learn more. Finally, recent advances in our knowledge about the factors that control the cellular levels ELL2 levels, including SIAH1 and PARP1 (96,173), may provide more targets for the designing of corresponding drugs.

It is important to point out that the conclusions in this dissertation about effects of SEC, KAT5, and proteasomes in HIV latency reversal have been made on the basis of results in $CD4^+$ T cells, which is the major, but probably not exclusive reservoir that contribute to HIV persistence (135). Other anatomical compartments and cellular reservoirs, including gut-associated lymphoid tissue (GALT), microglial cells and perivascular macrophages in the central nervous system may also contribute to HIV persistence (114,190,191). Therefore, it remains to be seen if the mechanisms that maintain HIV latency described here also play a vital role in these additional viral reservoirs.

Since the purpose of reversing HIV latency is to kill the latent reservoir cells (170,192), future research needs to focus on how the manipulation of SEC, KAT5, and proteasomes will affect the size of the latent reservoir. Ideally, the LRAs that reverse latency would also activate cytotoxic natural killer cells and $CD8^+$ T cells, or at least not antagonize their functions of killing HIV-infected cells. To achieve the goal of complete eradication, therapeutic agents, just as broadly neutralizing antibodies (193,194), dual-affinity re-targeting molecules (195,196), and immune checkpoint antibodies (197) may need to serve as part of the combined kick-and-kill approaches to orchestrate the destruction of the HIV reservoirs. Last but not least, since the size of latent HIV reservoir

is determined in the early stage of acute HIV infection (198), positively correlated with the difficulty of viral eradication (199), and varies greatly in different individuals (74), quick diagnosis and early initiation of cART in infected individuals will limit the size of latent reservoirs and facilitate future viral eradication (200,201).

Work Cited

1. Drew, W.L., Mintz, L., Miner, R.C., Sands, M. and Ketterer, B. (1981) Prevalence of cytomegalovirus infection in homosexual men. *J Infect Dis*, **143**, 188-192.
2. Gottlieb, M.S., Schroff, R., Schanker, H.M., Weisman, J.D., Fan, P.T., Wolf, R.A. and Saxon, A. (1981) Pneumocystis carinii pneumonia and mucosal candidiasis in previously healthy homosexual men: evidence of a new acquired cellular immunodeficiency. *N Engl J Med*, **305**, 1425-1431.
3. Gottlieb, M.S., Howard M. Schanker, Peng Thim Fan, Andrew Saxon, Joel D. Weisman, and Irving Pozalski. (1981) Pneumocystis pneumonia--Los Angeles. *MMWR Morb Mortal Wkly Rep*, **30**, 250-252.
4. Korber, B., Muldoon, M., Theiler, J., Gao, F., Gupta, R., Lapedes, A., Hahn, B.H., Wolinsky, S. and Bhattacharya, T. (2000) Timing the ancestor of the HIV-1 pandemic strains. *Science*, **288**, 1789-1796.
5. Sharp, P.M., Bailes, E., Chaudhuri, R.R., Rodenburg, C.M., Santiago, M.O. and Hahn, B.H. (2001) The origins of acquired immune deficiency syndrome viruses: where and when? *Philos Trans R Soc Lond B Biol Sci*, **356**, 867-876.
6. Sharp, P.M. and Hahn, B.H. (2010) The evolution of HIV-1 and the origin of AIDS. *Philos Trans R Soc Lond B Biol Sci*, **365**, 2487-2494.
7. Chitnis, A., Rawls, D. and Moore, J. (2000) Origin of HIV type 1 in colonial French Equatorial Africa? *AIDS Res Hum Retroviruses*, **16**, 5-8.
8. Worobey, M., Gemmel, M., Teuwen, D.E., Haselkorn, T., Kunstman, K., Bunce, M., Muyembe, J.J., Kabongo, J.M., Kalengayi, R.M., Van Marck, E. *et al.* (2008) Direct evidence of extensive diversity of HIV-1 in Kinshasa by 1960. *Nature*, **455**, 661-664.
9. Pepin, J. and Labbe, A.C. (2008) Noble goals, unforeseen consequences: control of tropical diseases in colonial Central Africa and the iatrogenic transmission of blood-borne viruses. *Trop Med Int Health*, **13**, 744-753.
10. Gilbert, M.T., Rambaut, A., Wlasiuk, G., Spira, T.J., Pitchenik, A.E. and Worobey, M. (2007) The emergence of HIV/AIDS in the Americas and beyond. *Proc Natl Acad Sci U S A*, **104**, 18566-18570.
11. Worobey, M., Watts, T.D., McKay, R.A., Suchard, M.A., Granade, T., Teuwen, D.E., Koblin, B.A., Heneine, W., Lemey, P. and Jaffe, H.W. (2016) 1970s and 'Patient 0' HIV-1 genomes illuminate early HIV/AIDS history in North America. *Nature*, **539**, 98-101.
12. Hammer, S.M., Squires, K.E., Hughes, M.D., Grimes, J.M., Demeter, L.M., Currier, J.S., Eron, J.J., Jr., Feinberg, J.E., Balfour, H.H., Jr., Deyton, L.R. *et al.* (1997) A controlled trial of two nucleoside analogues plus indinavir in persons with human immunodeficiency virus infection and CD4 cell counts of 200 per cubic millimeter or less. AIDS Clinical Trials Group 320 Study Team. *N Engl J Med*, **337**, 725-733.
13. Gulick, R.M., Mellors, J.W., Havlir, D., Eron, J.J., Gonzalez, C., McMahon, D., Richman, D.D., Valentine, F.T., Jonas, L., Meibohm, A. *et al.* (1997) Treatment with indinavir, zidovudine, and lamivudine in adults with human immunodeficiency virus infection and prior antiretroviral therapy. *N Engl J Med*, **337**, 734-739.
14. Saag, M.S., Benson, C.A., Gandhi, R.T., Hoy, J.F., Landovitz, R.J., Mugavero, M.J., Sax, P.E., Smith, D.M., Thompson, M.A., Buchbinder, S.P. *et al.* (2018) Antiretroviral Drugs for Treatment and Prevention of HIV Infection in Adults: 2018 Recommendations of the International Antiviral Society-USA Panel. *JAMA*, **320**, 379-396.

15. Bangsberg, D.R., Kroetz, D.L. and Deeks, S.G. (2007) Adherence-resistance relationships to combination HIV antiretroviral therapy. *Curr HIV/AIDS Rep*, **4**, 65-72.
16. Bangalore, S., Kamalakkannan, G., Parkar, S. and Messerli, F.H. (2007) Fixed-dose combinations improve medication compliance: a meta-analysis. *Am J Med*, **120**, 713-719.
17. Cohen, J. (2011) Breakthrough of the year. HIV treatment as prevention. *Science*, **334**, 1628.
18. Cohen, M.S., Smith, M.K., Muessig, K.E., Hallett, T.B., Powers, K.A. and Kashuba, A.D. (2013) Antiretroviral treatment of HIV-1 prevents transmission of HIV-1: where do we go from here? *Lancet*, **382**, 1515-1524.
19. Jiang, J., Yang, X., Ye, L., Zhou, B., Ning, C., Huang, J., Liang, B., Zhong, X., Huang, A., Tao, R. *et al.* (2014) Pre-exposure prophylaxis for the prevention of HIV infection in high risk populations: a meta-analysis of randomized controlled trials. *PLoS One*, **9**, e87674.
20. Spinner, C.D., Boesecke, C., Zink, A., Jessen, H., Stellbrink, H.J., Rockstroh, J.K. and Esser, S. (2016) HIV pre-exposure prophylaxis (PrEP): a review of current knowledge of oral systemic HIV PrEP in humans. *Infection*, **44**, 151-158.
21. Goulder, P.J. and Watkins, D.I. (2004) HIV and SIV CTL escape: implications for vaccine design. *Nat Rev Immunol*, **4**, 630-640.
22. Walker, B.D. and Burton, D.R. (2008) Toward an AIDS vaccine. *Science*, **320**, 760-764.
23. McMichael, A.J. and Hanke, T. (2003) HIV vaccines 1983-2003. *Nat Med*, **9**, 874-880.
24. Barouch, D.H., Kunstman, J., Kuroda, M.J., Schmitz, J.E., Santra, S., Peyerl, F.W., Krivulka, G.R., Beaudry, K., Lifton, M.A., Gorgone, D.A. *et al.* (2002) Eventual AIDS vaccine failure in a rhesus monkey by viral escape from cytotoxic T lymphocytes. *Nature*, **415**, 335-339.
25. Pitisuttithum, P., Gilbert, P., Gurwith, M., Heyward, W., Martin, M., van Griensven, F., Hu, D., Tappero, J.W. and Choopanya, K. (2006) Randomized, double-blind, placebo-controlled efficacy trial of a bivalent recombinant glycoprotein 120 HIV-1 vaccine among injection drug users in Bangkok, Thailand. *J Infect Dis*, **194**, 1661-1671.
26. Rerks-Ngarm, S., Pitisuttithum, P., Nitayaphan, S., Kaewkungwal, J., Chiu, J., Paris, R., Premsri, N., Namwat, C., de Souza, M., Adams, E. *et al.* (2009) Vaccination with ALVAC and AIDSVAX to prevent HIV-1 infection in Thailand. *N Engl J Med*, **361**, 2209-2220.
27. Pitisuttithum, P., Rerks-Ngarm, S., Bussaratid, V., Dhitavat, J., Maekanantawat, W., Pungpak, S., Suntharasamai, P., Vanijanonta, S., Nitayapan, S., Kaewkungwal, J. *et al.* (2011) Safety and reactogenicity of canarypox ALVAC-HIV (vCP1521) and HIV-1 gp120 AIDSVAX B/E vaccination in an efficacy trial in Thailand. *PLoS One*, **6**, e27837.
28. Granich, R., Gupta, S., Hall, I., Aberle-Grasse, J., Hader, S. and Mermin, J. (2017) Status and methodology of publicly available national HIV care continua and 90-90-90 targets: A systematic review. *PLoS Med*, **14**, e1002253.
29. Gisslen, M., Svedhem, V., Lindborg, L., Flamholc, L., Norrgren, H., Wendahl, S., Axelsson, M. and Sonnerborg, A. (2017) Sweden, the first country to achieve the Joint United Nations Programme on HIV/AIDS (UNAIDS)/World Health Organization (WHO) 90-90-90 continuum of HIV care targets. *HIV Med*, **18**, 305-307.
30. Sabapathy, K., Hensen, B., Varsaneux, O., Floyd, S., Fidler, S. and Hayes, R. (2018) The cascade of care following community-based detection of HIV in sub-Saharan Africa - A systematic review with 90-90-90 targets in sight. *PLoS One*, **13**, e0200737.
31. Grobler, A., Cawood, C., Khanyile, D., Puren, A. and Kharsany, A.B.M. (2017) Progress of UNAIDS 90-90-90 targets in a district in KwaZulu-Natal, South Africa, with high HIV burden, in the HIPSS study: a household-based complex multilevel community survey. *Lancet HIV*, **4**, e505-e513.

32. Kojima, N. and Klausner, J.D. (2018) Strategies to increase human immunodeficiency virus testing among men to reach UNAIDS 90-90-90 targets. *Clin Infect Dis*.
33. Abgrall, S., Ingle, S.M., May, M.T., Costagliola, D., Mercie, P., Cavassini, M., Reekie, J., Samji, H., Gill, M.J., Crane, H.M. *et al.* (2013) Durability of first ART regimen and risk factors for modification, interruption or death in HIV-positive patients starting ART in Europe and North America 2002-2009. *AIDS*, **27**, 803-813.
34. Al-Dakkak, I., Patel, S., McCann, E., Gadkari, A., Prajapati, G. and Maiese, E.M. (2013) The impact of specific HIV treatment-related adverse events on adherence to antiretroviral therapy: a systematic review and meta-analysis. *AIDS Care*, **25**, 400-414.
35. Dahab, M., Charalambous, S., Hamilton, R., Fielding, K., Kielmann, K., Churchyard, G.J. and Grant, A.D. (2008) "That is why I stopped the ART": patients' & providers' perspectives on barriers to and enablers of HIV treatment adherence in a South African workplace programme. *BMC Public Health*, **8**, 63.
36. Johnson, A.A., Ray, A.S., Hanes, J., Suo, Z., Colacino, J.M., Anderson, K.S. and Johnson, K.A. (2001) Toxicity of antiviral nucleoside analogs and the human mitochondrial DNA polymerase. *J Biol Chem*, **276**, 40847-40857.
37. Birkus, G., Hitchcock, M.J. and Cihlar, T. (2002) Assessment of mitochondrial toxicity in human cells treated with tenofovir: comparison with other nucleoside reverse transcriptase inhibitors. *Antimicrob Agents Chemother*, **46**, 716-723.
38. Usach, I., Melis, V. and Peris, J.E. (2013) Non-nucleoside reverse transcriptase inhibitors: a review on pharmacokinetics, pharmacodynamics, safety and tolerability. *J Int AIDS Soc*, **16**, 1-14.
39. Walmsley, S. (2007) Protease inhibitor-based regimens for HIV therapy: safety and efficacy. *J Acquir Immune Defic Syndr*, **45 Suppl 1**, S5-13; quiz S28-31.
40. Lee, F.J. and Carr, A. (2012) Tolerability of HIV integrase inhibitors. *Curr Opin HIV AIDS*, **7**, 422-428.
41. Schackman, B.R., Gebo, K.A., Walensky, R.P., Losina, E., Muccio, T., Sax, P.E., Weinstein, M.C., Seage, G.R., 3rd, Moore, R.D. and Freedberg, K.A. (2006) The lifetime cost of current human immunodeficiency virus care in the United States. *Med Care*, **44**, 990-997.
42. Sloan, C.E., Champenois, K., Choisy, P., Losina, E., Walensky, R.P., Schackman, B.R., Ajana, F., Melliez, H., Paltiel, A.D., Freedberg, K.A. *et al.* (2012) Newer drugs and earlier treatment: impact on lifetime cost of care for HIV-infected adults. *AIDS*, **26**, 45-56.
43. Gilks, C.F., Crowley, S., Ekpini, R., Gove, S., Perriens, J., Souteyrand, Y., Sutherland, D., Vitoria, M., Guerma, T. and De Cock, K. (2006) The WHO public-health approach to antiretroviral treatment against HIV in resource-limited settings. *Lancet*, **368**, 505-510.
44. Hogan, D.R., Baltussen, R., Hayashi, C., Lauer, J.A. and Salomon, J.A. (2005) Cost effectiveness analysis of strategies to combat HIV/AIDS in developing countries. *BMJ*, **331**, 1431-1437.
45. Mbonye, U. and Karn, J. (2014) Transcriptional control of HIV latency: cellular signaling pathways, epigenetics, happenstance and the hope for a cure. *Virology*, **454-455**, 328-339.
46. Karn, J. (2011) The molecular biology of HIV latency: breaking and restoring the Tat-dependent transcriptional circuit. *Curr Opin HIV AIDS*, **6**, 4-11.
47. Rouzine, I.M., Weinberger, A.D. and Weinberger, L.S. (2015) An evolutionary role for HIV latency in enhancing viral transmission. *Cell*, **160**, 1002-1012.
48. Finzi, D., Blankson, J., Siliciano, J.D., Margolick, J.B., Chadwick, K., Pierson, T., Smith, K., Lisziewicz, J., Lori, F., Flexner, C. *et al.* (1999) Latent infection of CD4+ T cells provides a

mechanism for lifelong persistence of HIV-1, even in patients on effective combination therapy. *Nat Med*, **5**, 512-517.

49. Siliciano, J.D., Kajdas, J., Finzi, D., Quinn, T.C., Chadwick, K., Margolick, J.B., Kovacs, C., Gange, S.J. and Siliciano, R.F. (2003) Long-term follow-up studies confirm the stability of the latent reservoir for HIV-1 in resting CD4+ T cells. *Nat Med*, **9**, 727-728.
50. Hutter, G., Nowak, D., Mossner, M., Ganepola, S., Mussig, A., Allers, K., Schneider, T., Hofmann, J., Kucherer, C., Blau, O. *et al.* (2009) Long-term control of HIV by CCR5 Delta32/Delta32 stem-cell transplantation. *N Engl J Med*, **360**, 692-698.
51. Allers, K., Hutter, G., Hofmann, J., Loddenkemper, C., Rieger, K., Thiel, E. and Schneider, T. (2011) Evidence for the cure of HIV infection by CCR5Delta32/Delta32 stem cell transplantation. *Blood*, **117**, 2791-2799.
52. Sengupta, S. and Siliciano, R.F. (2018) Targeting the Latent Reservoir for HIV-1. *Immunity*, **48**, 872-895.
53. Margolis, D.M., Garcia, J.V., Hazuda, D.J. and Haynes, B.F. (2016) Latency reversal and viral clearance to cure HIV-1. *Science*, **353**, aaf6517.
54. Siliciano, R.F. and Greene, W.C. (2011) HIV latency. *Cold Spring Harb Perspect Med*, **1**, a007096.
55. Mbonye, U. and Karn, J. (2011) Control of HIV latency by epigenetic and non-epigenetic mechanisms. *Curr HIV Res*, **9**, 554-567.
56. Williams, S.A., Chen, L.F., Kwon, H., Ruiz-Jarabo, C.M., Verdin, E. and Greene, W.C. (2006) NF-kappaB p50 promotes HIV latency through HDAC recruitment and repression of transcriptional initiation. *EMBO J*, **25**, 139-149.
57. Coull, J.J., Romerio, F., Sun, J.M., Volker, J.L., Galvin, K.M., Davie, J.R., Shi, Y., Hansen, U. and Margolis, D.M. (2000) The human factors YY1 and LSF repress the human immunodeficiency virus type 1 long terminal repeat via recruitment of histone deacetylase 1. *J Virol*, **74**, 6790-6799.
58. Keedy, K.S., Archin, N.M., Gates, A.T., Espeseth, A., Hazuda, D.J. and Margolis, D.M. (2009) A limited group of class I histone deacetylases acts to repress human immunodeficiency virus type 1 expression. *J Virol*, **83**, 4749-4756.
59. Nabel, G. and Baltimore, D. (1987) An inducible transcription factor activates expression of human immunodeficiency virus in T cells. *Nature*, **326**, 711-713.
60. Liu, J., Perkins, N.D., Schmid, R.M. and Nabel, G.J. (1992) Specific NF-kappa B subunits act in concert with Tat to stimulate human immunodeficiency virus type 1 transcription. *J Virol*, **66**, 3883-3887.
61. Kinoshita, S., Chen, B.K., Kaneshima, H. and Nolan, G.P. (1998) Host control of HIV-1 parasitism in T cells by the nuclear factor of activated T cells. *Cell*, **95**, 595-604.
62. Giffin, M.J., Stroud, J.C., Bates, D.L., von Koenig, K.D., Hardin, J. and Chen, L. (2003) Structure of NFAT1 bound as a dimer to the HIV-1 LTR kappa B element. *Nat Struct Biol*, **10**, 800-806.
63. Palangat, M., Meier, T.I., Keene, R.G. and Landick, R. (1998) Transcriptional pausing at +62 of the HIV-1 nascent RNA modulates formation of the TAR RNA structure. *Mol Cell*, **1**, 1033-1042.
64. Zhang, Z., Klatt, A., Gilmour, D.S. and Henderson, A.J. (2007) Negative elongation factor NELF represses human immunodeficiency virus transcription by pausing the RNA polymerase II complex. *J Biol Chem*, **282**, 16981-16988.
65. Ott, M., Geyer, M. and Zhou, Q. (2011) The control of HIV transcription: keeping RNA polymerase II on track. *Cell Host Microbe*, **10**, 426-435.

66. Kao, S.Y., Calman, A.F., Luciw, P.A. and Peterlin, B.M. (1987) Anti-termination of transcription within the long terminal repeat of HIV-1 by tat gene product. *Nature*, **330**, 489-493.
67. Muesing, M.A., Smith, D.H. and Capon, D.J. (1987) Regulation of mRNA accumulation by a human immunodeficiency virus trans-activator protein. *Cell*, **48**, 691-701.
68. Dingwall, C., Ernberg, I., Gait, M.J., Green, S.M., Heaphy, S., Karn, J., Lowe, A.D., Singh, M. and Skinner, M.A. (1990) HIV-1 tat protein stimulates transcription by binding to a U-rich bulge in the stem of the TAR RNA structure. *EMBO J*, **9**, 4145-4153.
69. Roy, S., Delling, U., Chen, C.H., Rosen, C.A. and Sonenberg, N. (1990) A bulge structure in HIV-1 TAR RNA is required for Tat binding and Tat-mediated trans-activation. *Genes Dev*, **4**, 1365-1373.
70. Weeks, K.M., Ampe, C., Schultz, S.C., Steitz, T.A. and Crothers, D.M. (1990) Fragments of the HIV-1 Tat protein specifically bind TAR RNA. *Science*, **249**, 1281-1285.
71. Weinberger, L.S., Burnett, J.C., Toettcher, J.E., Arkin, A.P. and Schaffer, D.V. (2005) Stochastic gene expression in a lentiviral positive-feedback loop: HIV-1 Tat fluctuations drive phenotypic diversity. *Cell*, **122**, 169-182.
72. Razooky, B.S., Pai, A., Aull, K., Rouzine, I.M. and Weinberger, L.S. (2015) A hardwired HIV latency program. *Cell*, **160**, 990-1001.
73. Weinberger, L.S., Dar, R.D. and Simpson, M.L. (2008) Transient-mediated fate determination in a transcriptional circuit of HIV. *Nat Genet*, **40**, 466-470.
74. Ho, Y.C., Shan, L., Hosmane, N.N., Wang, J., Laskey, S.B., Rosenbloom, D.I., Lai, J., Blankson, J.N., Siliciano, J.D. and Siliciano, R.F. (2013) Replication-competent noninduced proviruses in the latent reservoir increase barrier to HIV-1 cure. *Cell*, **155**, 540-551.
75. Weinberger, A.D. and Weinberger, L.S. (2013) Stochastic fate selection in HIV-infected patients. *Cell*, **155**, 497-499.
76. Mancebo, H.S., Lee, G., Flygare, J., Tomassini, J., Luu, P., Zhu, Y., Peng, J., Blau, C., Hazuda, D., Price, D. *et al.* (1997) P-TEFb kinase is required for HIV Tat transcriptional activation in vivo and in vitro. *Genes Dev*, **11**, 2633-2644.
77. Zhu, Y., Pe'ery, T., Peng, J., Ramanathan, Y., Marshall, N., Marshall, T., Amendt, B., Mathews, M.B. and Price, D.H. (1997) Transcription elongation factor P-TEFb is required for HIV-1 tat transactivation in vitro. *Genes Dev*, **11**, 2622-2632.
78. Wei, P., Garber, M.E., Fang, S.M., Fischer, W.H. and Jones, K.A. (1998) A novel CDK9-associated C-type cyclin interacts directly with HIV-1 Tat and mediates its high-affinity, loop-specific binding to TAR RNA. *Cell*, **92**, 451-462.
79. Garber, M.E., Wei, P. and Jones, K.A. (1998) HIV-1 Tat interacts with cyclin T1 to direct the P-TEFb CTD kinase complex to TAR RNA. *Cold Spring Harb Symp Quant Biol*, **63**, 371-380.
80. Xie, Z. and Price, D.H. (1996) Purification of an RNA polymerase II transcript release factor from Drosophila. *J Biol Chem*, **271**, 11043-11046.
81. Price, D.H. (2000) P-TEFb, a cyclin-dependent kinase controlling elongation by RNA polymerase II. *Mol Cell Biol*, **20**, 2629-2634.
82. Peterlin, B.M. and Price, D.H. (2006) Controlling the elongation phase of transcription with P-TEFb. *Mol Cell*, **23**, 297-305.
83. Rahl, P.B., Lin, C.Y., Seila, A.C., Flynn, R.A., McCuine, S., Burge, C.B., Sharp, P.A. and Young, R.A. (2010) c-Myc regulates transcriptional pause release. *Cell*, **141**, 432-445.
84. Nguyen, V.T., Kiss, T., Michels, A.A. and Bensaude, O. (2001) 7SK small nuclear RNA binds to and inhibits the activity of CDK9/cyclin T complexes. *Nature*, **414**, 322-325.

85. Yang, Z., Zhu, Q., Luo, K. and Zhou, Q. (2001) The 7SK small nuclear RNA inhibits the CDK9/cyclin T1 kinase to control transcription. *Nature*, **414**, 317-322.
86. Xue, Y., Yang, Z., Chen, R. and Zhou, Q. (2010) A capping-independent function of MePCE in stabilizing 7SK snRNA and facilitating the assembly of 7SK snRNP. *Nucleic Acids Res*, **38**, 360-369.
87. Yik, J.H., Chen, R., Nishimura, R., Jennings, J.L., Link, A.J. and Zhou, Q. (2003) Inhibition of P-TEFb (CDK9/Cyclin T) kinase and RNA polymerase II transcription by the coordinated actions of HEXIM1 and 7SK snRNA. *Mol Cell*, **12**, 971-982.
88. Zhou, Q. and Yik, J.H. (2006) The Yin and Yang of P-TEFb regulation: implications for human immunodeficiency virus gene expression and global control of cell growth and differentiation. *Microbiol Mol Biol Rev*, **70**, 646-659.
89. Barboric, M., Yik, J.H., Czudnochowski, N., Yang, Z., Chen, R., Contreras, X., Geyer, M., Matija Peterlin, B. and Zhou, Q. (2007) Tat competes with HEXIM1 to increase the active pool of P-TEFb for HIV-1 transcription. *Nucleic Acids Res*, **35**, 2003-2012.
90. He, N., Liu, M., Hsu, J., Xue, Y., Chou, S., Burlingame, A., Krogan, N.J., Alber, T. and Zhou, Q. (2010) HIV-1 Tat and host AFF4 recruit two transcription elongation factors into a bifunctional complex for coordinated activation of HIV-1 transcription. *Mol Cell*, **38**, 428-438.
91. Sobhian, B., Laguette, N., Yatim, A., Nakamura, M., Levy, Y., Kiernan, R. and Benkirane, M. (2010) HIV-1 Tat assembles a multifunctional transcription elongation complex and stably associates with the 7SK snRNP. *Mol Cell*, **38**, 439-451.
92. Lin, C., Smith, E.R., Takahashi, H., Lai, K.C., Martin-Brown, S., Florens, L., Washburn, M.P., Conaway, J.W., Conaway, R.C. and Shilatifard, A. (2010) AFF4, a component of the ELL/P-TEFb elongation complex and a shared subunit of MLL chimeras, can link transcription elongation to leukemia. *Mol Cell*, **37**, 429-437.
93. Shilatifard, A., Duan, D.R., Haque, D., Florence, C., Schubach, W.H., Conaway, J.W. and Conaway, R.C. (1997) ELL2, a new member of an ELL family of RNA polymerase II elongation factors. *Proc Natl Acad Sci U S A*, **94**, 3639-3643.
94. Shilatifard, A., Lane, W.S., Jackson, K.W., Conaway, R.C. and Conaway, J.W. (1996) An RNA polymerase II elongation factor encoded by the human ELL gene. *Science*, **271**, 1873-1876.
95. Shilatifard, A., Conaway, R.C. and Conaway, J.W. (2003) The RNA polymerase II elongation complex. *Annu Rev Biochem*, **72**, 693-715.
96. Liu, M., Hsu, J., Chan, C., Li, Z. and Zhou, Q. (2012) The ubiquitin ligase Siah1 controls ELL2 stability and formation of super elongation complexes to modulate gene transcription. *Mol Cell*, **46**, 325-334.
97. He, N., Chan, C.K., Sobhian, B., Chou, S., Xue, Y., Liu, M., Alber, T., Benkirane, M. and Zhou, Q. (2011) Human Polymerase-Associated Factor complex (PAFc) connects the Super Elongation Complex (SEC) to RNA polymerase II on chromatin. *Proc Natl Acad Sci U S A*, **108**, E636-645.
98. Takahashi, H., Parmely, T.J., Sato, S., Tomomori-Sato, C., Banks, C.A., Kong, S.E., Szutorisz, H., Swanson, S.K., Martin-Brown, S., Washburn, M.P. *et al.* (2011) Human mediator subunit MED26 functions as a docking site for transcription elongation factors. *Cell*, **146**, 92-104.
99. Chou, S., Upton, H., Bao, K., Schulze-Gahmen, U., Samelson, A.J., He, N., Nowak, A., Lu, H., Krogan, N.J., Zhou, Q. *et al.* (2013) HIV-1 Tat recruits transcription elongation factors dispersed along a flexible AFF4 scaffold. *Proc Natl Acad Sci U S A*, **110**, E123-131.

100. Schulze-Gahmen, U., Upton, H., Birnberg, A., Bao, K., Chou, S., Krogan, N.J., Zhou, Q. and Alber, T. (2013) The AFF4 scaffold binds human P-TEFb adjacent to HIV Tat. *Elife*, **2**, e00327.
101. Schulze-Gahmen, U., Echeverria, I., Stjepanovic, G., Bai, Y., Lu, H., Schneidman-Duhovny, D., Doudna, J.A., Zhou, Q., Sali, A. and Hurley, J.H. (2016) Insights into HIV-1 proviral transcription from integrative structure and dynamics of the Tat:AFF4:P-TEFb:TAR complex. *Elife*, **5**.
102. Lu, H., Li, Z., Xue, Y., Schulze-Gahmen, U., Johnson, J.R., Krogan, N.J., Alber, T. and Zhou, Q. (2014) AFF1 is a ubiquitous P-TEFb partner to enable Tat extraction of P-TEFb from 7SK snRNP and formation of SECs for HIV transactivation. *Proc Natl Acad Sci U S A*, **111**, E15-24.
103. Schulze-Gahmen, U., Lu, H., Zhou, Q. and Alber, T. (2014) AFF4 binding to Tat-P-TEFb indirectly stimulates TAR recognition of super elongation complexes at the HIV promoter. *Elife*, **3**, e02375.
104. Lin, C., Garrett, A.S., De Kumar, B., Smith, E.R., Gogol, M., Seidel, C., Krumlauf, R. and Shilatifard, A. (2011) Dynamic transcriptional events in embryonic stem cells mediated by the super elongation complex (SEC). *Genes Dev*, **25**, 1486-1498.
105. Yang, Z., Yik, J.H., Chen, R., He, N., Jang, M.K., Ozato, K. and Zhou, Q. (2005) Recruitment of P-TEFb for stimulation of transcriptional elongation by the bromodomain protein Brd4. *Mol Cell*, **19**, 535-545.
106. Bisgrove, D.A., Mahmoudi, T., Henklein, P. and Verdin, E. (2007) Conserved P-TEFb-interacting domain of BRD4 inhibits HIV transcription. *Proc Natl Acad Sci U S A*, **104**, 13690-13695.
107. Filippakopoulos, P., Qi, J., Picaud, S., Shen, Y., Smith, W.B., Fedorov, O., Morse, E.M., Keates, T., Hickman, T.T., Felletar, I. *et al.* (2010) Selective inhibition of BET bromodomains. *Nature*, **468**, 1067-1073.
108. Li, Z., Guo, J., Wu, Y. and Zhou, Q. (2013) The BET bromodomain inhibitor JQ1 activates HIV latency through antagonizing Brd4 inhibition of Tat-transactivation. *Nucleic Acids Res*, **41**, 277-287.
109. Banerjee, C., Archin, N., Michaels, D., Belkina, A.C., Denis, G.V., Bradner, J., Sebastiani, P., Margolis, D.M. and Montano, M. (2012) BET bromodomain inhibition as a novel strategy for reactivation of HIV-1. *J Leukoc Biol*, **92**, 1147-1154.
110. Zhu, J., Gaiha, G.D., John, S.P., Pertel, T., Chin, C.R., Gao, G., Qu, H.J., Walker, B.D., Elledge, S.J. and Brass, A.L. (2012) Reactivation of Latent HIV-1 by Inhibition of BRD4. *Cell Reports*, **2**, 807-816.
111. Darcis, G., Kula, A., Bouchat, S., Fujinaga, K., Corazza, F., Ait-Ammar, A., Delacourt, N., Melard, A., Kabeya, K., Vanhulle, C. *et al.* (2015) An In-Depth Comparison of Latency-Reversing Agent Combinations in Various In Vitro and Ex Vivo HIV-1 Latency Models Identified Bryostatin-1+JQ1 and Ingenol-B+JQ1 to Potently Reactivate Viral Gene Expression. *PLoS Pathog*, **11**, e1005063.
112. Jiang, G., Mendes, E.A., Kaiser, P., Wong, D.P., Tang, Y., Cai, I., Fenton, A., Melcher, G.P., Hildreth, J.E., Thompson, G.R. *et al.* (2015) Synergistic Reactivation of Latent HIV Expression by Ingenol-3-Angelate, PEP005, Targeted NF-kB Signaling in Combination with JQ1 Induced p-TEFb Activation. *PLoS Pathog*, **11**, e1005066.
113. Zack, J.A., Arrigo, S.J., Weitsman, S.R., Go, A.S., Haislip, A. and Chen, I.S. (1990) HIV-1 entry into quiescent primary lymphocytes: molecular analysis reveals a labile, latent viral structure. *Cell*, **61**, 213-222.

114. Perelson, A.S., Essunger, P., Cao, Y., Vesanen, M., Hurley, A., Saksela, K., Markowitz, M. and Ho, D.D. (1997) Decay characteristics of HIV-1-infected compartments during combination therapy. *Nature*, **387**, 188-191.
115. Kulkosky, J., Nunnari, G., Otero, M., Calarota, S., Dornadula, G., Zhang, H., Malin, A., Sullivan, J., Xu, Y., DeSimone, J. *et al.* (2002) Intensification and stimulation therapy for human immunodeficiency virus type 1 reservoirs in infected persons receiving virally suppressive highly active antiretroviral therapy. *J Infect Dis*, **186**, 1403-1411.
116. Prins, J.M., Jurriaans, S., van Praag, R.M., Blaak, H., van Rij, R., Schellekens, P.T., ten Berge, I.J., Yong, S.L., Fox, C.H., Roos, M.T. *et al.* (1999) Immuno-activation with anti-CD3 and recombinant human IL-2 in HIV-1-infected patients on potent antiretroviral therapy. *AIDS*, **13**, 2405-2410.
117. Delagreverie, H.M., Delaugerre, C., Lewin, S.R., Deeks, S.G. and Li, J.Z. (2016) Ongoing Clinical Trials of Human Immunodeficiency Virus Latency-Reversing and Immunomodulatory Agents. *Open Forum Infect Dis*, **3**, ofw189.
118. Spivak, A.M. and Planelles, V. (2016) HIV-1 Eradication: Early Trials (and Tribulations). *Trends Mol Med*, **22**, 10-27.
119. Pearson, R., Kim, Y.K., Hokello, J., Lassen, K., Friedman, J., Tyagi, M. and Karn, J. (2008) Epigenetic silencing of human immunodeficiency virus (HIV) transcription by formation of restrictive chromatin structures at the viral long terminal repeat drives the progressive entry of HIV into latency. *J Virol*, **82**, 12291-12303.
120. Bullen, C.K., Laird, G.M., Durand, C.M., Siliciano, J.D. and Siliciano, R.F. (2014) New ex vivo approaches distinguish effective and ineffective single agents for reversing HIV-1 latency in vivo. *Nat Med*, **20**, 425-429.
121. Luo, Z., Lin, C. and Shilatifard, A. (2012) The super elongation complex (SEC) family in transcriptional control. *Nat Rev Mol Cell Biol*, **13**, 543-547.
122. Lu, H., Li, Z., Zhang, W., Schulze-Gahmen, U., Xue, Y. and Zhou, Q. (2015) Gene target specificity of the Super Elongation Complex (SEC) family: how HIV-1 Tat employs selected SEC members to activate viral transcription. *Nucleic Acids Res*.
123. Shilatifard, A. (1998) Factors regulating the transcriptional elongation activity of RNA polymerase II. *Faseb J*, **12**, 1437-1446.
124. Ran, F.A., Hsu, P.D., Wright, J., Agarwala, V., Scott, D.A. and Zhang, F. (2013) Genome engineering using the CRISPR-Cas9 system. *Nat Protoc*, **8**, 2281-2308.
125. Lassen, K.G., Bailey, J.R. and Siliciano, R.F. (2004) Analysis of human immunodeficiency virus type 1 transcriptional elongation in resting CD4(+) T cells in vivo. *Journal of Virology*, **78**, 9105-9114.
126. Wang, T., Wei, J.J., Sabatini, D.M. and Lander, E.S. (2014) Genetic Screens in Human Cells Using the CRISPR-Cas9 System. *Science*, **343**, 80-84.
127. Tyagi, M., Pearson, R.J. and Karn, J. (2010) Establishment of HIV latency in primary CD4+ cells is due to epigenetic transcriptional silencing and P-TEFb restriction. *J Virol*, **84**, 6425-6437.
128. Kim, Y.K., Mbonye, U., Hokello, J. and Karn, J. (2011) T-cell receptor signaling enhances transcriptional elongation from latent HIV proviruses by activating P-TEFb through an ERK-dependent pathway. *J Mol Biol*, **410**, 896-916.
129. Jordan, A., Bisgrove, D. and Verdin, E. (2003) HIV reproducibly establishes a latent infection after acute infection of T cells in vitro. *EMBO J*, **22**, 1868-1877.
130. Donahue, D.A., Kuhl, B.D., Sloan, R.D. and Wainberg, M.A. (2012) The viral protein Tat can inhibit the establishment of HIV-1 latency. *J Virol*, **86**, 3253-3263.

131. Baud, V. and Karin, M. (2009) Is NF-kappaB a good target for cancer therapy? Hopes and pitfalls. *Nat Rev Drug Discov*, **8**, 33-40.
132. Ghose, R., Liou, L.Y., Herrmann, C.H. and Rice, A.P. (2001) Induction of TAK (cyclin T1/P-TEFb) in purified resting CD4(+) T lymphocytes by combination of cytokines. *J Virol*, **75**, 11336-11343.
133. Sung, T.L. and Rice, A.P. (2006) Effects of prostratin on Cyclin T1/P-TEFb function and the gene expression profile in primary resting CD4+ T cells. *Retrovirology*, **3**, 66.
134. Ferrari, G., Haynes, B.F., Koenig, S., Nordstrom, J.L., Margolis, D.M. and Tomaras, G.D. (2016) Envelope-specific antibodies and antibody-derived molecules for treating and curing HIV infection. *Nat Rev Drug Discov*.
135. Martin, A.R. and Siliciano, R.F. (2016) Progress Toward HIV Eradication: Case Reports, Current Efforts, and the Challenges Associated with Cure. *Annu Rev Med*, **67**, 215-228.
136. Laird, G.M., Bullen, C.K., Rosenbloom, D.I., Martin, A.R., Hill, A.L., Durand, C.M., Siliciano, J.D. and Siliciano, R.F. (2015) Ex vivo analysis identifies effective HIV-1 latency-reversing drug combinations. *J Clin Invest*, **125**, 1901-1912.
137. Filippakopoulos, P., Picaud, S., Mangos, M., Keates, T., Lambert, J.P., Barsyte-Lovejoy, D., Felletar, I., Volkmer, R., Muller, S., Pawson, T. *et al.* (2012) Histone recognition and large-scale structural analysis of the human bromodomain family. *Cell*, **149**, 214-231.
138. Jang, M.K., Mochizuki, K., Zhou, M., Jeong, H.S., Brady, J.N. and Ozato, K. (2005) The bromodomain protein Brd4 is a positive regulatory component of P-TEFb and stimulates RNA polymerase II-dependent transcription. *Mol Cell*, **19**, 523-534.
139. Hargreaves, D.C., Horng, T. and Medzhitov, R. (2009) Control of inducible gene expression by signal-dependent transcriptional elongation. *Cell*, **138**, 129-145.
140. Conrad, R.J., Fozouni, P., Thomas, S., Sy, H., Zhang, Q., Zhou, M.M. and Ott, M. (2017) The Short Isoform of BRD4 Promotes HIV-1 Latency by Engaging Repressive SWI/SNF Chromatin-Remodeling Complexes. *Mol Cell*, **67**, 1001-1012 e1006.
141. Van Lint, C., Emiliani, S., Ott, M. and Verdin, E. (1996) Transcriptional activation and chromatin remodeling of the HIV-1 promoter in response to histone acetylation. *EMBO J*, **15**, 1112-1120.
142. Kimura, A. and Horikoshi, M. (1998) Tip60 acetylates six lysines of a specific class in core histones in vitro. *Genes Cells*, **3**, 789-800.
143. Smith, E.R., Cayrou, C., Huang, R., Lane, W.S., Cote, J. and Lucchesi, J.C. (2005) A human protein complex homologous to the Drosophila MSL complex is responsible for the majority of histone H4 acetylation at lysine 16. *Mol Cell Biol*, **25**, 9175-9188.
144. Gilbert, L.A., Horlbeck, M.A., Adamson, B., Villalta, J.E., Chen, Y., Whitehead, E.H., Guimaraes, C., Panning, B., Ploegh, H.L., Bassik, M.C. *et al.* (2014) Genome-Scale CRISPR-Mediated Control of Gene Repression and Activation. *Cell*, **159**, 647-661.
145. Nguyen, K., Das, B., Dobrowolski, C. and Karn, J. (2017) Multiple Histone Lysine Methyltransferases Are Required for the Establishment and Maintenance of HIV-1 Latency. *MBio*, **8**.
146. Aguilar-Cordova, E., Chinen, J., Donehower, L., Lewis, D.E. and Belmont, J.W. (1994) A sensitive reporter cell line for HIV-1 tat activity, HIV-1 inhibitors, and T cell activation effects. *AIDS Res Hum Retroviruses*, **10**, 295-301.
147. Ott, M., VERDIN, E.M. and Zhou, M.M. (2015). US20150133434 A1, US Patent.
148. Kaidi, A. and Jackson, S.P. (2013) KAT5 tyrosine phosphorylation couples chromatin sensing to ATM signalling. *Nature*, **498**, 70-74.
149. Nelson, J.D., Denisenko, O. and Bomsztyk, K. (2006) Protocol for the fast chromatin immunoprecipitation (ChIP) method. *Nat Protoc*, **1**, 179-185.

150. Schroder, S., Cho, S., Zeng, L., Zhang, Q., Kaehlcke, K., Mak, L., Lau, J., Bisgrove, D., Schnolzer, M., Verdin, E. *et al.* (2012) Two-pronged binding with bromodomain-containing protein 4 liberates positive transcription elongation factor b from inactive ribonucleoprotein complexes. *J Biol Chem*, **287**, 1090-1099.
151. Verdin, E., Paras, P., Jr. and Van Lint, C. (1993) Chromatin disruption in the promoter of human immunodeficiency virus type 1 during transcriptional activation. *EMBO J*, **12**, 3249-3259.
152. Beisel, C. and Paro, R. (2011) Silencing chromatin: comparing modes and mechanisms. *Nat Rev Genet*, **12**, 123-135.
153. Huynh, J.L. and Casaccia, P. (2013) Epigenetic mechanisms in multiple sclerosis: implications for pathogenesis and treatment. *Lancet Neurol*, **12**, 195-206.
154. Ghizzoni, M., Wu, J., Gao, T., Haisma, H.J., Dekker, F.J. and George Zheng, Y. (2012) 6-alkylsalicylates are selective Tip60 inhibitors and target the acetyl-CoA binding site. *Eur J Med Chem*, **47**, 337-344.
155. Kanno, T., Kanno, Y., LeRoy, G., Campos, E., Sun, H.W., Brooks, S.R., Vahedi, G., Heightman, T.D., Garcia, B.A., Reinberg, D. *et al.* (2014) BRD4 assists elongation of both coding and enhancer RNAs by interacting with acetylated histones. *Nat Struct Mol Biol*, **21**, 1047-1057.
156. Kouzarides, T. (2007) Chromatin modifications and their function. *Cell*, **128**, 693-705.
157. Lu, H., Xue, Y., Yu, G.K., Arias, C., Lin, J., Fong, S., Faure, M., Weisburd, B., Ji, X., Mercier, A. *et al.* (2015) Compensatory induction of MYC expression by sustained CDK9 inhibition via a BRD4-dependent mechanism. *Elife*, **4**, e06535.
158. Li, Z., Lu, H. and Zhou, Q. (2016) A Minor Subset of Super Elongation Complexes Plays a Predominant Role in Reversing HIV-1 Latency. *Mol Cell Biol*, **36**, 1194-1205.
159. Grow, E.J., Flynn, R.A., Chavez, S.L., Bayless, N.L., Wossidlo, M., Wesche, D.J., Martin, L., Ware, C.B., Blish, C.A., Chang, H.Y. *et al.* (2015) Intrinsic retroviral reactivation in human preimplantation embryos and pluripotent cells. *Nature*, **522**, 221-225.
160. Friedman, J., Cho, W.K., Chu, C.K., Keedy, K.S., Archin, N.M., Margolis, D.M. and Karn, J. (2011) Epigenetic silencing of HIV-1 by the histone H3 lysine 27 methyltransferase enhancer of Zeste 2. *J Virol*, **85**, 9078-9089.
161. Lu, H., Li, Z., Xue, Y. and Zhou, Q. (2013) Viral-host interactions that control HIV-1 transcriptional elongation. *Chem Rev*, **113**, 8567-8582.
162. Kamine, J., Elangovan, B., Subramanian, T., Coleman, D. and Chinnadurai, G. (1996) Identification of a cellular protein that specifically interacts with the essential cysteine region of the HIV-1 Tat transactivator. *Virology*, **216**, 357-366.
163. Creaven, M., Hans, F., Mutskov, V., Col, E., Caron, C., Dimitrov, S. and Khochbin, S. (1999) Control of the histone-acetyltransferase activity of Tip60 by the HIV-1 transactivator protein, Tat. *Biochemistry*, **38**, 8826-8830.
164. du Chene, I., Basyuk, E., Lin, Y.L., Triboulet, R., Knezevich, A., Chable-Bessia, C., Mettling, C., Baillat, V., Reynes, J., Corbeau, P. *et al.* (2007) Suv39H1 and HP1gamma are responsible for chromatin-mediated HIV-1 transcriptional silencing and post-integration latency. *EMBO J*, **26**, 424-435.
165. Jasencakova, Z., Meister, A., Walter, J., Turner, B.M. and Schubert, I. (2000) Histone H4 acetylation of euchromatin and heterochromatin is cell cycle dependent and correlated with replication rather than with transcription. *Plant Cell*, **12**, 2087-2100.
166. Grezy, A., Chevillard-Briet, M., Trouche, D. and Escaffit, F. (2016) Control of genetic stability by a new heterochromatin compaction pathway involving the Tip60 histone acetyltransferase. *Mol Biol Cell*, **27**, 599-607.

167. Jha, S., Vande Pol, S., Banerjee, N.S., Dutta, A.B., Chow, L.T. and Dutta, A. (2010) Destabilization of TIP60 by human papillomavirus E6 results in attenuation of TIP60-dependent transcriptional regulation and apoptotic pathway. *Mol Cell*, **38**, 700-711.
168. Gupta, A., Jha, S., Engel, D.A., Ornelles, D.A. and Dutta, A. (2013) Tip60 degradation by adenovirus relieves transcriptional repression of viral transcriptional activator EIA. *Oncogene*, **32**, 5017-5025.
169. Mbonye, U. and Karn, J. (2017) The Molecular Basis for Human Immunodeficiency Virus Latency. *Annu Rev Virol*, **4**, 261-285.
170. Thorlund, K., Horwitz, M.S., Fife, B.T., Lester, R. and Cameron, D.W. (2017) Landscape review of current HIV 'kick and kill' cure research - some kicking, not enough killing. *BMC Infect Dis*, **17**, 595.
171. Bartholomeeusen, K., Xiang, Y., Fujinaga, K. and Peterlin, B.M. (2012) Bromodomain and extra-terminal (BET) bromodomain inhibition activate transcription via transient release of positive transcription elongation factor b (P-TEFb) from 7SK small nuclear ribonucleoprotein. *J Biol Chem*, **287**, 36609-36616.
172. Abdel-Mohsen, M., Chavez, L., Tandon, R., Chew, G.M., Deng, X., Danesh, A., Keating, S., Lanteri, M., Samuels, M.L., Hoh, R. *et al.* (2016) Human Galectin-9 Is a Potent Mediator of HIV Transcription and Reactivation. *PLoS Pathog*, **12**, e1005677.
173. Yu, D., Liu, R., Yang, G. and Zhou, Q. (2018) The PARP1-Siah1 Axis Controls HIV-1 Transcription and Expression of Siah1 Substrates. *Cell Rep*, **23**, 3741-3749.
174. Gilbert, L.A., Larson, M.H., Morsut, L., Liu, Z., Brar, G.A., Torres, S.E., Stern-Ginossar, N., Brandman, O., Whitehead, E.H., Doudna, J.A. *et al.* (2013) CRISPR-mediated modular RNA-guided regulation of transcription in eukaryotes. *Cell*, **154**, 442-451.
175. Horlbeck, M.A., Gilbert, L.A., Villalta, J.E., Adamson, B., Pak, R.A., Chen, Y., Fields, A.P., Park, C.Y., Corn, J.E., Kampmann, M. *et al.* (2016) Compact and highly active next-generation libraries for CRISPR-mediated gene repression and activation. *Elife*, **5**.
176. Bliss, C.I. (1939) The toxicity of poisons applied jointly. *Annals of Applied Biology*, **26**, 585-615.
177. Williams, S.A., Chen, L.F., Kwon, H., Fenard, D., Bisgrove, D., Verdin, E. and Greene, W.C. (2004) Prostratin antagonizes HIV latency by activating NF-kappaB. *J Biol Chem*, **279**, 42008-42017.
178. Manganaro, L., Pache, L., Herrmann, T., Marlett, J., Hwang, Y., Murry, J., Miorin, L., Ting, A.T., Konig, R., Garcia-Sastre, A. *et al.* (2014) Tumor suppressor cylindromatosis (CYLD) controls HIV transcription in an NF-kappaB-dependent manner. *J Virol*, **88**, 7528-7540.
179. Lu, P., Hankel, I.L., Hostager, B.S., Swartzendruber, J.A., Friedman, A.D., Brenton, J.L., Rothman, P.B. and Colgan, J.D. (2011) The developmental regulator protein Gon4l associates with protein YY1, co-repressor Sin3a, and histone deacetylase 1 and mediates transcriptional repression. *J Biol Chem*, **286**, 18311-18319.
180. Lander, G.C., Estrin, E., Matyskiela, M.E., Bashore, C., Nogales, E. and Martin, A. (2012) Complete subunit architecture of the proteasome regulatory particle. *Nature*, **482**, 186-191.
181. Chen, D., Frezza, M., Schmitt, S., Kanwar, J. and Dou, Q.P. (2011) Bortezomib as the first proteasome inhibitor anticancer drug: current status and future perspectives. *Curr Cancer Drug Targets*, **11**, 239-253.
182. Kuhn, D.J., Chen, Q., Voorhees, P.M., Strader, J.S., Shenk, K.D., Sun, C.M., Demo, S.D., Bennett, M.K., van Leeuwen, F.W., Chanan-Khan, A.A. *et al.* (2007) Potent activity of carfilzomib, a novel, irreversible inhibitor of the ubiquitin-proteasome pathway, against preclinical models of multiple myeloma. *Blood*, **110**, 3281-3290.

183. Mehla, R., Bivalkar-Mehla, S., Zhang, R., Handy, I., Albrecht, H., Giri, S., Nagarkatti, P., Nagarkatti, M. and Chauhan, A. (2010) Bryostatin modulates latent HIV-1 infection via PKC and AMPK signaling but inhibits acute infection in a receptor independent manner. *PLoS One*, **5**, e11160.
184. Krishnan, V. and Zeichner, S.L. (2004) Host cell gene expression during human immunodeficiency virus type 1 latency and reactivation and effects of targeting genes that are differentially expressed in viral latency. *J Virol*, **78**, 9458-9473.
185. Pan, X.Y., Zhao, W., Wang, C.Y., Lin, J., Zeng, X.Y., Ren, R.X., Wang, K., Xun, T.R., Shai, Y. and Liu, S.W. (2016) Heat Shock Protein 90 Facilitates Latent HIV Reactivation through Maintaining the Function of Positive Transcriptional Elongation Factor b (p-TEFb) under Proteasome Inhibition. *J Biol Chem*, **291**, 26177-26187.
186. Manasanch, E.E. and Orlowski, R.Z. (2017) Proteasome inhibitors in cancer therapy. *Nat Rev Clin Oncol*, **14**, 417-433.
187. Teicher, B.A. and Tomaszewski, J.E. (2015) Proteasome inhibitors. *Biochem Pharmacol*, **96**, 1-9.
188. Singh, A., Razooky, B., Cox, C.D., Simpson, M.L. and Weinberger, L.S. (2010) Transcriptional bursting from the HIV-1 promoter is a significant source of stochastic noise in HIV-1 gene expression. *Biophys J*, **98**, L32-34.
189. Qi, S., Li, Z., Schulze-Gahmen, U., Stjepanovic, G., Zhou, Q. and Hurley, J.H. (2017) Structural basis for ELL2 and AFF4 activation of HIV-1 proviral transcription. *Nat Commun*, **8**, 14076.
190. Chun, T.W., Nickle, D.C., Justement, J.S., Meyers, J.H., Roby, G., Hallahan, C.W., Kottilil, S., Moir, S., Mican, J.M., Mullins, J.I. *et al.* (2008) Persistence of HIV in gut-associated lymphoid tissue despite long-term antiretroviral therapy. *J Infect Dis*, **197**, 714-720.
191. Valcour, V., Sithinamsuwan, P., Letendre, S. and Ances, B. (2011) Pathogenesis of HIV in the central nervous system. *Curr HIV/AIDS Rep*, **8**, 54-61.
192. Kim, Y., Anderson, J.L. and Lewin, S.R. (2018) Getting the "Kill" into "Shock and Kill": Strategies to Eliminate Latent HIV. *Cell Host Microbe*, **23**, 14-26.
193. Halper-Stromberg, A. and Nussenzweig, M.C. (2016) Towards HIV-1 remission: potential roles for broadly neutralizing antibodies. *J Clin Invest*, **126**, 415-423.
194. Halper-Stromberg, A., Lu, C.L., Klein, F., Horwitz, J.A., Bournazos, S., Nogueira, L., Eisenreich, T.R., Liu, C., Gazumyan, A., Schaefer, U. *et al.* (2014) Broadly neutralizing antibodies and viral inducers decrease rebound from HIV-1 latent reservoirs in humanized mice. *Cell*, **158**, 989-999.
195. Sung, J.A., Pickeral, J., Liu, L., Stanfield-Oakley, S.A., Lam, C.Y., Garrido, C., Pollara, J., LaBranche, C., Bonsignori, M., Moody, M.A. *et al.* (2015) Dual-Affinity Re-Targeting proteins direct T cell-mediated cytolysis of latently HIV-infected cells. *J Clin Invest*, **125**, 4077-4090.
196. Sloan, D.D., Lam, C.Y., Irrinki, A., Liu, L., Tsai, A., Pace, C.S., Kaur, J., Murry, J.P., Balakrishnan, M., Moore, P.A. *et al.* (2015) Targeting HIV Reservoir in Infected CD4 T Cells by Dual-Affinity Re-targeting Molecules (DARTs) that Bind HIV Envelope and Recruit Cytotoxic T Cells. *PLoS Pathog*, **11**, e1005233.
197. Velu, V., Shetty, R.D., Larsson, M. and Shankar, E.M. (2015) Role of PD-1 co-inhibitory pathway in HIV infection and potential therapeutic options. *Retrovirology*, **12**, 14.
198. Ananworanich, J., Chomont, N., Eller, L.A., Kroon, E., Tovanabutra, S., Bose, M., Nau, M., Fletcher, J.L.K., Tipsuk, S., Vandergeeten, C. *et al.* (2016) HIV DNA Set Point is Rapidly Established in Acute HIV Infection and Dramatically Reduced by Early ART. *EBioMedicine*, **11**, 68-72.

199. Bruner, K.M., Hosmane, N.N. and Siliciano, R.F. (2015) Towards an HIV-1 cure: measuring the latent reservoir. *Trends Microbiol*, **23**, 192-203.
200. Zhang, F., Dou, Z., Ma, Y., Zhang, Y., Zhao, Y., Zhao, D., Zhou, S., Bulterys, M., Zhu, H. and Chen, R.Y. (2011) Effect of earlier initiation of antiretroviral treatment and increased treatment coverage on HIV-related mortality in China: a national observational cohort study. *Lancet Infect Dis*, **11**, 516-524.
201. Archin, N.M. and Margolis, D.M. (2014) Emerging strategies to deplete the HIV reservoir. *Curr Opin Infect Dis*, **27**, 29-35.